Evaluating ^{238}U External Background for SNO+ Experiment using Radon Assays and ^{214}Bi Analysis

by

Syed Muhammad Adil Hussain

A thesis submitted in partial fulfillment of the requirements for the degree of Master of Science (MSc) in Physics

The Office of Graduate Studies
Laurentian University
Sudbury, Ontario, Canada

THESIS DEFENCE COMMITTEE/COMITÉ DE SOUTENANCE DE THÈSE
Laurentian Université/Université Laurentienne
Office of Graduate Studies/Bureau des études supérieures

Title of Thesis
Titre de la thèse: Evaluating ^{238}U External Background for SNO+ Experiment using Radon Assays and ^{214}Bi Analysis

Name of Candidate
Nom du candidat: Hussain, Syed Muhammad Adil

Degree
Diplôme: Master of Science

Department/Program
Département/Programme: Physics

Date of Defence
Date de la soutenance avril 11, 2022

APPROVED/APPROUVÉ

Thesis Examiners/Examinateurs de thèse:

Dr. Christine Kraus
(Supervisor/Directeur(trice) de thèse)

Dr. Chris Jillings
(Committee member/Membre du comité)

Dr. Szymon Manecki
(Committee member/Membre du comité)

Dr. Tina Pollmann
(External Examiner/Examinateur externe)

Approved for the Office of Graduate Studies
Approuvé pour le Bureau des études supérieures
Tammy Eger, PhD
Vice-President Research (Office of Graduate Studies)
Vice-rectrice à la recherche (Bureau des études supérieures)
Laurentian University / Université Laurentienne

ACCESSIBILITY CLAUSE AND PERMISSION TO USE

Abstract

SNO+ is large multipurpose detector located at SNOLAB filled with liquid scintillator. The scintillator will then be loaded with Te isotope, allowing to look for neutrino-less double beta decay which is extremely rare. This will determine if the neutrino is its own antiparticle. One of the main concerns for these rare event experiments is the presence of backgrounds, which could mask the signals of interest. This thesis will focus on ^{222}Rn, one of the most common backgrounds due to its excessive prevalence in the mine environment. Radon decays into daughter nuclei where the energies lie within the region of interest for neutrino-less double beta decay. The detector is housed in a large cavity that is filled with ultrapure water and has a nitrogen cover-gas in order to avoid contamination. Radon Assay is a technique that was developed for the original SNO experiment to keep track of the radon content within the cavity and the covergas systems. The Assay system itself is well calibrated with low backgrounds. Assays are performed frequently at different positions of the cavity and cover-gas to monitor the radon levels. During a radon assay, radon is cryogenically trapped, concentrated, and shared into a ZnS coated Lucas cell for a period of time and known amount of flow. This Lucas cell is then connected to a PMT, which detects the decayed alphas that are used to calculate the number of radon atoms in the assay. This technique is a crucial part of measuring and monitoring the low backgrounds for the experiment which is then verified from the *in-situ* Bi^{214} analysis for accuracy.

Acknowledgements

First and foremost, I would like to thank my supervisor Dr Christine Kraus for her continuous support throughout my degree. Your perseverance and patience is admirable. You adhered to your students during the hard times of Laurentian University, even when your own future wasn't exactly clear. I am very grateful to you for the opportunity and independence during the course of this degree.

Special thanks to Dr Nasim Fatemighomi for training me with all the Assay related work underground. Your guidance has played an enormous role in my learning and development. I also want to thank Dr Ryan Bayes for always being readily available and prompting physics discussions in order to stimulate my thinking. Thank you Dr Aleksandra for always supporting my work and helping me get underground shifts. I also want to thank my committee members for reading my thesis and giving valuable feedback.

I would like to extend my appreciation to the operations group and scientific support group at SNOLAB. Your continuous support enabled my underground work to go smoothly. I would like to thank the SNO+ on site crew including Pouya, Jamie, Matt, Mark, Cindy, Caroline, and Shengzhao.

I would like to thank my parents for always supporting me and encouraging me in the pursuit of my dreams and showering me with unconditional love throughout my life. Special thanks to my mother for her endless support and resilience, I wouldn't have been able to do this without you and I am forever indebted to you for providing me with wonderful opportunities. I am forever thankful to my amazing sisters, Hareem and Fahama, who have always been there for me and continued to extend their support, love, and encouragement. To my beautiful niece Wareesha, the world is your oyster!

I would like to thank my amazing friends: Raafay, Mahad, Reshayl, Yumeka, and Tariq. Your affection and continuous support is greatly appreciated and your presence in my life has made a huge impact on my personal development. Lastly I would like to thank all my uncles and aunts for showering me with love and constant support, especially Ali Uncle, Ausaf Aunty, and Sajjad Uncle.

List of Figures

List of Tables

Contents

Chapter 1

Neutrino Physics

1.1 Neutrinos

The Neutrino, a neutral and weakly interacting particle, was first proposed by Wolfgang Pauli in 1930 to explain the non conserved energy from the continuous beta decay emission spectrum. Initially named neutrons, neutrinos were suggested to have an angular momentum of $\hbar(1/2)$ and a magnetic moment, but no charge [29]. While neutrons were discovered [30], neutrino was the alternative name given derived from the "little neutral one".

Neutrinos remained a proposed particle until its first detection in 1956 [63]. Since then a lot of work has been done in understanding all the properties of neutrinos, most prominent one being observing neutrino oscillations which implied that neutrinos can not only change flavors and but also have a non zero-mass [9] [66] [32]. However, several properties of neutrinos such as their absolute mass and Majorana or Dirac nature are still unknown. The incomplete theory of neutrinos has provided a lot of motivation for neutrino-less double beta decay experiments which attempt to resolve the Majorana nature of the neutrino [69].

Since its first discovery, three flavors of Neutrinos have been discovered: electron neutrino, muon neutrino and tau neutrino; denoted by ν_e, ν_μ, and ν_τ. Apart from the three flavors of neutrinos, there is another proposed flavor of neutrino known as the "sterile neutrino" which only interacts with gravity [4]. Neutrino is a fermion with 1/2 integer spin which interact with

matter with a weak force, therefore, they pass through the matter unhindered. Due to the small cross section and weak interactions, neutrino detection attempts were made successful by developing big underground detectors. The underground presence helped eliminate the cosmic flux which could severely impact the detection of neutrinos. Moreover, detectors were relatively big in order to increase the interaction cross section of neutrinos with the active medium of the detectors.

1.1.1 Electron Neutrino

In 1956, Frederick Reines and Clyde L. Cowan attempted to detect the anti-neutrino from a nuclear reactor using inverse beta decay [20]. Nuclear reactor was considered a suitable source as it was expected to produce large flux of anti-neutrinos. In order to detect the neutrino, a large scintillator detector was built next to the reactor site [63]. In inverse beta decay, the anti neutrinos produced within the nuclear reactor would interact with a proton in the detector and produce a neutron and a positron, as shown in equation 1.1

$$\bar{\nu_e} + p \rightarrow n + e^+ \tag{1.1}$$

The positron interacted with the electrons in the detector and annihilated producing scintillation light or prompt signal, while neutron travelled for another 200 μs before being captured by another proton producing a 2.22 MeV gamma or delayed signal. These coincident events within the detector successfully measured the inverse beta decay and led to the discovery of the neutrino. This neutrino was named as the electron anti-neutrino.

1.1.2 Muon Neutrino

The muon neutrino was first proposed by Shoichi Sakata and Takesi Inoue's two-meson theory of 1942 [53]. However, it wasn't detected until 1962 in the Brookhaven National Laboratory using a proton beam produced by Alternating Gradient Synchrotron (AGS) [35][64]. The generated proton beam had an energy of 15 GeV which was slammed into a beryllium target creating

pions [55]. The pions then decayed into muons and neutrinos using the equations 1.2 and 1.3 .

$$\pi^{\pm} \rightarrow \mu^{\pm} + \nu_{\mu} \tag{1.2}$$

$$\mu^{\pm} \rightarrow e^{\pm} + \nu_{e} + \bar{\nu}_{\mu} \tag{1.3}$$

The pions, muons, and the proton beam passed through a 13.5m thick steel wall. An additional 10 ton spark chamber was constructed consisting of aluminium plates separated by gas filled gaps. The neutrino would interact with the proton of the aluminium disks and create neutrons and either muons or electrons. The electrons or muons would ionize the gas creating sparks. The experiment concluded that pion decay only produced muons which suggested that the neutrinos measured were different than the ones from the beta decay [55]. This discovery led to the 1988 Nobel prize for Melvin Schwartz, Leon Lederman, and Jack Steinberger.

1.1.3 Tau neutrino

The evidence of the tau neutrinos were strengthened after the tau particle was discovered in 1975 at Stanford Linear Accelerator Center—Lawrence Berkeley Laboratory during electron and positron annihilation [61]. The DONUT(Direct Observation of the Nu Tau) collaboration was an experiment located at FERMILAB to detect the tau neutrinos using a 800 GeV accelerated proton beam from the decay of charmed mesons [52]. The tau neutrinos are produced as a result of decay of D_s mesons into τ and $\bar{\nu_{\tau}}$, and the subsequent decay of τ into ν_{τ}. The neutrinos were made to interact with the emulsion targets and out of a total of 213 neutrino interactions, only four were registered as the tau neutrino interactions. The probability of these interactions occurring from background events were low, therefore, these events were accepted as charged current interactions for tau neutrinos [52].

1.2 Standard Model

The standard model contains all of the elementary particles and is an exceptional tool in classifying interactions of these particles with matter. The standard model (SM) was first formulated in the 1970s but with the passage of time new particles were added to the model [50]. The standard model even though very comprehensive still stands incomplete due to unknown properties of the neutrinos.

The standard model consists of 17 elementary particles which are classified into two groups based on their intrinsic quantum spin: Fermions and Bosons. Fermions are particles with non integer spin of $\hbar(1/2, 3/2, ..)$ and are building blocks of matter interacting through the fields, while bosons are particles with integer spin of $\hbar(0, 1, 2, ..)$ and are force carriers that mediates interaction among fermions [33]. Fermions are classified into two further categories: leptons and Quarks. Quarks form composite particles binded by strong force known as hadrons such as the proton and neutrons. Leptons on the other hand are weakly interacting particles which consists of charged and uncharged particles. Charged leptons include electron, muon, and tau; while uncharged leptons includes electron neutrino, muon neutrino, and tau neutrino. Initially, neutrinos were thought to be mass-less in the standard model until SNO experiment successfully measured the neutrino oscillations which indicated a flavor change during propagation and a non zero mass [9]. Neutrinos even though has mass, its absolute value is still not determined due to experimental constraints.

Bosons are usually force carriers which transmit interactions. The standard model have five different guage bosons; $W^{\pm}$ boson, Z boson, photon, gluon, and higgs boson. In standard model, quarks, leptons, and guage bosons obtain their mass through higgs mechanism, which gives rise to another field with a single neutral particle, the Higgs Boson [41] [65].

1.3 Solar Neutrino Problem

Neutrinos are messengers that due to their low cross-section area can travel astronomical distances without interacting with matter [3]. They are produced in galactic events such as a

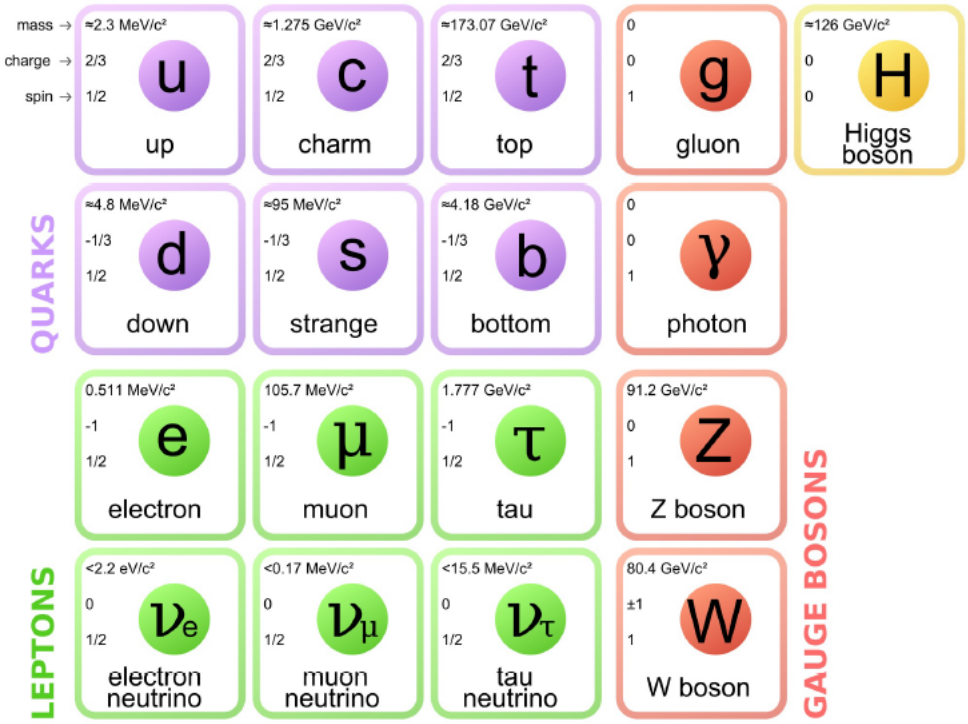

Figure 1.1: Most upto date Standard model of Particle Physics consisting of Fermions and Bosons, and the recently discovered Higgs Boson [45].

supernova, or from the fusion processes occurring inside the sun and within other stars. Moreover, neutrinos are also produced within the earth's crust from U^{238}, Th^{232}, and K^{40} decay chains, as well from the decay decay of radioactive isotopes [46].

One of the biggest neutrino flux on earth is from the sun. With the detection of neutrinos in 1956, motivation began to physically observe and determine the ν_e flux coming directly from sun [20]. Neutrinos were believed to be the only particle that can help understand the nuclear fusion processes occurring in the core of the sun, which were believed to be the reason behind the radiant energy [32]. The fusion reactions within the sun are now well understood and they mostly come from the interaction between the two protons, known as the *pp* chain [70], and the interactions from carbon-nitrogen-oxygen also commonly as the CNO cycle [6]. The dominant cycle the solar flux comes from the *pp* cycle which constitutes to about 99 % of the total solar flux and CNO cycle constitutes to about 1% of the total solar flux [6]. Among these two cycles, series of further reaction takes place which produce a wide spectrum of solar neutrinos with

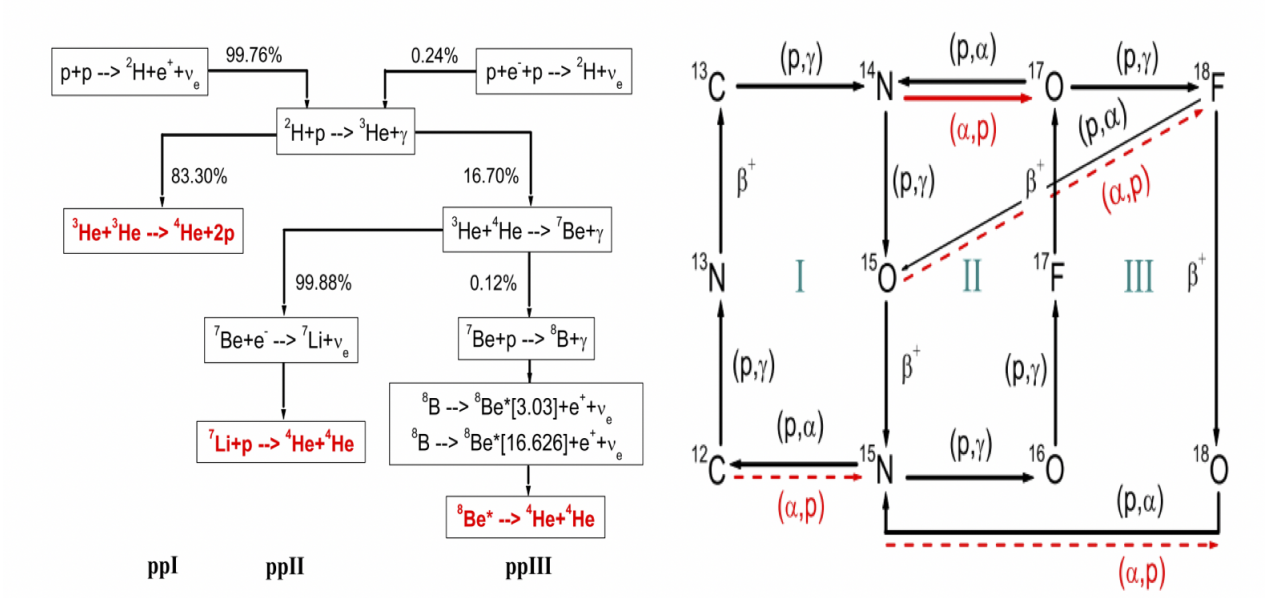

Figure 1.2: The three branches of the proton-proton fusion chain of the solar neutrino flux shown on left. The three branches of the CNO cycle shown on the right [70].

different cross sections and different energies. Most of these reactions occur within the core of the sun but due to the low interaction cross section, they leave the sun immediately almost uninterrupted as opposed to a photon created in the core of the sun, which can take up to thousands of years to reach the surface of the sun. The flight of solar neutrinos after leaving the surface of the earth takes about eight minutes before reaching the earth.

Most recent energy composition of the solar neutrinos is shown in figure 1.3. Neutrinos coming from the pp chain even though the most dominant, have the lowest energy. Neutrinos from the CNO cycle and the pep and hep chain, even though have lower flux, dominate the high energy solar neutrino spectrum [6].

In the 1960s, solar models mentioned in section 1.3 had been developed with a lot of confidence which led to to the first experiment to measure the solar neutrinos led by R. David in 1968 [32]. The experiment was designed from the developed solar models with estimated flux and energy compositions of the neutrinos. Most recent energy composition of the solar neutrinos is shown in figure 1.3.

R. Davis built two 500 gallon tanks of of tetracholorethylene(C_2Cl_4). This detector was situated in a gold mine, 2300 feet below the surface of the earth [36]. The interaction of solar

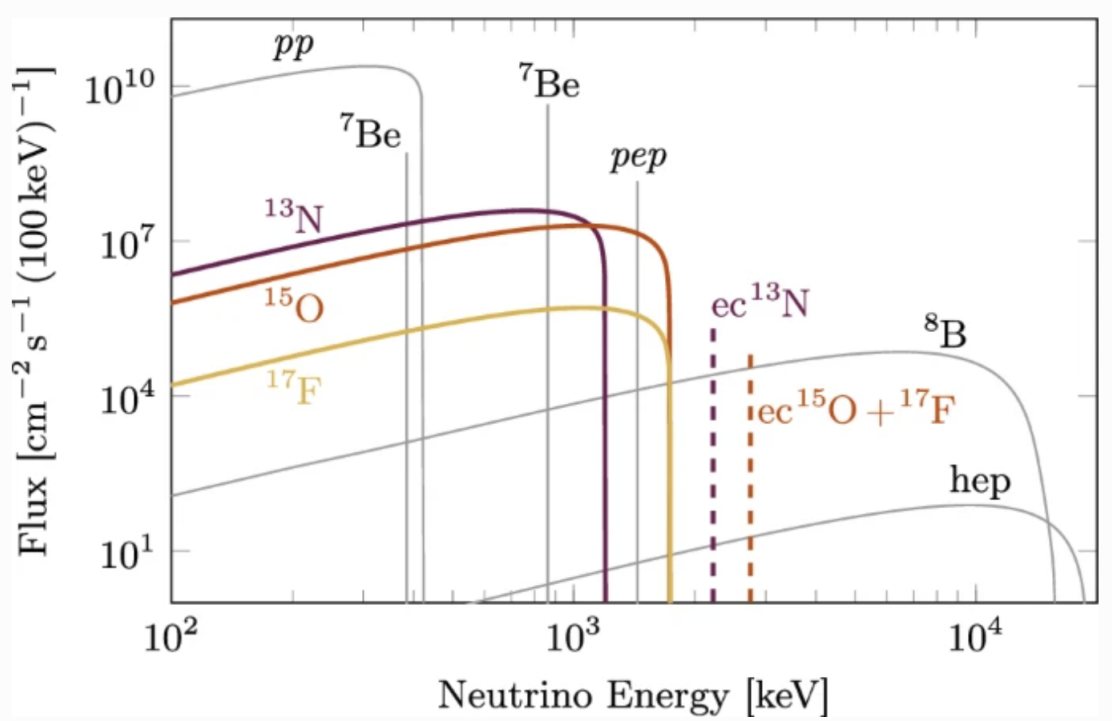

Figure 1.3: Solar neutrino flux versus the energy of the neutrinos for all fusion processes within the sun[6].

neutrino with chlorine would turn chlorine into an argon atom, as shown in Equation 1.4.

$$\nu_e + Cl^{37} \rightarrow Ar^{37} + e^- \tag{1.4}$$

The detector successfully measured the total flux of neutrinos above 0.814 MeV [31], however, the measured neutrino flux was only one third of the expected flux. The discrepancy between the measurements and the theory was not a result of any inconsistency or error within the experiment but was rather due to an incomplete theoretical model. Similar inconsistencies were measured by other leading experiments like Kamiokande [66] [49], SAGE [5], and Gallex [34] [14]. This problem persisted until SNO experiment measured all three different flavors of neutrinos and got the expected flux which solidified the neutrino oscillations theory [8].

1.3.1 SNO Experiment

In 1984 Professor Herb Chen suggested the use of heavy water (D_2O) for the measurement of all three flavors of neutrinos and potentially solve the solar neutrino problem. The detector was

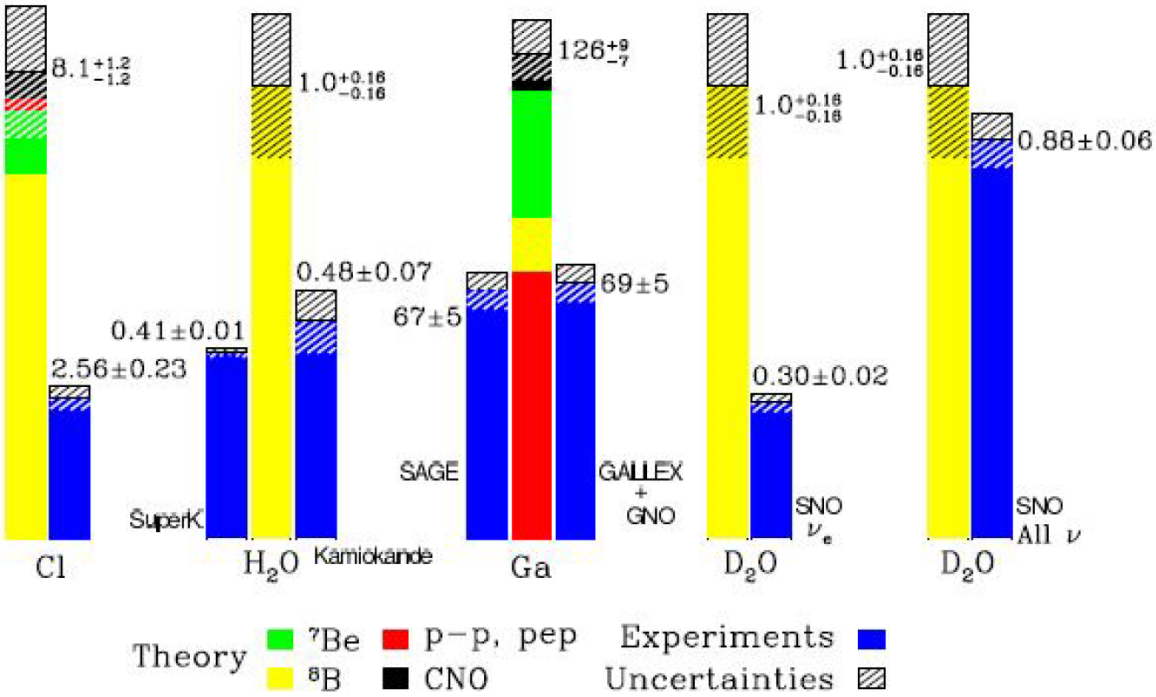

Figure 1.4: Discrepancies within the solar flux shown based on different results of different experiments. SNO measured the total flux while measuring all three flavors of the neutrinos.

built underground in a mine in Sudbury, Canada. The actual depth was 6800 feet below surface and consisted of large Acrylic vessel consisting of 1000 tonnes of Heavy water (D_2O) housed in a 7000 tonnes of ultra-purified water cavity [9]. The Acrylic vessel (AV) is surrounded by a large geodesic structure called the PSUP, which held approximately 10000 PMTs, used to view the events within the AV and the water volume between the PSUP and AV [9]. Additionally, hold up ropes were installed to prevent the AV from sinking due to the downward buoyant force exerted from the heavy water on to the light water due to a higher density.

The neutrino reactions with the deuterium is as follows:

$$\text{Charged Current(CC)} : \nu_e + d \rightarrow e^- + p + p \tag{1.5}$$

$$\text{Neutral Current(NC)} : \nu_x + d \rightarrow \nu_x + n + p \tag{1.6}$$

$$\text{Elastic Scattering(ES)} : \nu_x + d \rightarrow \nu_x + e^- \tag{1.7}$$

The charged current(CC) interactions are only sensitive to electron neutrinos and elastic scattering(ES) is mainly dominant by the electron neutrinos as well [8]. The neutral current interactions are equally sensitive to all three flavors of the neutrinos [8]. In the first phase SNO only measured interactions from the neutral current by observing the neutron capture from the deuterons. During the second phase of the experiment, 2000 Kg of NaCl was added which enhanced the neutron detection efficiency and separated the NC and CC signals, while improving the accuracy of ν_x and ν_e measurement [8].

In 2001 after the first phase of the experiment, SNO reported evidence of neutrinos changing flavors on the way to the earth and the measured flux was in agreement with the solar model predictions [58]. The results concluded that the electron neutrino flux is only a third of the total flux measured which confirmed that the rest of the solar flux transformed into different neutrino flavors; a theory known as neutrino oscillations theory and ruled out the possibility of neutrinos being mass-less. SNO proceeded with other phases of the experiment in order to improve the statistical and systematic uncertainties. The success of SNO experiment led to the formation of a successor experiment; SNO+, which is currently looking to observe neutrinoless double beta decay [11].

1.4 Neutrinoless Double Beta Decay

In a beta decay, the neutrons in a nuclei are converted into protons while emitting an electron and an anti-electron neutrino. The down quark of the neutron is converted into the up quark producing a proton. The double beta decay is a rare radioactive decay which was first proposed by M Goeppert-Mayer in 1935 [47]. In which two beta decay occurs simultaneously with the formation of two electrons, two protons, and two anti-neutrinos. It changes the atomic number(Z) of the atom by two due to the formation of two protons while keeping the atomic mass(A) the same:

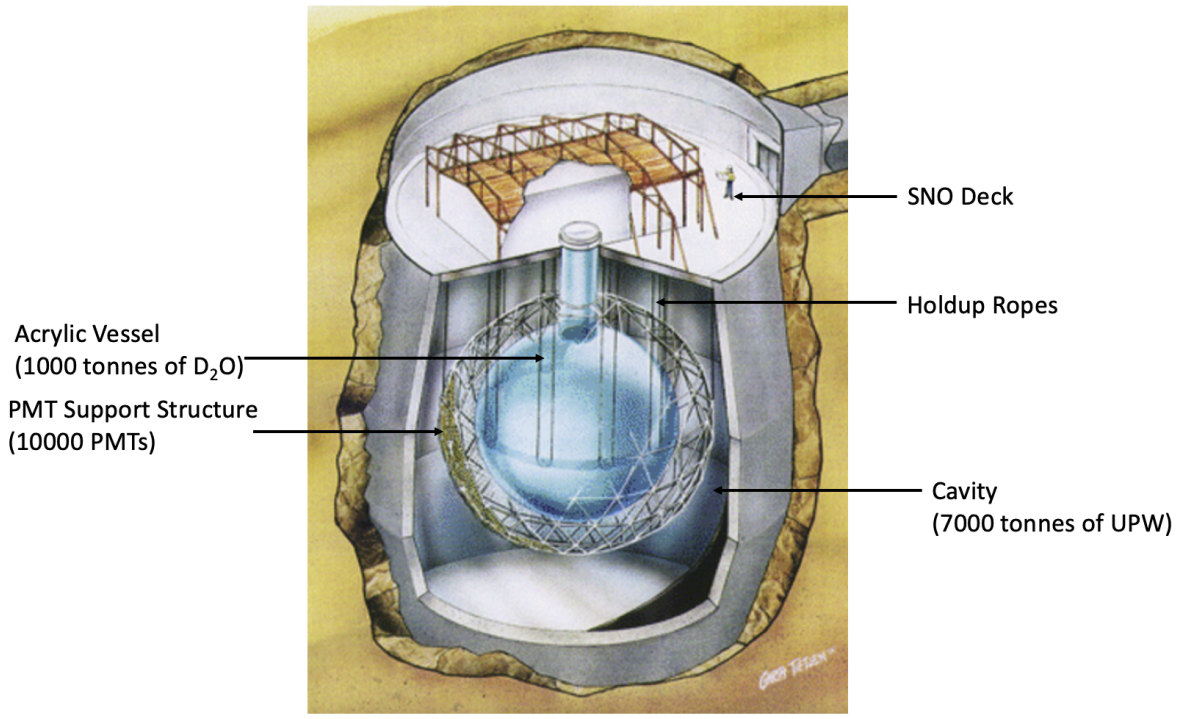

Figure 1.5: Schematic of the SNO detector built in 1990s to measure neutrino oscillations.Consisting of 1000 Tonnes of Heavy water(D_2O viewed by 10000 PMTs and was housed in a large UPW cavity [58]

$$(A, Z) \rightarrow (A, Z + 2) + 2e^{-} + 2\bar{\nu}_e \tag{1.8}$$

Double beta decay is one of the very rare kind of decay as it is predicted to happen in only 36 isotopes and have been experimentally observed in 11 isotopes [46]. Moreover, it can only occur in atoms with nuclei of even atomic and mass number and for these nuclei a single beta decay is energetically forbidden. The transition energy also known as the Q value of this process is defined as the difference of mass of the initial isotope to the sum of masses of the decay products. The equation is as follows:

$$Q_{2\nu\beta\beta} = m(A, Z) - \left[m(A, Z + 2) + 2m_e\right] \tag{1.9}$$

For a double beta decay, reactions with higher Q values are preferred. Another important factor that needs to be considered is the rate of decay for this process. The rate of decay is given by

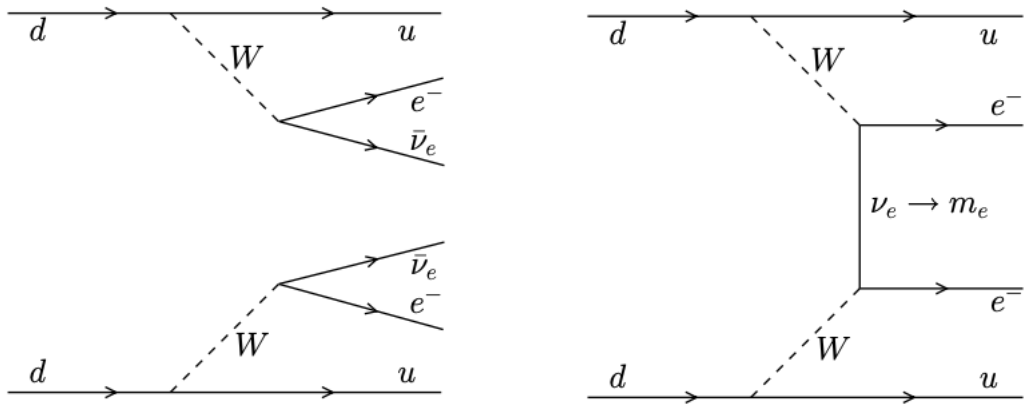

(a) (b)

Figure 1.6: (a) Feynman diagram of 2νββ decay showing two protons, two electrons, and two anti-electron neutrino (b) Feynman diagram of 0νββ decay showing two protons and two electrons without the emission of anti-electron neutrinos [46]

equation 1.10.

$$\Gamma^{1/2}_{2\nu\beta\beta} = G^{2\nu} \cdot |M^{2\nu\beta\beta}|^2 \tag{1.10}$$

Where the $G^{2\nu}$ is the phase space integral which scales the transition energy or the Q value while the $M^{2\nu}$ is the nuclear matrix element.

Discovery of double beta decay gave way to a proposed radioactive decay known as neutrinoless double beta decay in which a neutron is converted into protons and only two electrons are emitted without the emission of two electron anti-neutrinos. It was first proposed by W.H Furry in 1939 which suggested the Majorana nature of neutrinos i.e. that neutrino is its own antiparticle [44]. If neutrino is its own antiparticle, then the anti-electron neutrinos will be emitted but would get absorbed by one another, transferring all the energy to the electrons. Moreover, this decay will also exhibit lepton number violation which will give information beyond the standard model and will also help determine the anti-matter matter asymmetry of the universe.

$$(\mathrm{A}, \mathrm{Z}) \rightarrow (\mathrm{A}, \mathrm{Z}+2) + 2\mathrm{e}^{-} \tag{1.11}$$

The decay rate of this reaction is as follows:

Isotope	Q Value(Mev)	Natural Abundance(%)	$T^{1/2}_{0\nu\beta\beta}$yr	Experiment	Ref
^{48}Ca	4.272	0.187	$> 5.8 \times 10^{22}$	ELEGANT VI	[68]
^{82}Se	2.995	9.2	$> 2.4 \times 10^{24}$	CUPID-0	[22]
^{76}Ge	2.039	7.8	$> 1.8 \times 10^{26}$	GERDA	[7]
^{100}Mo	3.034	9.6	$> 1.5 \times 10^{24}$	CUPID-Mo	[18]
^{116}Cd	2.805	7.49	$> 1.0 \times 10^{23}$	NEMO-3	[19]
^{130}Te	2.52	34.5	$> 5.9 \times 10^{24}$	SNO+, CUORE	[40][11]
^{136}Xe	2.457	8.96	$> 5.0 \times 10^{25}$	EXO-200	[15]
^{150}Nd	3.367	5.6	$> 1.8 \times 10^{22}$	NEMO-3	[17]

Table 1.1: Double beta decay isotopes with their most recent $0\nu\beta\beta$ half lives, along with the experiments that measured them [48][46].

$$\Gamma^{1/2}_{0\nu\beta\beta} = G^{0\nu} \cdot |M^{0\nu\beta\beta}|^2 \cdot < m_{\beta\beta} >^2 \tag{1.12}$$

Where, $G^{0\nu}$ is the space factor which is determined by the q value of the isotope used and $M^{0\nu\beta\beta}$ is the nuclear matrix vector and is completely model dependent. The decay rate $\Gamma^{1/2}_{0\nu\beta\beta}$ is directly proportional to the effective majorana mass squared $< m_{\beta\beta} >^2$. If $0\nu\beta\beta$ is observed, it can help determine the effective mass of the neutrino, otherwise the measurement of the life times can help set a limit on the mass scale of a neutrino.

$$< \mathrm{m}_{\beta\beta} >^2 = | \sum_{\mathrm{k}=1}^{3} \mathrm{U}_{\alpha\mathrm{k}} |\mathrm{m}_\mathrm{k}> |^2 \tag{1.13}$$

The $\mathrm{m}_{\beta\beta}$ is the effective majorana mass which is written as a sum of the mass eigenstates, $|\mathrm{m}_\mathrm{k}>$ $(\mathrm{k} = 1, 2, 3)$. Where $\mathrm{U}_{\alpha\mathrm{k}}$ is the Pontecorvo Maki Nakagawa Sakata(PMNS) mixing matrix and alpha equals ν_e in this case. Figure 1.7 shows the $2\nu\beta\beta$ spectrum as well as the high energy $0\nu\beta\beta$ sharp peak.

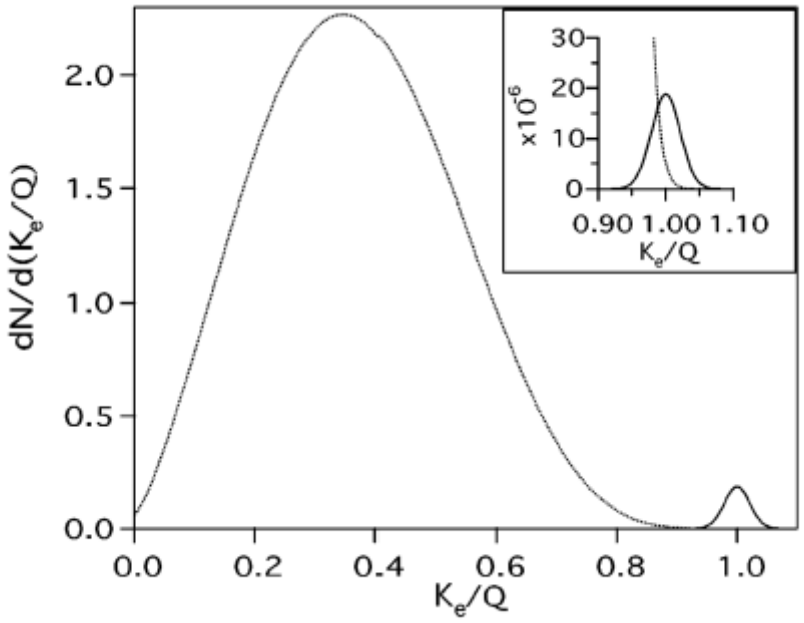

Figure 1.7: Energy spectrum of $0\nu\beta\beta$ and $2\nu\beta\beta$. $0\nu\beta\beta$ is the short peak shown on the right and $2\nu\beta\beta$ is the continuous spectrum shown on the left [38]

Chapter 2

SNO+ Experiment

2.1 SNO+ Detector

SNO+ experiment is a multipurpose scintillator detector located 6800 feet underground in the Vale Creighton mine near Sudbury, Ontario. SNO+ acquired the detector from the historic SNO experiment which was designed to detect neutrinos and observe all three neutrinos flavors [9]. SNO experiment ran successfully from 1999 to 2006 and measured the expected solar flux which confirmed the neutrino oscillation theory and earned it a Nobel prize in 2015. This success led to the establishment of SNOLAB; a level 2000 clean lab facility which prevents radioactive contamination from the mine dust and surrounding rocks to ensure low background sensitivity for all the experiments, including SNO+. SNOLAB now hosts several experiments on dark matter, neutrino physics, low background counting experiments, etc. Figure 2.1 shows the schematic of SNOLAB.

The depth of SNOLAB provides a rock overburden of 2070m which provides effective shielding from the cosmic muon flux that corresponds to 6010 metre of equivalent water [39]. Shielding from backgrounds is necessary in order to see the rare interactions required by sensitive experiments located at SNOLAB. The Table 2.1 shows the muon flux and the water equivalent depth for various underground labs in the world. SNO+ inherited most of the detector from the original SNO experiment but due to different physics goals, the detector was upgraded and

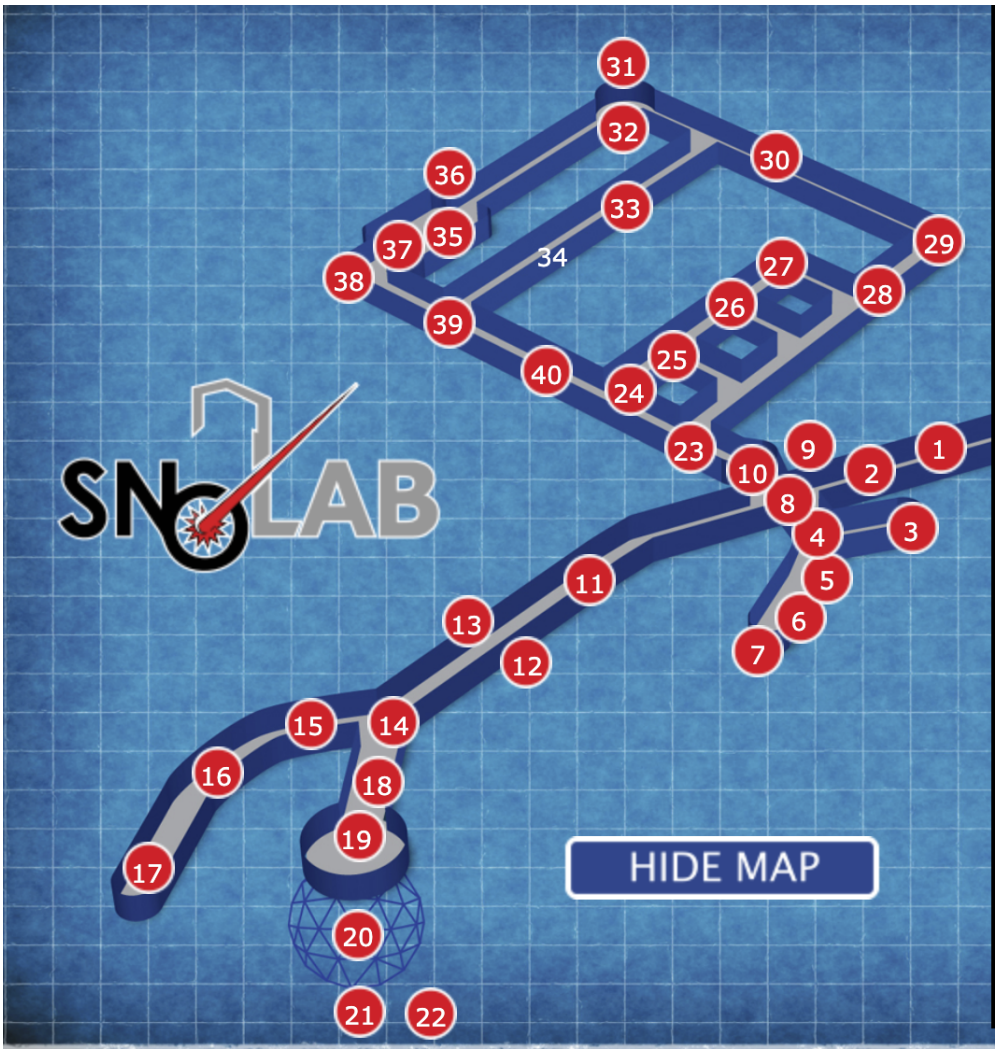

Figure 2.1: SNOLAB's virtual map. Pointers 20, 21, and 22 indicate the location of the SNO+ detector. Pointers 15 and 16 points towards the water and scintillator purification plant [1].

made compatible.

The components of the detector are as follows:

- **Cavity:** SNO+ detector is housed in a 22 metre wide and 34 metre tall cavity which is submerged in ultra pure water to provide effective shielding against the radiations from the surrounding rocks and emanation from detector components. The cavity consists of two components: Outer cavity and the Inner cavity. The inner cavity holds 1700 tonnes of ultra pure water and consists of the volume between the Acrylic Vessel (AV) and the Photo-multiplier Structure (PSUP). The external cavity consists of 5700 tonnes of ultra-

Site	Total flux $cm^{-1}sec^{-1}$	Depth km.w.e.
WIPP	$(4.77 \pm 0.09) \times 10^{-7}$	1.585 ± 0.011
Soudan	$(2.0 \pm 0.20) \times 10^{-7}$	1.95 ± 0.15
Kamioka	$(1.58 \pm 0.21) \times 10^{-7}$	2.05 ± 0.15
Boulby	$(4.09 \pm 0.15) \times 10^{-8}$	2.80 ± 0.015
Gran Sasso	$(2.58 \pm 0.30) \times 10^{-8}$	3.10 ± 0.2
Frejus	$(5.47 \pm 0.10) \times 10^{-9}$	4.15 ± 0.2
Homestake	$(4.40 \pm 0.10) \times 10^{-9}$	4.30 ± 0.2
Sudbury	$(3.77 \pm 0.41) \times 10^{-10}$	6.011 ± 0.1

Table 2.1: Summary of the Muon flux of various underground laboratories and their respective metres water equivalent depth [59]

pure water (UPW) which is the volume between the PSUP and the cavity walls. There is a UPW plant located at SNOLAB which is used to purify water for the cavity (see section 3.9). SNO+ uses the same ultra-pure water purification plant that was developed for the SNO experiment but was upgraded for smooth operations of SNO+.

- **Acrylic Vessel (AV):** The detector consists of a transparent 12 metre diameter Acrylic vessel(AV) which is 5.5 cm thick. The AV contains active medium, a hydrocarbon liquid Alkylbenzene (LAB) as a main solvent and 2,5 diphenyloxale (PPO) as a flour. A total of 780 tonnes of LAB is loaded in the AV with a PPO concentration of 2g/L. Finally, the AV will be loaded with about 4 tonnes of tellurium as the main double beta isotope. Scintillator and tellurium purification plants(see section 3.10) have been developed at SNOLAB to facilitate the purified filling of LAB and tellurium into the detector.

- **Photomultiplier Tubes (PMT) and PMT Support Structure (PSUP):** The AV is viewed by 9300 photo-multiplier tubes (PMTs) situated in a $\sim$ 18 metre geodesic stainless steel structure (PSUP) facing towards the centre of the vessel. PSUP is approximately 8.9 metre in radius and consists of triangular panels of PMTs, each panel holds 500 PMTS and the electronics is grouped into crates and the entire PSUP has a total of 19 crates. PMTs are the main detection mechanism for SNO+ as they account for all the events that happen within the AV and the inner cavity. Before the beginning of SNO+, the

PMTs from the SNO experiment were serviced and the previously broken PMTs were repaired and reinstalled.

- **Hold-Up and Hold-Down Ropes:** SNO experiment used heavy water (D_2O) which had a density of 1.11 g/cm^3 generating buoyancy force acting downwards [9]. To mitigate the effect of the force, hold up ropes were installed. However, SNO+ uses LAB that has a density of 0.85 g/cm^3 which means that once the AV is filled with LAB, it will have an upwards buoyancy due to the ultra pure water in the cavity. In order to compensate for this effect, 20 hold down ropes were installed which were anchored to the cavity floor [11].

- **Cover-gas system** SNOLAB has a radon content of 123Bq/m^3 while SNO+ detector has an ingress budget of 5.5 atoms/m^3 of air [11]. Cover-gas systems containing pure nitrogen gas are in place to prevent radon diffusion into the detector. SNO+ has two cover-gas systems; one which includes the volume above the scintillator in the AV and second one includes volume between the cavity water and the deck floor. Both systems are in place to maintain the background levels of the UPW and LAB in the detector. The LAB cover-gas system consists of a Universal Interface (UI) and three bags filled with nitrogen gas acting as a barrier against radon contamination and a mechanism to accommodate the pressure changes in the mine. This is done by inflating and deflating the bags to allow up to 360L of allowable expansion or contraction volume that can compensate for sudden pressure changes in the mine and wouldn't allow radon dispersion into the detector [11]. The cavity cover-gas system includes a flow-through system which constantly flushes nitrogen gas at 5 LPM, this system was acquired from the SNO experiment [26]. The AV cover gas system is also connected to a radon monitor that continuously monitors the background levels within the UI.

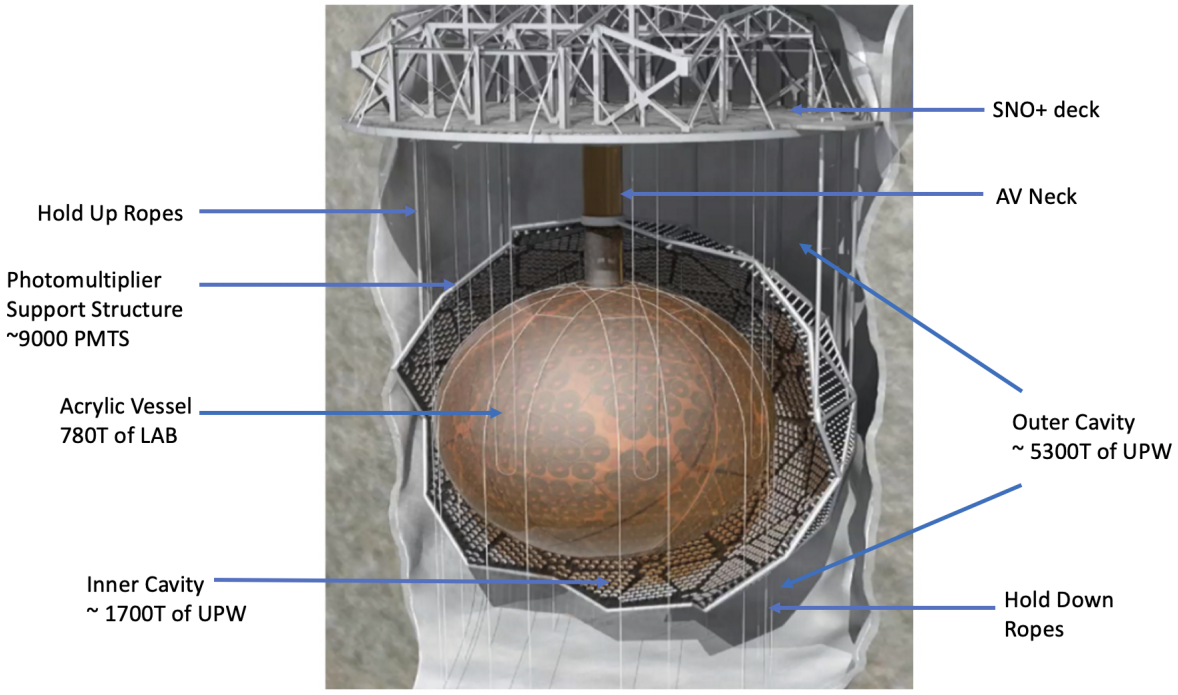

Figure 2.2: Pictoral representation of SNO+ Detector located underground showing all the essential components [11]

2.2 Phases of SNO+

The phase of SNO+ experiment is determined by the active medium within the AV. SNO+ experiment is divided into three main phases: water phase, scintillator phase, and tellurium phase. All these three phases allows a wide variety of exotic physics searches. The three phases of SNO+ and their respective physics goals are described in Table 2.2 below:

2.2.1 Water Phase

In the first phase of the experiment, the acrylic vessel was filled with Ultra pure water. The water phase of the experiment ran from may 2017 to July 2019 and it was crucial for the other phases because it allowed optical calibration of the detector and determined the PMTs response. Moreover, external background contributions coming from the leaching of AV, ropes, PSUP, PMTs, mine walls were characterized. At the end of the water phase, LAB-PPO was added to the AV via volume displacement.

2.2.2 Partial Fill Phase

The AV fill was a long and hefty process which took several years to finish. The partial fill phase officially began when LAB and PPO went into the AV and ended the water phase of the experiment in 2019. It took about two years to fill 780 tonnes of LAB into the AV by volume displacement. The filling was stopped twice for prolonged periods of time, firstly from July 2019 - October 2019 due to problems in the scintillator purification plant, and secondly from April 2020 to August 2020 due to COVID-19 pandemic. Both these regions were termed as stable periods where several background analysis were carried out (see Chapter 6).

2.2.3 Scintillator Phase

Since Since April 2021 to the time of writing this thesis, SNO+ was in the pure LAB phase of the experiment. A total of 780 tonnes of pure LAB was loaded into the AV along with a PPO concentration of 1 g/litre of LAB. PPO is still being added to achieve the target level of 2 g/L. During this phase, background will be characterized and the optical model will be verified. The background levels will be very low due to the high purity content of LAB. This will allow observance of low energy Solar neutrinos, Reactor anti-neutrinos, and Geo anti-neutrinos. This phase of the experiment is suppose to last for about a year until the addition of tellurium.

2.2.4 Tellurium Loaded Phase

The most exciting part of the experiment will begin when ^{130}Te will be added to the AV. It is the main beta decay isotope and once it is added, the search for neutrino-less double beta decay will begin. The proposed concentration of tellurium is 0.3 % which corresponds to about 4 tonnes in the AV [24]. Tellurium is a naturally occurring element which has a high natural abundance of 34 % therefore does not require any enrichment. However, purification standards are the same as for all the other mediums entering the AV. In order to ensure low backgrounds in tellurium, a tellurium purification plant is being built at SNOLAB to remove any radioactive contamination. The loading of tellurium is achieved by adding telluric acid to a butane diol

Target	Phase			Limit
	H_2O	LAB	Te	
Nucleon decay	✓			Measured proton and neutron decay lifetimes
Reactor Antineutrinos	✓	✓		Measure neutrino oscillation parameters
Geo Antineutrinos	✓	✓		Understand Earth's thermal history
Supernova Neutrinos	✓	✓	✓	Study Supernova neutrinos
Solar Neutrinos	✓	✓	✓	Measure solar neutrinos from pep chain and CNO cycle
$0\nu\beta\beta$			✓	Determine if neutrino is a Majorana particle

Table 2.2: Physics goals of SNO+ summarized for each perspective phase[51].

solution and then loading the mixture into the detector. SNO+ has the capability of looking for $0\nu\beta\beta$ at different concentrations of the tellurium isotope into the detector. This phase of the experiment is suppose to last for a few years in order to reach the required neutrino mass sensitivity.

2.3 Physics Goals for SNO+

2.3.1 Nucleon Decay

The water phase of the experiment lasted for over two years. In this phase, SNO+ was able to achieve the background target levels initiating the search for invisible modes of nucleon decay. Nucleon decays that deposit direct energy by the decay products such as positrons, pions, and koans, have not been observed, therefore, SNO+ aimed to look for decay modes that do not directly deposit energy but instead leaves the nucleus in an excited state which will then produce a detectable signal. SNO+ searched for invisible decay modes of ^{16}O. Upon a neutron decay, ^{16}O goes into an excited state of $^{15}O^*$, which 44% of the time emits a 6.18 MeV γ and 2% of the time emits a 7.03 MeV γ. Secondly, upon a proton decay ^{16}O goes into an excited state of $^{15}N^*$, which 41% of the time emits a 6.32 MeV γ along with 7.01, 7.03, and 9.93 MeV γ's produced 2%, 2%, and 3% of the time, respectively [13].

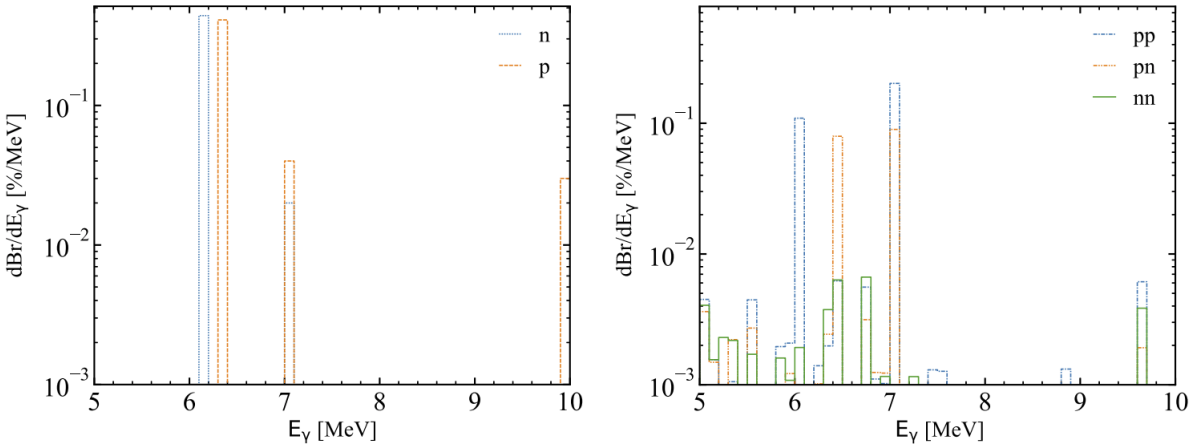

Figure 2.3: Gamma ray spectrum of invisible modes of O^{16} for single nucleon (left) and dinucleon decay (right) [13].

	Spectral Analysis	Counting Analysis	Existing Limits
n	2.5×10^{29} y	2.6×10^{29} y	5.8×10^{29} y [16]
p	3.6×10^{29} y	3.4×10^{29} y	2.1×10^{29} y [10]
pp	4.7×10^{28} y	4.1×10^{28} y	5.0×10^{25} y [23]
pn	2.6×10^{28} y	2.3×10^{28} y	2.1×10^{25} y [67]
nn	1.3×10^{28} y	0.6×10^{28} y	1.4×10^{30}y[16]

Table 2.3: Lifetime limits of invisible modes of nucleon decay at 90% CI for both spectral and counting analysis, including all the statistical and systematic uncertainties. Existing limits from various experiments are also shown [13].

Invisible Di-nucleon modes also exist where two nucleon decays from ^{16}O and leaves the nucleus in an excited state. Three different modes of decays from the oxygen molecule exists that create unstable nuclei $^{14}O^*$, $^{14}N^*$, and $^{14}C^*$ after *nn*, *pn*, and *pp* decays, respectively. The *pn* decay produces a 6.45 MeV γ at 7.7 % and 7.03 MeV γ at 8.9%, while *pp* produces a 6.09 MeV γ at 10.9 % and 7.01 MeV γ at 20.1% probability . The *nn* decay produces a series of gammas ranging between 5 MeV and 9 MeV with a branching ratio of 4.53% [13].

SNO+ observed all of the invisible nucleon decay modes of ^{16}O. The proton decay mode of lifetime of 3.6×10^{29}y shows a significant improvement from the SNO measurement while the neutron decay limit of 2.5×10^{29}y is weaker than the KAMLAND measurement. Moreover, the limits set by di-nucleon modes of *pp* and *pn* are 4.7×10^{28}y and 2.6×10^{29} y respectively. These limits show an improvement of 3 orders of magnitude to the existing limits while *nn* does not

show any improvement [13].

2.3.2 Reactor Anti-neutrinos

The nuclear fission within the nuclear reactor emits electron anti-neutrinos as a product of the beta decay of fission products. The anti neutrino flux of each reactor is carefully measured and is dependent upon the fuel used. In SNO+, anti-neutrinos are detected by an inverse beta decay reaction with anti neutrinos greater than 1.8 MeV:

$$\mathrm{p} + \bar{\nu}_{\mathrm{e}} \rightarrow \mathrm{n} + \mathrm{e}^{+} \tag{2.1}$$

The positron annihilates with another electron in the detector producing a scintillation light also known as the prompt signal. The neutron travels within the detector for another 220 μs before it is captured by another proton and produces a characteristic 2.22 MeV gamma which is detected by the detector. The delayed coincidence signal which are separated by a definite time allows for a detection mechanism of the $\bar{\nu}$s in SNO+. The anti-neutrino energy is calculated by:

$$\mathrm{E}_{\bar{\nu}_{\mathrm{e}}} \simeq \mathrm{E}_{\mathrm{prompt}} + (\mathrm{m}_{\mathrm{neutron}} + \mathrm{m}_{\mathrm{proton}}) - \mathrm{m}_{\mathrm{electron}} \simeq \mathrm{E}_{\mathrm{prompt}} + 0.8\mathrm{MeV} \tag{2.2}$$

Where $\mathrm{m}_{\mathrm{neutron}}$, $\mathrm{m}_{\mathrm{proton}}$, and $\mathrm{m}_{\mathrm{electron}}$ are the masses of neutron, protons, and electrons. The location of SNO+ allows for detection of anti-neutrinos from three different nuclear reactors. SNO+ is about 240 km from Bruce nuclear station and about 330 km from Darlington and Pickering nuclear reactors. A total flux of 90 reactor anti-neutrino events are expected from these reactors with an expected 40% signal contribution from Bruce and 20% from reactors in Darlington and Pickering and the rest 40 % from either USA or elsewhere [39] .

The known flux and a comprehensive understanding of the reactor anti-neutrino spectrum allows for a precise measurement of the neutrino oscillation parameters. The neutrinos from the 240 km and 330 km reactors induce a very clear neutrino oscillation pattern which gives a high sensitivity on $\Delta \mathrm{m}^2_{12}$ oscillation parameter.

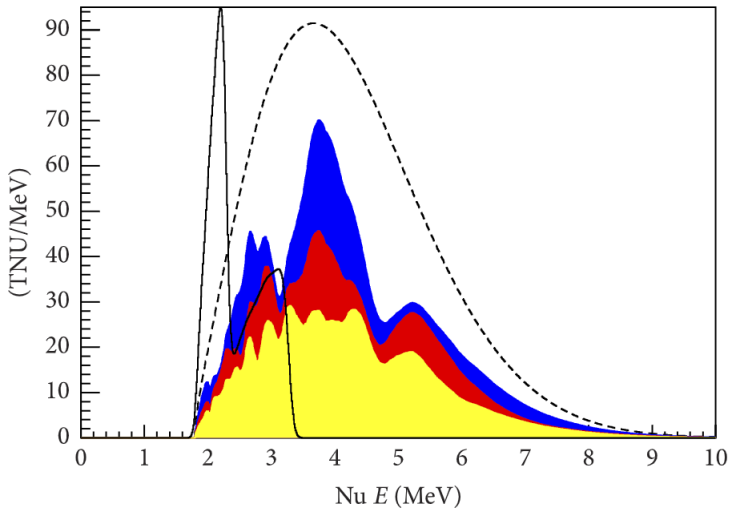

Figure 2.4: Expected anti-neutrino spectrum for SNO+. Non-oscillated reactor spectrum (dashed line) and geo neutrino spectrum(solid line). Three stacked oscillated reactor spectrum are shown: Bruce at 240 km(blue), Darlington and Pickering at 330 km(red), and all other reactors(yellow) [39].

2.3.3 Geo Neutrinos

The long lived isotopes present within the earths crust undergo radioactive decays and emits anti neutrinos which provides vital information about the thermal history of the earth. The decay process only emits electron anti neutrinos and they are called as "Geo Neutrinos". The major flux of geo neutrinos come from the decay chains of ^{238}U, ^{232}Th, and ^{40}K. The decay processes of these long lived isotopes are shown below:

$$^{238}\mathrm{U} \rightarrow ^{206}\mathrm{Pb} + 8\alpha + 8\mathrm{e}^{-} + 6\bar{\nu}_{\mathrm{e}} + 51.7\mathrm{MeV} \tag{2.3}$$

$$^{232}\mathrm{Th} \rightarrow ^{208}\mathrm{Pb} + 6\alpha + 4\mathrm{e}^{-} + 4\bar{\nu}_{\mathrm{e}} + 42.7\mathrm{MeV} \tag{2.4}$$

$$^{40}\mathrm{K} \rightarrow ^{40}\mathrm{Ca} + \mathrm{e}^{-} + \bar{\nu}_{\mathrm{e}} + 1.31\mathrm{MeV} \tag{2.5}$$

The Geo-neutrinos can be detected in SNO+ via inverse beta decay reaction just like that mentioned in Eq 2.1 and their detection mechanism consists of the same coincidence signal used

for detecting reactor anti-neutrinos. The geo-neutrino spectrum is shown in Figure 2.4. The energy threshold for anti-neutrinos for inverse beta decay is 1.81 MeV, therefore, geo-neutrinos from the ^{40}K will not be detected due to their lower energy level.

2.3.4 Solar Neutrinos

The solar neutrino problem was resolved by SNO when it successfully measured the neutrino oscillations. There are still a lot of interesting solar neutrino measurements to be done. The water phase of the SNO+ experiment was able to measure the ^{8}B flux measurement. Elastic scattering of neutrinos was used to make this measurement as the scattered electrons direction is correlated to the direction of the incident neutrino. Therefore, the scattered electron produced cherenkov radiation that is directed away from the direction of the sun [12].

The flux is given as:

$$\Phi_{^8\mathrm{B}} = 5.95^{+0.75}_{-0.71}(\mathrm{stat.})^{+0.28}_{-0.30}(\mathrm{syst.}) \times 10^{6}\mathrm{cm}^{-1}\mathrm{s}^{-1} \tag{2.6}$$

The ^{8}B flux measurement is consistent with the SNO measurement and with that of KamLAND. SNO measured the ^{8}B flux as $\Phi_{^8\mathrm{B}} = (5.25 \pm 0.20) \times 10^{6}\mathrm{cm}^{-1}\mathrm{s}^{-1}$ with all the statistical and systematical uncertainties combined [12].

The pure LAB phase of SNO+ will allow sensitivity of below 0.5 MeV which will enable to see the low energy solar neutrino flux coming from the pep, CNO cycle, and low energy ^{8}B. Neutrinos from these cycles will be detected by the same electron scattering mechanism as was used in the ^{8}B measurement. The solar neutrino spectrum with all the dominant background is shown in figure 2.5.

2.3.5 Supernova Neutrinos

Supernova is referred to as a rapid collapse of a massive star. When this happens, neutrinos are emitted and 99% of the binding energy is transferred and carried by the neutrinos. During a supernova, a star emits more neutrinos within a span of seconds then it does in its entire

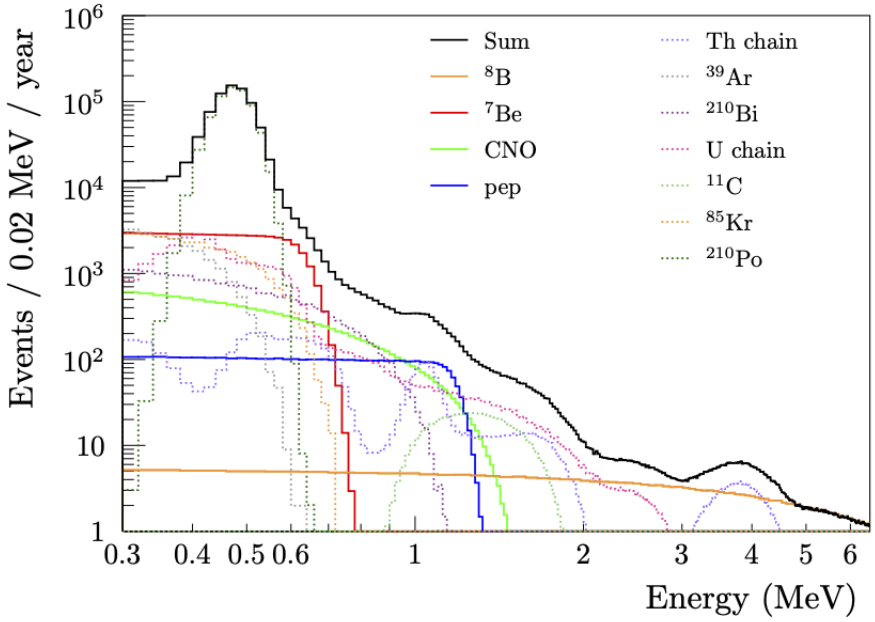

Figure 2.5: Expected solar neutrino fluxes along with backgrounds. Events shown in the LAB-PPO phase with 400 N_{hits}/MeV with a fiducial volume cut of 5.5 m radius [21] [39].

life. The location and specifications of SNO+ detector makes it an ideal detector to detect these neutrinos and even supernovas at large distances will produce a big neutrino flux for the detector. Supernova neutrino astronomy is motivated by observation of 24 $\bar{\nu}_e$ events detected through through inverse beta decay reaction from the collapse of SN1987A that happened at a distance of 50 kpc [39]. The neutrino flux expected from a supernova consists of all three flavors with their antiparticle counterparts with equal consistency between the flavors, particles and anti-particles.

Supernova neutrinos, if observed, can provide more information about the supernova and the propagation of neutrinos over long distances. SNO+ detector can detect all three flavors of supernova neutrinos and anti-neutrinos. This flavor separation will provide valuable information about the flavour changes and give more insights on neutrino oscillation parameters. Supernova neutrinos are expected to arrive at earth earlier than light, therefore, SNO+ will participate in the development of a Supernova Early Warning System(SNEWS). The goal is to provide an early alert for the astronomical community in regards to a supernova based on burst signals detected from neutrino detectors [39].

2.3.6 Neutrino-less Double Beta Decay

Discovery of double beta decay gave way to a proposed radioactive decay known as neutrino-less double beta decay in which two neutrons are converted into protons and only two electrons are emitted without the emission of two electron anti-neutrino. The main goal of SNO+ is to look for neutrino-less double beta decay and determine whether neutrino is a Majorana particle using ^{130}Te as the double beta isotope. The choice of tellurium as the isotope is due its high Q value (Q value = 2.536 MeV), and high natural abundance (34%), which will allow large amounts of tellurium to be added to scintillator without the need for any enrichment process. In order to achieve low backgrounds, purification process is necessary to remove any contamination, therefore, a purification plant is being developed at SNOLAB to facilitate in purifying tellurium before loading into the SNO+ detector. In phase I, 0.3% natural tellurium will be loaded in the detector which will mark the beginning of the 0νββ search. If required, a possibility of phase II exists in which the concentration of natural tellurium will be increased to 3%. ^{130}Te has a long half life of 7×10^{20}y which is significantly higher than other beta decay isotopes.

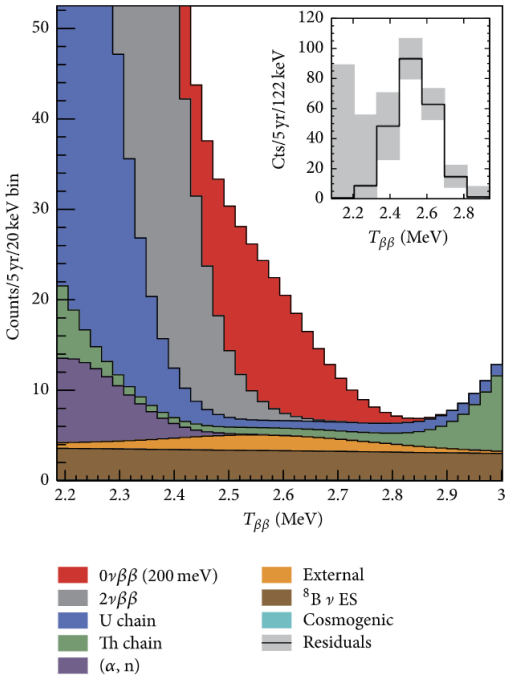

Figure 2.6: SNO+ 0νββ signal with stacked backgrounds for 5 year of data taking. With 0.3% natural tellurium loading and 200 Nhits/MeV light yield [39].

Figure 2.6 shows the expected $0\nu\beta\beta$ signal with 0.3% tellurium loading for over 5 years of data taking amongst the dominant backgrounds of SNO+. A fiducial volume cut is applied at 3.5m. At this fiducial cut a background rejection rate of $> 99.99\%$ for ^{214}Bi-Po and $> 98\%$ for ^{212}Bi-Po is assumed (See Chapter 3) [39]. The signal shown is for $m_{\beta\beta} = 200$ meV which corresponds to long half life of $T_{1/2}^{0\nu\beta\beta}$ of $\sim 1 \times 10^{25}$ years [39].

Chapter 3

SNO+ Backgrounds

3.1 Introduction

Physics goals of SNO+ includes detecting very rare signals which could be easily masked by any low energy interactions. Any no physics interaction that can fall under the region of interest (ROI) for SNO+ is labelled as a background event. In SNO+, backgrounds are classified into two categories: Internal and External background. The internal backgrounds consist of non signal interactions that occur within the Acrylic Vessel for the region r $<$ 6m or within the detector volume/medium. Each phase of SNO+ has different internal background target levels. The external backgrounds consists of events that doesn't occur within the AV but have the capability of propagating to the detector volume such as contamination coming from hold-up and hold-down ropes, PSUP, mine walls, and cavity water.

SNO+ stringent background levels requires constant and thorough *in situ* analysis and *ex situ* assays in order to monitor and maintain the background levels throughout the components of the detector. One of the major occurring radioactive background comes from the decay chains of long lived isotopes of ^{238}U and ^{232}Th. These radioactive isotopes are abundantly present in the notrite rock surrounding SNOLAB and have very long half lives of 4.47$\times$ 10^{9} yr and 1.4$\times 10^{10}$ yr, respectively [39].

Materials used to develop the SNO+ detector included careful selection of materials that

have low radioactive emanation in order to ensure low background contributions from detector components itself. Uranium and thorium levels are kept to a minimum, as slight ingress of these radioactive isotopes can break the secular equilibrium within the detector and cause the production of radioactive isotopes.

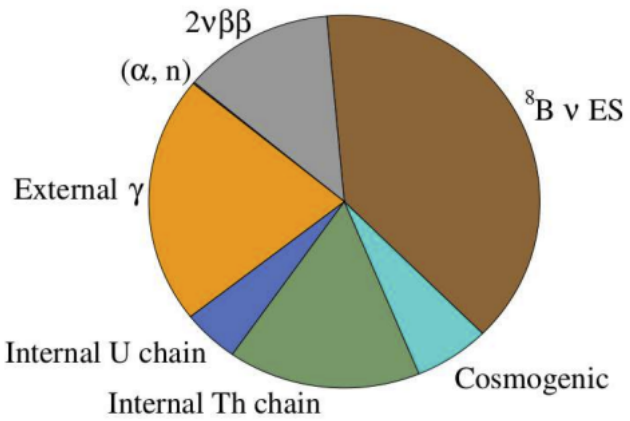

Figure 3.1: Expected background contribution from sources at 0.5 % ^{130}Te loaded phase for ROI after 1 year of data taking [62].

The background budget for SNO+ can be seen in figure 3.1 for the fiducial volume and ROI after 1 year of data taking. Several background mitigation strategies are underway to not only keep the background levels limited but also have successful mechanism that can characterize and reject these background events.

3.2 Cosmogenics

The location of SNO+ detector in a mine deep underground plays a crucial role in shielding SNO+ detector from cosmic rays. Being 6800 feet underground provides a 6000m water equivalent shielding which results in a muon flux of 3.77×10^{-10} μ cm^{-2}sec^{-1} corresponding to about 70 muons/day [59]. Despite being deep underground, the risk of cosmogenic activation of backgrounds still exists within the LAB and tellurium. LAB and tellurium are produced elsewhere and transported underground. During this process, cosmic rays can interact with the LAB nuclei and produce a variety of spallation products known as cosmogenics.

Isotope	Half life/days	Q-value/Mev
^{14}Sb	60.2	2.90
^{22} Na	950.6	2.84
^{60}Co	1925	2.82
^{110}Ag	249.8	2.89
^{88}Y	106.6	3.62

Table 3.1: Spallation products produced as a result of cosmic ray interactions with the tellurium nuclei [39].

One of the most common and problematic cosmogenic background in LAB is ^{7}Be with a long half of 53.2 days; It is expected to accumulate within the LAB from the time it is produced until it is shipped underground. The interaction of cosmic rays with the carbon nuclei of LAB further produces spallation products such as ^{14}C and ^{11}C. While ^{11}C has a short half life of 20 minutes and can be greatly reduced by using fudicial cuts, ^{14}C however, has a long half life of 5700yr. This is problematic and a source of direct background for solar pp neutrinos. The scintillator purification plant underground was successful in removing these cosmogenics from the LAB before loading it into the detector.

Other backgrounds produced due to muon interactions are very short lived, on the orders of milliseconds to seconds. These events are rejected by characterizing the muon interaction and vetoing the detector for a few minutes. The same concern for cosmogenic exposure exists for tellurium as well. Tellurium goes through the same logistics of being produced elsewhere and getting shipped underground. Tellurium purification plant is being developed underground which is expected to remove cosmogenic backgrounds before loading into AV. The cosmogenics products of tellurium are summarized in Table 3.1.

3.3 2νββ

The 2νββ is an inevitable and irreducible background of SNO+ because it a consequence for the search of neutrino-less double beta decay. This background will only be seen in the tellurium phase of the experiment and a good energy resolution will be required to discriminate them from other backgrounds and 0νββ signal.

3.4 ^{8}B Neutrinos

As discussed in section 2.3.4, ^{8}B is a part of pp chain which produces solar electron neutrinos and dominate the high energy part of the solar spectrum. It was the measurement of ^{8}B flux by SNO experiment and Super-K that resolved the solar neutrino problem (Ref [12]). The ^{8}B neutrino flux, however is one of the major background in the search of neutrino less double beta decay for SNO+. It can be seen in 2.6 that it is a flat continuum background that comes from the elastic scattering of electrons of an incident neutrino [12]. The solar flux and mixing parameters are used to identify and reject the ^{8}B neutrino interactions that may fall in the region of interest.

3.5 (α, n) Reactions

The alphas produced in the detector can produce neutrons within the detector. The most common ones in SNO+ comes from the interaction of alphas with ^{13}C and ^{18}O producing neutrons. One of the common source of alpha backgrounds comes from ^{210}Po, a daughter isotope of uranium decay chain, which decays while producing a 5.3 MeV alpha that interacts with ^{13}C and produces a neutron and a 6 MeV γ. The gamma is seen by the detector almost immediately contributing to a prompt signal, while the neutron travels for another 200 microsecond where it is captured by proton which produces a characteristic 2.22 MeV γ. The delayed coincident signal can act as a background for inverse beta decay (see section 2.3.2), and 2.22 MeV γ signal also acts a direct background for $0\nu\beta\beta$ signal.

3.6 ^{238}U Decay Chain

One of the most inevitable consequence of being located underground is the elevated levels of radioactive decay chains: ^{238}U and ^{232}Th. ^{238}U is a one of the most dominant backgrounds of SNO+ and is abundantly present within the rocks surrounding the detector. Even though ^{238}U has a very long half life of 4.5×10^{9} years but it eventually decays and creates problematic

isotopes that are direct backgrounds in the search for $0\nu\beta\beta$ decay. The radioactive isotopes of the decay chain consists of ^{214}Bi, ^{222}Rn, ^{224}Po etc, which have shorter half lives and upon decaying produces alphas, betas, and gammas throughout the detector. The contributions from these radiations are of great concern because they can mask the signal of interest.

One of the most problematic progeny of ^{238}U decay chain is ^{222}Rn which has a half life of 3.82 days and and is a chemically inert gas. Radon is abundantly present in the mine air and has the ability to travel long distances before decaying. These unique characteristics of radon makes it one of the biggest concerns for underground detectors as a slight ingress of radon into the detector volume or component can break the secular equilibrium of the decay chain. The radon decays by emitting alpha particles into short lived isotopes, for every radon decay there are three alpha decays. This characteristic decay of radon led to the development of radon assay systems which is a direct measurement in determining the ^{222}Rn content of the detector(See Chapter 4). Moreover, this unique method allows to measure the radon content in cavity water, AV scintillator volume, and cover-gas systems.

Down the decay chain of ^{238}U there is another isotope called ^{214}Bi which is of great concern for the sensitivity of the $0\nu\beta\beta$ signal. ^{214}Bi has a half life of 19.8 minutes and Q value of 3.27 MeV. The beta decay of bismuth and some gammas results in a spectrum that crosses the tail of the ^{130}Te spectrum and is at a greater risk of falling in the ROI. Bismuth decays into ^{214}Po 99.9 % of times by emitting an beta particle which 162 μs later decays into lead-210 by an alpha decay. This characteristic beta-alpha decay with a known time delay gave rise to what is called the $\beta - \alpha$ coincidence, which will be used to determine the radon concentration and reject almost all of the non signals that fall within the ROI [39]. This method will be effective in both the scintillator and tellurium phase but not in the water phase due to alpha quenching in water.

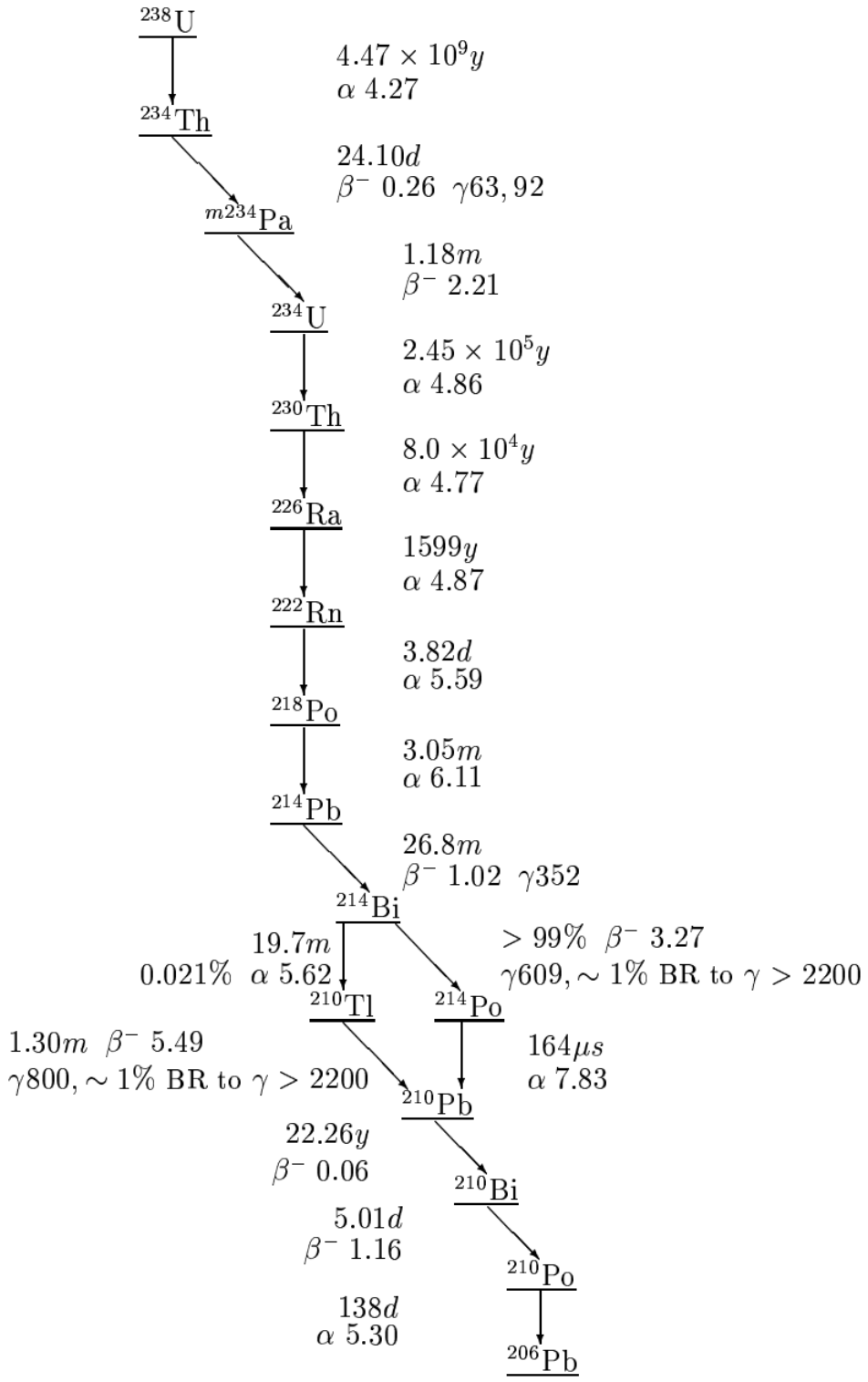

Figure 3.2: ^{238}U decay chain with the type of emission and half life of each isotope [60].

Target Levels	Water Phase	LAB-PPO phase	Tellurium loaded phase
$\mathbf{g^{238}U/gH_2O}$	3.5×10^{-14}	1.6×10^{-17}	2.5×10^{-15}
$\mathbf{g^{232}Th/gH_2O}$	3.5×10^{-15}	6.8×10^{-18}	2.8×10^{-16}

Table 3.2: SNO+ target background levels for ^{238}U and ^{232}Th decay chains for each phase of the experiment [39].

3.7 ^{232}Th Decay Chain

Thorium decay chain is also a commonly found long lived radioactive isotope (1.47×10^{10}y) that exists within the rock surrounding the SNO+ detector. The ^{232}Th although has long life will eventually decay and produce daughter isotopes. Out of all of the isotopes, ^{210}Bi and ^{208}Tl are the most problematic. ^{210}Bi has a half life of 60.2 minutes and q value of 2.25 MeV which beta decays to ^{212}Po 64 % of the time. ^{212}Po then alpha decays 0.299 μs later into ^{208}Pb. The time difference of 0.299 μs between a $\beta - \alpha$ event gives rise to a coincident signal which is used to reject all the ^{210}Bi events in the detector that lie within the ROI and tail end of the ^{130}Te spectrum [39].

The rest of the 36 % of the times ^{210}Bi alpha decays into ^{208}Tl which then beta decays 3.1 minutes later. The $\alpha - \beta$ signal with a 3.1 minute time difference leads to a coincident signal which is used to reject all of the ^{208}Tl from the detector. Moreover, thorium chain also has a radon isotope Rn^{220} with a half life of 55.6 seconds. Due to its lower half life it is not as problematic as ^{222}Rn. Even if the ingress of ^{220}Rn were to happen secular equilibrium would be disrupted but would be restored almost immediately due to shorter half life.

Each phase of SNO+ has different target levels for ^{232}Th and ^{238}U levels. The difference in target levels comes from the limitations based off the active medium in the AV and purification techniques. The Table 3.2 mentions all the target levels for the phases of the experiment.

3.8 External Backgrounds

External backgrounds are defined as events that originate outside the detector volume. External background comes from the mine rocks, cavity water, AV ropes, PSUP, and PMT arrays. One

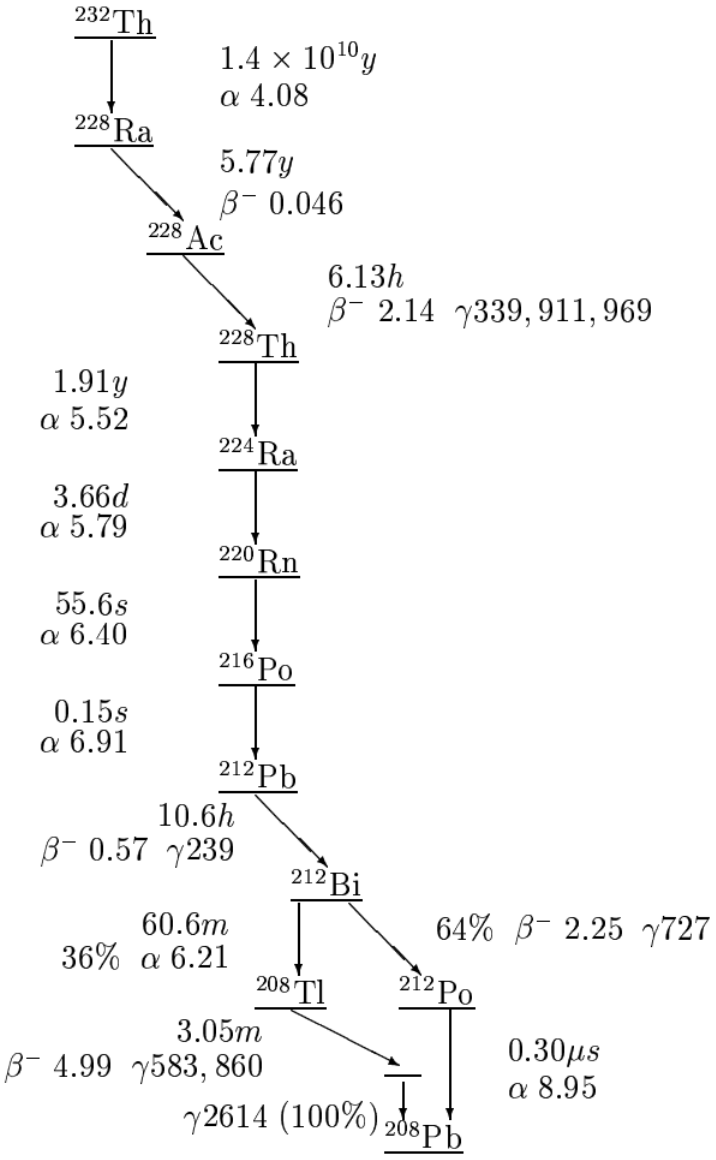

Figure 3.3: ^{232}Th decay chain showing all emissions and half life of each isotope [60].

of the major concerns is the high energy gammas coming from ^{208}Tl, ^{214}Bi, and ^{40}K which are produced outside the AV volume but can propagate into the AV and fall into ROI. Fiducial volume cuts can be applied to avoid reconstruction into the ROI and reduces these external events by several orders of magnitude.

External background characterization and levels are consistent throughout all three phases of SNO+. There are *in situ* and *ex situ* analysis through which we can determine the levels of background coming from external sources. One of the most common ways of measuring the radon levels is through radon assay of the water which helps determine the g^{238}U/gH_2O concentration (See Chapter 4). The ^{238}U background concentration is then checked by determining the concentration through analysis of the detector data (See Chapter 6). Moreover, radium assays are also performed on the cavity which helps determine the concentration of the ^{232}Th decay chain and possible lead concentration in the cavity.

The temperature profile of the cavity is set in a way that prevents radon or any backgrounds to spread over the cavity due to convection currents. The bottom part of the cavity is set at approximately 12 degrees, middle at 13 degrees and top at 15 degrees. Keeping the bottom of the cavity colder prevents convection modes and contain the backgrounds preventing mixing of backgrounds.

The overall background contributions to ROI for $0\nu\beta\beta$ analysis is summarized in the table 3.4

Sources	Measured Concentrations	Decays/yr
Water Shielding	^{214}Bi : 2.1×10^{-13} gU/g	1.32×10^{8}
	^{208}Tl : 5.2×10^{-14} gTh/g	3.92×10^{6}
Internal Ropes	^{214}Bi : $(2.8 \pm 5.4) \times 10^{-10}$ gU/g	4955
	^{208}Tl: $< 2.0 \times 10^{-10}$ gTh/g	< 418
Hold-Down Ropes	^{214}Bi : $(4.7 \pm 3.2) \times 10^{-11}$ gU/g	2.06×10^{6}
	^{208}Tl : $(2.27 \pm 1.13) \times 10^{-10}$ gTh/g	2.32×10^{6}
Hold-Up Ropes	^{214}Bi : $(4.7 \pm 3.2) \times 10^{-11}$ gU/g	8.34×10^{5}
	^{208}Tl : $(2.27 \pm 1.13) \times 10^{-10}$ gTh/g	4.78×10^{5}
Acrylic Vessel	^{214}Bi: $< 1.1 \times 10^{-12}$ gU/g	1.28×10^{7}
	^{208}Tl: $< 1.1 \times 10^{-12}$gTh/g	1.50×10^{6}
PMTs	^{214}Bi : 100×10^{-6} gU/PMT	3.7×10^{11}
	^{208}Tl : 100×10^{-6} gTh/pmt	4.4×10^{10}

Table 3.3: Measured levels for ^{238}U and ^{232} decay chains from external background sources along with their expected decays/yr [39].

Isotope	1 Year	5 Years
$2\nu\beta\beta$	6.3	31.6
^{8}B ν ES	7.3	36.3
Uranium Chain	2.1	10.4
Thorium Chain	1.7	8.7.
External	3.6	18.1
(α, n)	0.1	0.8
Cosmogenics	0.7	0.8
Total	21.8	106.8

Table 3.4: Total number of background events falling into the ROI after 1 and 5 years of data taking [39].

3.9 UltraPure Water Purification Plant

SNO originally had two working purification plants; Ultra-pure water and D_2O purification plant. Upon completion of SNO experiment, D_2O plant was decommissioned and removed. UPW plant however remained intact and serviced for the operations of SNO+. The purification plants are instrumental to the SNO+ experiment as they help remove all contaminant backgrounds. SNO+ required two additional purification plants: Scintillator purification plant and Tellurium purification plant. This chapter only covers UPW plant and Scintillator plant as Tellurium plant is still in commissioning phase.

SNO+ cavity is filled with ultra pure water which prevents radioactive contaminants emanating from mine walls to reach to the AV. Inner cavity consists of 1700 tonnes of UPW and outer cavity consists of 5700 tonnes of UPW. The UPW plant is used to produce ultra pure water for maintaining low backgrounds within the cavity. Figure 3.4 shows the flow chart of the vale water entering the purification system until it is filled within the cavity.

The water enters the filtration unit and passes through multiple filters, activated charcoal, softener, and reverse osmosis. After this treatment, clean enough water is exposed to UV rays (185 nm) to break down organics present within the water. Ionic compound products are removed by passing through an ion exchange columns. The water then enters a process degasser (PDG) which strips dissolved gases like Rn, Ar, Kr, and $_2O$ from water. PMTs do not operate well with the degassed water, therefore, water is re-gassed again with nitrogen. The re-gassed water now enters another set of UV rays (254 nm) that further prevents any biological growth. In order to maintain the temperature profile of the cavity, water enters a heat exchanger where excess heat is removed and the temperature of water is dropped to 12 degrees. Low temperature within the cavity keeps PMTs noise rate to a minimum and prevents any biological growth [51].

There exists an assay skid on the water plant which is being used to assay the different parts of the cavity for ^{238}U concentration. The acceptable target level for SNO+ ^{238}U decay chain is 2.1×10^{-13} g^{238}U/g H_2O and 5.2×10^{-14} g^{232}Th/g H_2O.

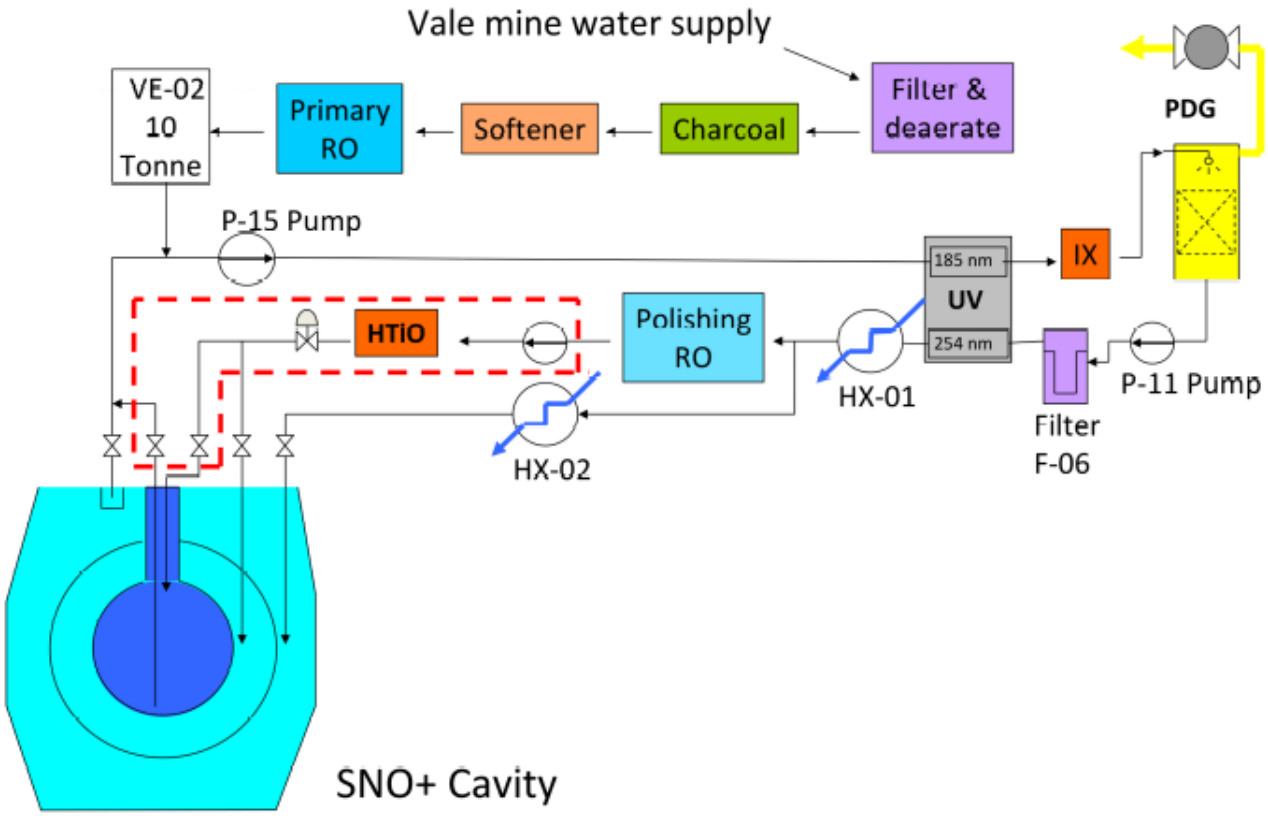

Figure 3.4: Flow diagram for Ultra pure water purification plant. It purifies and water for SNO+ and will be used during recirculation of the cavity water [51].

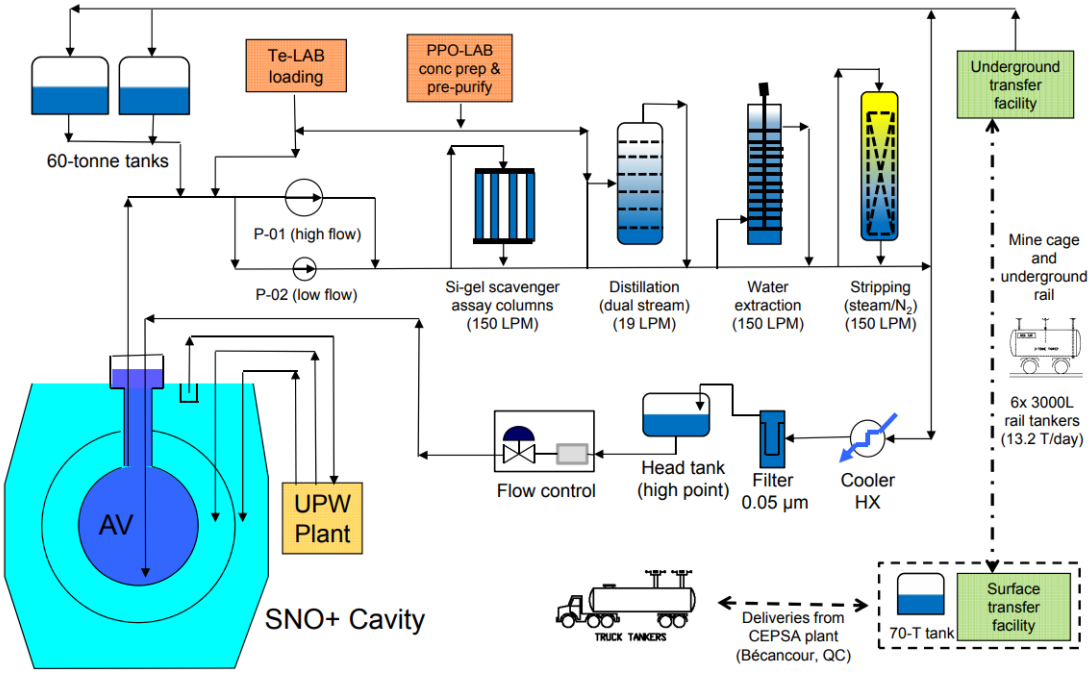

Figure 3.5: SNO+ Scintillator purification and fluid handling flow diagram. It consists of the Surface Transfer facility, Underground Transfer facility, 60T tanks, purification system, AV sample lines [2].

3.10 Scintillator Purification Plant

The development of a scintillator purification system was crucial for successfully removing radioactive backgrounds from the LAB before adding it into the detector. The design and process of the purification plant was constrained due to the underground location of the plant and the combustible nature of the LAB. The LAB is transferred to SNOLAB in 22 tonne LAB tankers, where it is stored temporarily in surface transfer facility (STF) in a 70 tonne tank. The LAB is then transported to underground transfer facility in 2.2 tonne rail-cars, where LAB is finally transferred to 60 tonne storage tanks [2]. The LAB is drawn from the storage tanks and entered into the purification systems before being added to the detector. The purification system include multistage distillation 3.10.1, solvent-solvent water extraction 3.10.2, gas stripping 3.10.4 , and metal scavenger 3.10.3.

3.10.1 Multi-stage Distillation

SNO+ uses multi-stage distillation as one of the first steps in purifying the LAB. Distillation is one of the oldest and most effective separation process used for removing contaminants within a solvent, in this case LAB. The separation is made possible by the differences in volatilities (boiling point) of different contaminants within the scintillator. Since the volatilities of heavy metals are low, distillation effectively removes Ra, Th, Po, Pb, Bi, and K [2]. Moreover, it is very effective in improving optical clarity of LAB by removing oxidized organic molecules, and achieving the desired detector resolution.

The distillation column consists of a 4.4m height tower with six stages. The scintillator feed is vaporized in the boiler before it enters the tower at 1000 kg/hr (19 LPM), 238 $^{\circ}$C , and 55 Torr [2]. The distillation is performed at 55 Torr to ensures safety because the atmospheric boiling point of LAB (278 - 314 $^{\circ}$C) is very close to the auto ignition temperature of 323 $^{\circ}$C. Additionally, the temperature needs to be kept as low as possible because of the past evidence of heat damage on LAB. The six stage distillation allows for an efficient separation of impurities from the scintillator.

The distillation also includes simultaneously purifying PPO, which also enables successful removal of PPO from LAB that is crucial to the decommissioning of SNO+. PPO+LAB is fed into a single stage kettle at 120 g/L. PPO is distilled at 242 $^{\circ}$C and 20 Torr vacuum [2]. The PPO concentrated solution enters the kettle where LAB flashes and PPO boils removing contaminants based on difference in volatilities. Upon completion of distillation, the purified LAB and PPO are then mixed and sent to the rest of the purification plant.

3.10.2 Solvent-Solvent Extraction with Water

Solvent-solvent extraction with water is a purification step that is intended to take place only during the re-circulation phase after the LAB fill is completed, in order remove the AV leaching and radon backgrounds. It is dependent upon the idea of bringing two immiscible solvents into close contact and then re-separating them. In this case, the two solvents are LAB and water.

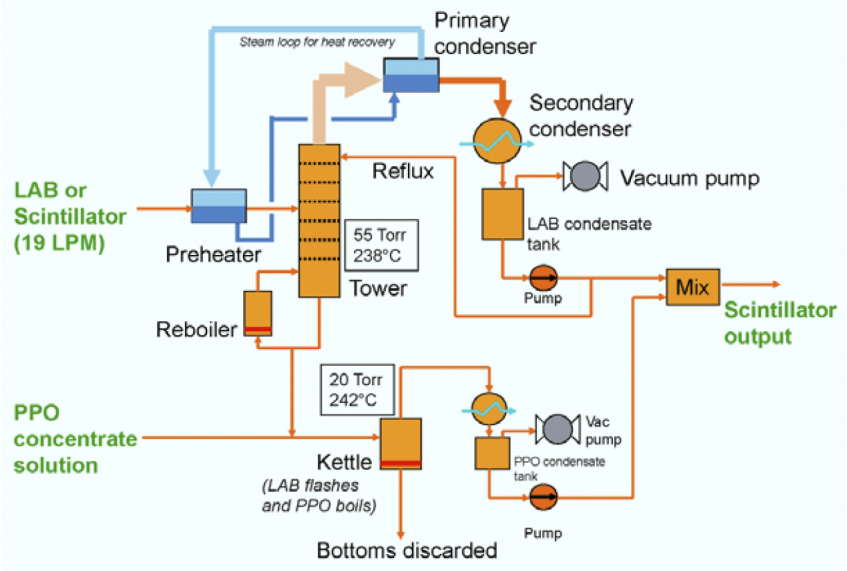

Figure 3.6: Flow Diagram for SNO+ Distillation System. The tower distillates the LAB while the Kettle purifies the PPO and upon completion both are blended together and sent to the scintillator plant [2]

The extraction occurs in a 18 feet tall purification column with 22 rotating stages and baffle plates [2].

This process will be used during high flow re-circulation, therefore, it is designed to operate at 150 LPM as opposed to 19 LPM in the multistage distillation. The lower flow of UPW was a major operational constraint in this process due to parallel purification of the cavity water by the UPW plant. The LAB enters the bottom and travels up with the pressure from a pump while the water entering from the top flows down due to gravity and higher density than LAB. The separation is dependent upon the insolubility of LAB with water, even when LAB is immiscible with water, many heavy metals like, U, Ra, and K are soluble in water and are pulled from LAB into water. The contaminated water is then returned to the UPW loop for purification. This process will be very crucial to recover ^{130}Te from the scintillator during the decommissioning of SNO+.

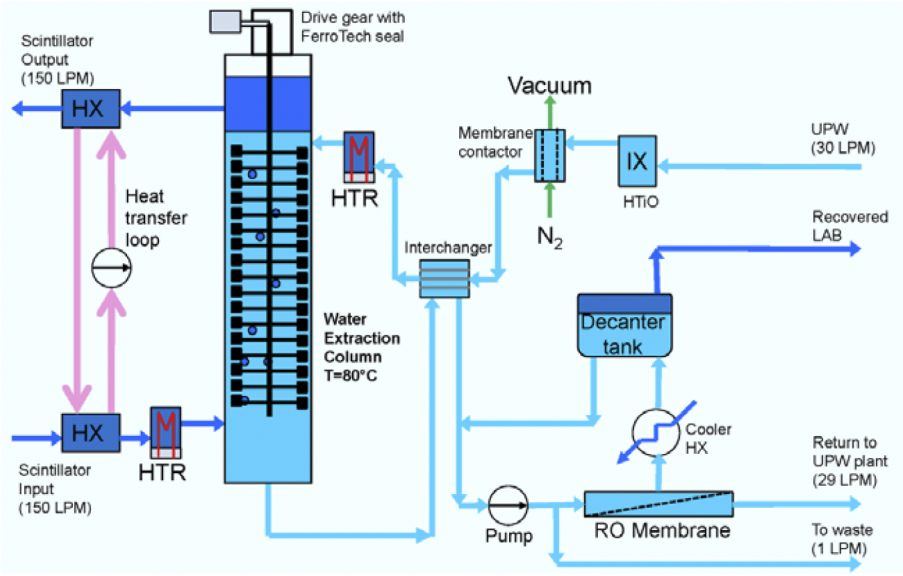

Figure 3.7: Flow diagram for water extraction purification system. It consists of an 18 feet tall column to purify scintillator at 150 LPM with flow of 30 LMP of UPW water [2].

3.10.3 Metal Scavengers

Metal scavengers are very effective in removing heavy metals from aqueous or aromatic solvents. The purification plant uses six metal scavengers designed to remove metallic contaminants from the LAB during high recirculation. The QuadraSil-AP^{TM} has a aminopropyl functional group on a 50µm silica gel and is found be really efficient in removing Pb and Ra [2].

3.10.4 Gas Stripping with Steam and Nitrogen

The Scintillator purification system has a 24 feet tall stripping column with 19 packed elements, which separates the scintillator from volatile impurities such as Rn, Ar, Kr, and O_2 by using steam and nitrogen gas. The concept behind the stripping column is based on the difference between the vapor-liquid partitioning of volatile species versus temperature [2]. The removal efficiency of gas from the scintillator depends on Henry coefficients, which suggests that the solubility of a gas within a liquid, LAB in our case, is directly proportional to the partial pressure of the gas in equilibrium with the liquid. The gas in this case consists of a mixture of steam and nitrogen gas [2].

The column is fed with scintillator at 150 LPM from the top, while nitrogen gas at 3 Kg/hr

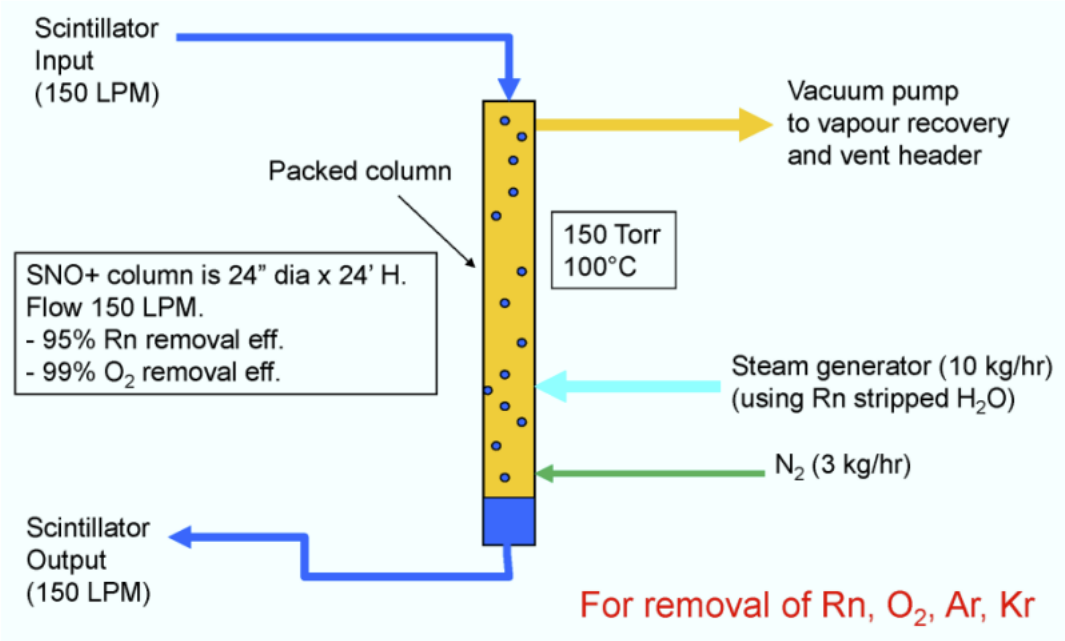

Figure 3.8: Flow diagram for the gas stripping column. Consisting of a 24 foot tall column with LAB being fed from the top and N_2 gas and steam being introduced from the bottom [2].

and steam at 10 Kg/hr is fed from the bottom. The column is set at 150 Torr and 100 $^{\circ}$C. The liquid falls down the bottom due to gravity while the gas is driven up the column by a vacuum pump. The purge gas of nitrogen and steam allows for a low partial pressure of contaminant such as Rn, Ar, Kr, and O_2. The high temperature of the stripping column is also used for removing water from the scintillator. The stripping column allows 95 % radon removal efficiency and 99 % O_2 removal efficiency [2]. The purified scintillator is then fed into a tank known as VO1 where it sits before being loaded into the detector.

Chapter 4

Water Radon Assays

4.1 Introduction

One purpose of the water in the SNO+ cavity is to mitigate the backgrounds that emanate from the surrounding rocks and detector components and prevent them from creating non signal events that can propagate into the ROI for neutrino-less double beta decay. The UPW plant continuously recirculates water from the cavity and purifies it before injecting it back again. The *in situ* analysis (see Chapter 6) are performed continuously to monitor uranium levels in the cavity water but a direct measurement is also required that can determine the radon concentration in the cavity water and determine the efficiency of the *in situ* analysis and UPW shielding. The method used to measure the radon levels is done by performing radon assays. Radon assays was a technique used by the SNO experiment to determine the ^{238}U background at different locations of the cavity and after service, SNO+ uses the same assay system for background measurements [25].

The radon assay technique is based on the characteristic alpha decay of radon. For every ^{222}Rn decay there are three subsequent alpha emissions. Radon emits alpha upon decaying while producing ^{218}Po, which then alpha decays 3 minutes later into ^{214}Pb. The lead isotope then beta decays into ^{214}Bi and then into ^{214}Po. The ^{214}Po then again alpha decays into stable ^{210}Pb isotope which has a half life of 22 years. This decay scheme of radon allowed

for the development of the assay technique which allows to accurately determine the radon concentration.

The SNO+ detector and purification plants uses a cover-gas system to act as a barrier from the highly radon contaminated mine air. In order to determine the effectiveness of the cover-gas system SNO+ has a radon gas system which can measure the radon content within the cover-gas and determine the radon detection factor (see Chapter 5). Moreover, there is another radon board under construction that will determine the radon concentration within the LAB and determine the efficiency of the Bi-Po coincidences.

4.2 Water Assay Technique

4.2.1 Monitor Degasser

Radon concentration in water is measured by an assay technique which involves passing water from the cavity through the MDG (Monitor Degasser) which extracts radon. Radon is then trapped, concentrated, and transferred into custom made Lucas cells for counting [25]. Water Assay technique is a complicated method that requires one whole shift. It makes use of two diaphragm pumps, where the first pump injects water into the MDG and other puts the water back into the water purification system, both pumps are essential in maintaining a stable flow throughout the assay. Figure 4.1 shows the schematic of the MDG.

The MDG consists of vertical stainless steel cylinder with 1.15 m height and 0.4 m diameter. It was custom made during the SNO time and is being reused for SNO+ assay system. Water is pumped into the degasser from the top and then sprayed upwards into three cone spray nozzles. The nozzles spray water upwards producing water droplets about $\approx$ 1 mm in diameter [25]. The water vapor with dissolved radon is then dispensed into the radon collector with the help of a vacuum pump. The temperature of the cavity around sample points is set around 13 $^{\circ}$C while the water is pumped at around 19 litres/minute. There are two viewable ports which are used to determine the level of water within the degasser inorder to prevent possible flooding.

SNO+ still uses the efficiency of the degasser that was measured during SNO time. The

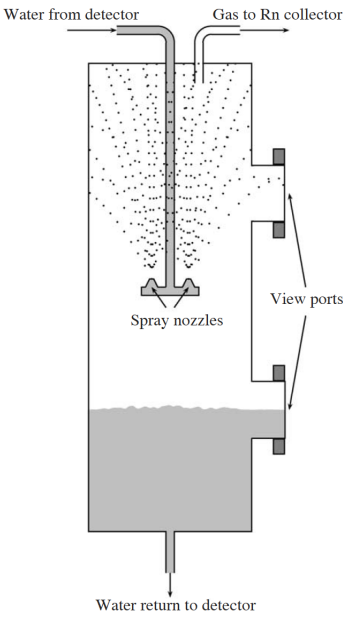

Figure 4.1: Schematic of the Monitor Degasser during a water assay. The water is injected from the top and drained from the bottom. The spray nozzles spray the water in the cavity of the degasser [25].

degassing efficiency was measured by enriching a small amount of water with radon by exposing it to mine air and allowing for an equilibrium to reach. The radon-enriched water was then injected into the MDG and radon was extracted and counted. Measured radon atoms were compared to the expected radon atoms and efficiency was determined. The degassing efficiency at 13 $^{\circ}$C of water and flow rate of 19 L/m is 0.58 $\pm$ 0.10 [25].

4.2.2 Radon Board and FTS

The gas collector consists of radon board which separates radon from other gases while refrigerant (FTS) column separates water vapor from radon. The components of this system were chosen based on the low emanation rate of radon. A typical water assay begins by pulling vacuum on all components of the gas collection system along with the MDG. This allows removal of any residual gas from previous assays or from emanation. It takes about three to four hours to pump down the whole system before extracting water from the cavity. Figure 4.2 shows the schematic of the components of the gas collector system.

The dispensed water vapor from the MDG is drawn into the radon collection system with

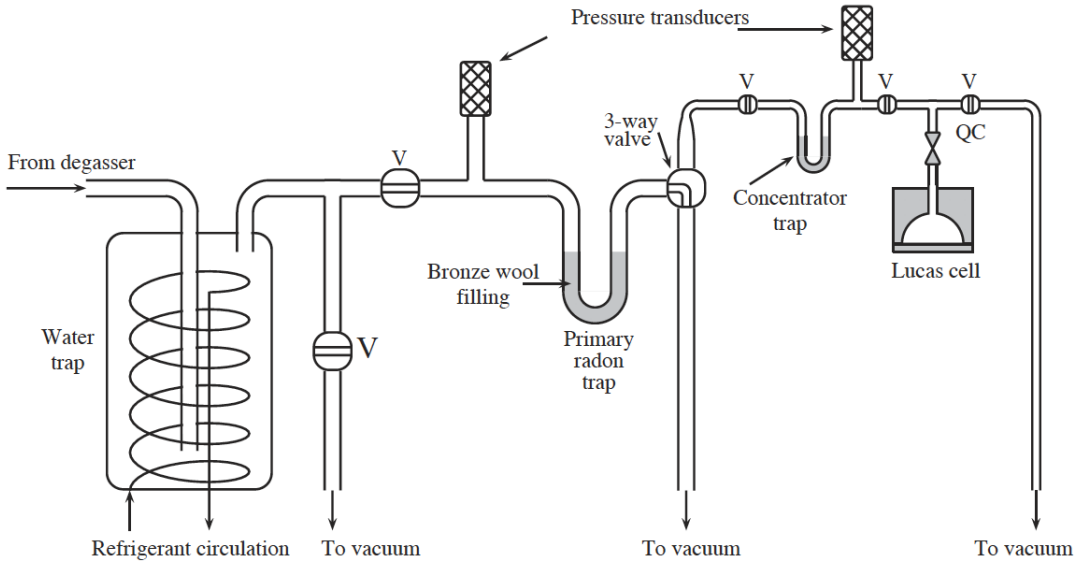

Figure 4.2: Schematic of the Radon Board and refrigerant column(FTS). The schematic shows the water trap along with primary and secondary traps that are stuffed with bronze wool. Lucas cell can also be seen that is used to store the trapped radon sample [25].

the vacuum pump. The vacuum pump also has a back-flow trap attached which prevents radon ingress into the system from the pump. The radon enriched water droplets from the degasser enters the FTS which consists of a refrigerant coil that freezes the vapor. The FTS is made of an acrylic cylinder with a volume of 42 litres and consists of stainless steel refrigeration coil [25]. The coil is kept at below -60°C during an assay but this number can fluctuate from anywhere between -55°C and -65°C. The FTS needs to be drained after each assay, therefore, a purging system exists which purges the FTS with nitrogen gas and allows successful draining while preventing mine air from entering the system.

After successfully establishing a stable flow, water is recirculated for at least 30 minutes before starting the assay to ensure any residual water in the piping is circled out of the MDG. The assay requires cryogenically trapping radon into the trap. Primary radon trap or also known Trap A is made of 10 mm diameter stainless steel tube bent in a U shape and stuffed with bronze wool [25]. This trap is immersed in a liquid nitrogen bath during an assay with temperature of the trap going below -180 °C. At this temperature, ^{222}Rn, CO_2, are stopped and other gases like Ar, O_2, and N_2 are evacuated via the vacuum pump. Primary trap is equipped with a pressure transducer which is an indicator of any water vapor that can enter

Efficiencies	Value
$\varepsilon_{\text{trap}}$	$100.5 \pm 2.3\%$
$\varepsilon_{\text{transfer}}$	$64 \pm 2.0\%$
$\varepsilon_{\text{count}}$	$3 \times 74 \pm 2.1\%$
$\varepsilon_{\text{degasser}}$	$58.0 \pm 1.0\%$

Table 4.1: Efficiencies measured by SNO experiment and are still being used by SNO+. The counting efficiency makes use of the three alphas emitted by the radon [25].

the trap. The presence of FTS makes it highly unlikely for vapor to enter the trap but there still exists a possibility. Presence of water vapor can over-pressurize the trap and greatly affect the efficiency of the lucas cell which can impact the assay results. Upon completion, trap is isolated from the system and inlet to the pump is remained open for a few minutes to allow residual gases other than radon to evacuate. The valve is then closed and nitrogen bath is removed.

Radon is then transferred from the primary to a secondary trap. During transfer primary trap is heated with a heat gun and radon is cryopumped into the secondary trap for about 15 minutes. Once the transfer is over, liquid nitrogen bath is removed from the secondary trap and brought to room temperature. Once the secondary trap is at room temperature, the valve is opened to a previously evacuated lucas cell and radon is transferred via volume sharing for about 10 minutes. After 10 minutes, the transfer is completed and lucas cell is removed and transported to surface lab for counting.

Efficiency measurements are required to understand each process of the transfer, therefore, SNO determined radon efficiency of three important steps; trapping efficiency of primary trap, transfer efficiency from the primary trap to the secondary trap and to the lucas cell, and counting efficiency of the lucas cell. All the efficiencies were measured by injecting known amount of radon into the traps and lucas cells and comparing them to the expected values. The Table 4.1 shows the efficiencies.

4.2.3 Lucas Cell and Data Acquisition system

Lucas Cell

The radon assay technique uses Lucas cells which contain the sample and count the alpha particles. They are custom made cells initially made for the SNO experiment with very low background, and are still being constructed to cater the assay demands for SNO+ experiment. Customised cells were a necessity as commercial cells had very high background. These cells are coated with silver activated Zinc Sulfide (ZnS(Ag)) scintillator. The cell as shown in figure 4.3 consists of an acrylic body with a base diameter of 5 cm and an inner volume of 15.5 cm^3. Acrylic body of the cell was chosen due to its low radioactivity, and the cell can be accessed by a Swagelock quick connect which allows secure installation of the cell to the radon board without injecting any mine air. The ZnS thickness of 10 mg/cm^2 was carefully chosen as this gives the highest pulse amplitude compared to the PMT noise with an acceptable background contribution [56]. Acrylic window on the base of the cell is not coated with ZnS and is used by the PMT to view the alpha pulses.

The emitted alphas from radon decay interact with the scintillator and emit scintillation light. In order to detect this light, lucas cells are placed in the PMT where it detects the light within the cell. The scintillation light in the lucas cell can be explained by the electron band theory. Alpha particle is a charged radiation which upon striking the ZnS (Ag) coating within the hemisphere of the Lucas cell excites the electrons in the valence band to the excited states. An array of photons are emitted upon de-excitation of the electron to its original ground state which are detected by the coupled PMT [56].

The Lucas cell background needs to be determined in order to accurately measure the sample from the assays. Lucas cell background (B_{LC}) is due to the long lived decay of ^{210}Po isotope down the ^{238}U decay chain. Lucas cell backgrounds are periodically checked, and lucas cells are often purged with N_2 gas in order to discharge any residual backgrounds from the previous assays.

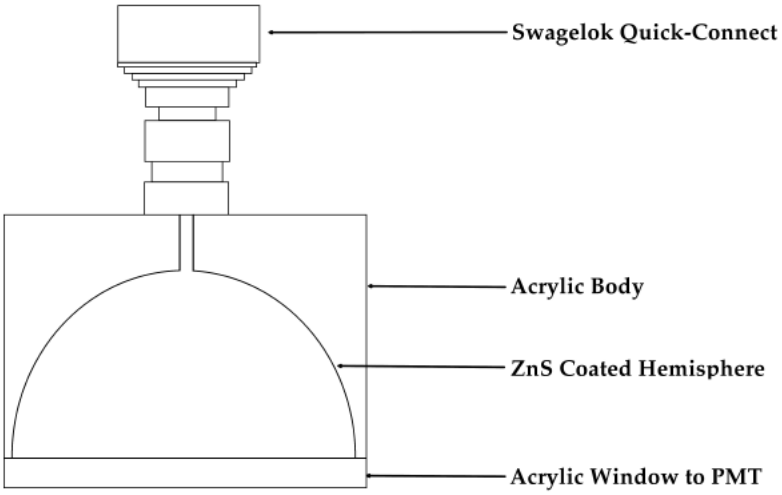

Figure 4.3: Schematic of the Lucas cell consisting of the hemispherical cavity along with an acrylic window for PMT viewing [51].

Data Acquisition System

The data acquisition system was developed as a joint venture between SNO+ and SNOLAB which was completed in 2020 and is located on the clean lab of SNOLAB. This data acquisition system allows an efficient way of counting the alpha decays. The lucas cell shown in figure 4.4 is placed in a dark box which is viewed from the PMT underneath that counts the alpha decays by counting the scintillation light signals. The system has eight channels which can run simultaneously. The Figure 4.4 shows the data acquisition with only one PMT channel.

The PMT is powered up by high voltage and it detects signals which pass through the digitizer that converts the analog signals to digital signals. The signals from the digitizer are then processed for the signals of interest which are then analyzed. All eight PMT channels were calibrated by using a hot source and optimal voltage was determined for each channel. Optimal voltage allowed no PMT noise signal to fall in the signal of interest. Figure 4.5 shows the alpha decay plot that the analyzing software produces.

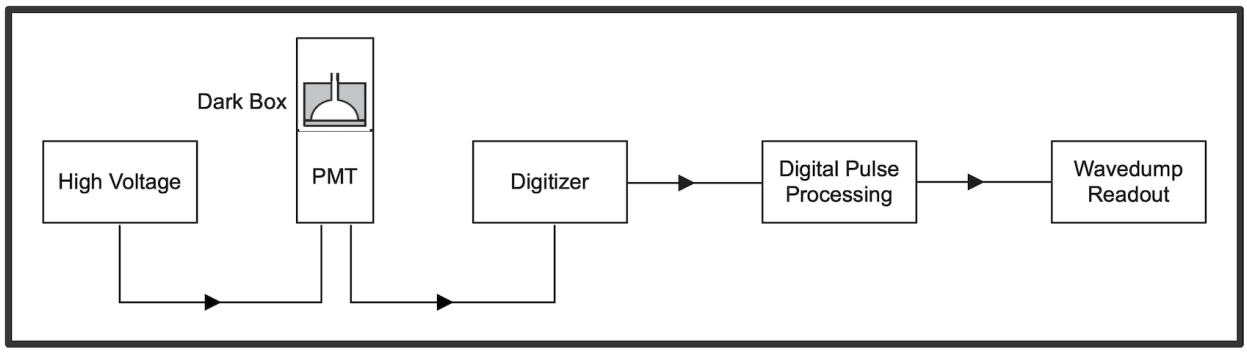

Figure 4.4: Data Acquisition system showing a lucas cell placed in the Dark box which is being viewed PMT. It consists of high voltage, digitizer, and signal processor The wavedump readout gives the total number of alphas in a given time.

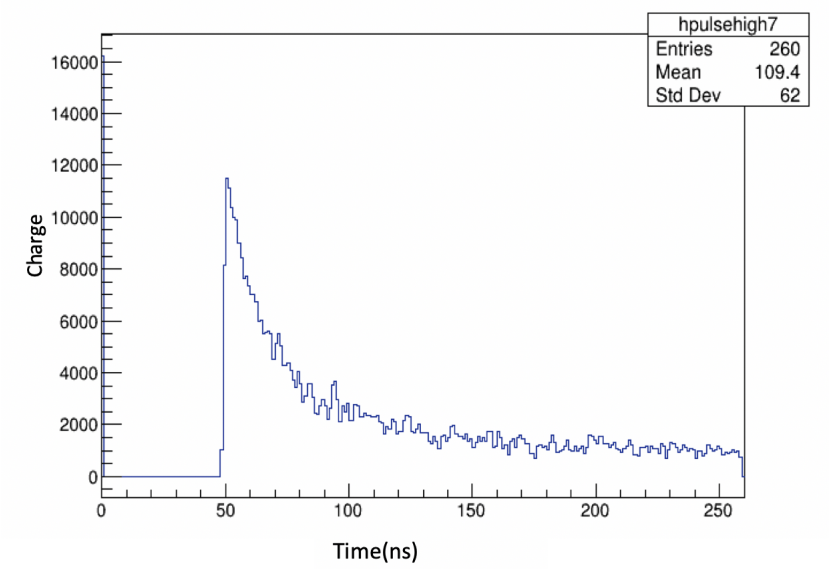

Figure 4.5: Time structure of a single Alpha pulse. Each time bin has a width of 4ns. The exponential decay represents the decay of electron from excited states to ground state.

4.2.4 Radon Calculations

Radon calculations depend upon the characteristic alpha decay of radon. Radon with a half life of 3.8 days emits 4 alphas down the Uranium-238 decay chain, the first three are emitted promptly while the fourth one is emitted after a half life of 140 days. In order to correctly calculate the number of radon atoms that were trapped in the primary trap, we need to take into account the assay time, delay time i.e the time between the end of the assay and start of counting , and counting time. Moreover, the efficiencies on each step needs to be included in order to accurately determine the radon concentration.

Data acquisition gives us the total number of alpha pulses at the end of the counting period. Radon decays using the following radioactive decay law:

$$\frac{dN}{dt} = -\lambda N \tag{4.1}$$

dN/dt represents the decay rate of radon and λ is the decay constant while N is the rate of radon at any given time of counting. With the help of this equation, the initial number of Radon atoms present at the start of counting (N_{soc}) can be determined by integrating over the decay law.

$$N(t_{count}) = N_{soc} e^{-\lambda t_{count}} \tag{4.2}$$

The alpha counting system affects the efficiency of the counting, therefore, our calculations must account for it. The counting efficiency is due to the optical coupling between the lucas cell and the PMT, and the lucas cell geometry. Moreover, we need to account for the background for the Lucas cell background accumulated over the total counting period.

$$\frac{dN}{dt} = \lambda \varepsilon_{count} N_{soc} e^{-\lambda t_{count}} + B_{LC} \tag{4.3}$$

Integrating this provides the number of alphas $N(t_{count})$, the total number of counts in the cell

over a period of time:

$$N(t_{count}) = \varepsilon_{count} N_{SOC}(1 - e^{-\lambda t_{count}}) + B_{LC} t \tag{4.4}$$

Assays are performed underground and alpha counters are installed on surface. There is a significant delay time which needs to be accounted as Radon will decay during that time. This will allow us to determine the number of radon atoms collected at the end of the assay. The decay law can be written as follows:

$$N_{SOC} = N_{EOA} e^{-\lambda t_{delay}} \tag{4.5}$$

Where N_{SOC} is the atoms present at the start of the counting and N_{EOA} represents the radon atoms present at the end of assay. The sample extracted at the end of the Assay needs to be accounted for the background of the Assay system. Therefore, $N_{EOA} = N_{sample} + N_{bcg}$. In this part the transfer efficiency of the system needs to be accounted in order to correctly determine the radon atoms that were trapped in the primary trap and later on transferred to the lucas cell. Equation 4.5 then becomes:

$$N_{SOC} = \varepsilon_{transfer}(N_{sample} + N_{bcg}) e^{-\lambda t_{delay}} \tag{4.6}$$

Radon is expected to decay within the primary trap. It is also expected to decay within the secondary trap but due to the short amount of time that decay is futile and can be ignored. The decay of the sample is considered and the correction factor is added into the calculations. The sample decays with the following radioactive decay equation within the primary trap:

$$\frac{dN_{sample}}{dt} = R - \lambda N \tag{4.7}$$

Where R represents the radon atoms from the cavity water sample or source. Integrating

equation 4.7 gives the following result equation:

$$N_{sample}(t_{assay}) = \frac{\varepsilon_{trap} R(1 - \exp^{-\lambda t_{assay}})}{\lambda} \tag{4.8}$$

The trapping efficiency is added into the equation. The N_{backg} also needs to take into account the atoms that decayed during the assay. The background decays with the following radioactive decay equation within the primary trap:

$$\frac{dN_{backg}}{dt} = R_{back} - \lambda N_{backg} \tag{4.9}$$

Integrating equation 4.9 gives the following result equation:

$$N_{sample}(t_{assay}) = \frac{\varepsilon_{trap} R_{bckg}(1 - \exp^{-\lambda t_{assay}})}{\lambda} \tag{4.10}$$

Now substituting equations 4.10 and 4.8 into 4.6, and finally substituting the resulting Equation 4.6 into 4.4 results in the following equation.

$$N(t_{count}) = \varepsilon_{total} \left[\frac{R(1 - \exp^{-\lambda t_{assay}})}{\lambda} + \frac{R_{bckg}(1 - \exp^{-\lambda t_{assay}})}{\lambda} \right] (1 - e^{-\lambda t_{count}})(e^{-\lambda t_{delay}}) + B_{LC} t \tag{4.11}$$

Where $\varepsilon_{total} = \varepsilon_{count}\varepsilon_{transfer}\varepsilon_{trap}\varepsilon_{degassing}$. The degassing efficiency has been accounted as well on order to account for the total number of radon atoms that was initially present in the water and did not enter the radon assay system. Now finally solving for R yields:

$$R(\text{atoms/day}) = \frac{(N - B_{LC} t_{count})\lambda}{\varepsilon_{count}\varepsilon_{transfer}\varepsilon_{trap}\varepsilon_{degassing}(1 - e^{-\lambda t_{count}})(1 - e^{-\lambda t_{assay}})(e^{-\lambda t_{delay}})} - R_{bcg} \tag{4.12}$$

There is another approach to solve the final equation from here, one if our assay time is less than one hour we only account for the Radon we collected in the sample and the background of the assay system. The steps followed from equation 4.6 till equation 4.10 will not be necessary.

$$R(\text{atoms/sample}) = \frac{N - B_{lc} t_{count}}{\varepsilon_{trap}\varepsilon_{transfer}\varepsilon_{count}\varepsilon_{degassing}(e^{-\lambda t_{delay}})(1 - e^{-\lambda t_{count}})} - R_{bg} \tag{4.13}$$

Equation 4.12 now can be used to determine the concentration of the water sample within the cavity. The flow F(L/min) rate at which the radon is extracted is taken into the account and the radon concentration is calculated.

$$C(\text{atoms/L}) = \frac{1}{F}\left[\frac{N - B_{LC} t_{count}}{\varepsilon_{count}\varepsilon_{transfer}\varepsilon_{trap}\varepsilon_{degassing}(1 - e^{-\lambda t_{count}})(1 - e^{-\lambda t_{assay}})(e^{-\lambda t_{delay}})} - R_{bcg}\right] \tag{4.14}$$

In order to estimate the concentration from atoms/day, the flow needs to be converted from L/min to L/day. Similarly, if concentration from atoms/sample is determined then flow will be converted to L/min to litres. In the cavity, radon concentration is assumed to be in secular equilibrium with ^{238}U concentration. If this is the case then the following relation holds true:

$$\frac{N_U}{N_{Rn}} = \frac{\lambda_{Rn}}{\lambda_U} \rightarrow \frac{N_U}{N_{Rn}} = \frac{T_{Rn}^{1/2}}{T_U^{1/2}} \tag{4.15}$$

Where N_U and N_{Rn} are the number of Uranium-238 and Radon-222 atom and the relation finally simplifies to the ratio between their half lives. SNO+ uses gU^{238}/gH_2O as a common unit to express the concentration. The following conversion is done to calculate the g/g concentration from atoms/L from equation 4.14.

$$C[gU^{238}/gH_2O] = C[\text{Rnatoms/L}] \times \frac{1.69 \times 10^{-13}}{\rho} \tag{4.16}$$

Here ρ is the density of the liquid and for this case it is water. Because ρ_{water} is 1.00 g/m^3 so equation 4.16 becomes:

$$C[gU^{238}/gH_2O] = C[\text{Rnatoms/L}] \times 1.69 \times 10^{-13} \tag{4.17}$$

Date	SNO Time	2015	April 2018
LC ID	-	LCT6	N19
$\mathbf{B}_{\mathrm{LC}}$ (cpd)	-	2.88	13
$\mathbf{t}_{\mathrm{assay}}$(minutes)	30	78	30
Alphas	-	67	949
$\mathbf{t}_{\mathrm{delay}}$(hours)	-	5.75	2
$\mathbf{t}_{\mathrm{count}}$(days)	-	12.82	12.4
$\mathbf{R}_{\mathrm{bcg}}$ (Rn/day)	460 ± 133	446 ± 157	31623 ± 3912

Table 4.2: MDG background results over the years.Consistent values are seen from SNO and in 2015. The system developed leaks which shows high counts in 2018 [51] [25] [71].

4.2.5 Assay System Background

As explained in section 4.2.1 and 4.2.2 MDG unit and radon collector is a part of the assay system. In order to measure the radon concentration within the cavity, the background of the system needs to be measured and subtracted from total radon atoms. This measurement is performed in two ways, one by doing a blank assay on the system under vacuum using the MDG and the radon collector without water re-circulation, second by using the MDG and some of the piping the from the UPW plant and pumping water into the MDG in a closed-loop configuration. This process requires using the the diaphragm pumps to fill and drain the water into the degasser. The background measurement follows the same assay procedure which allows radon to be trapped, concentrated, and volume shared into the Lucas cell. The only difference between this measurement and a normal cavity assay is that the closed loop configuration requires running the water in a loop with vent line open to the vacuum pump. Venting the lines prior to assay allow any residual radon to be dispensed out of the system and leaves only the constant background of the system. For operational purposes this measurement is known as the closed-loop assay. Background measurements have been made since the SNO time and the readings have changed significantly based on the history of leak rates during commissioning phase of SNO+.

The history of the background of MDG has changed over the years. SNO experiment used this system extensively to measure the background levels within the cavity. During SNO phase, background of the MDG was measured at 460 Rn/day and at this rate an expected 19 radon

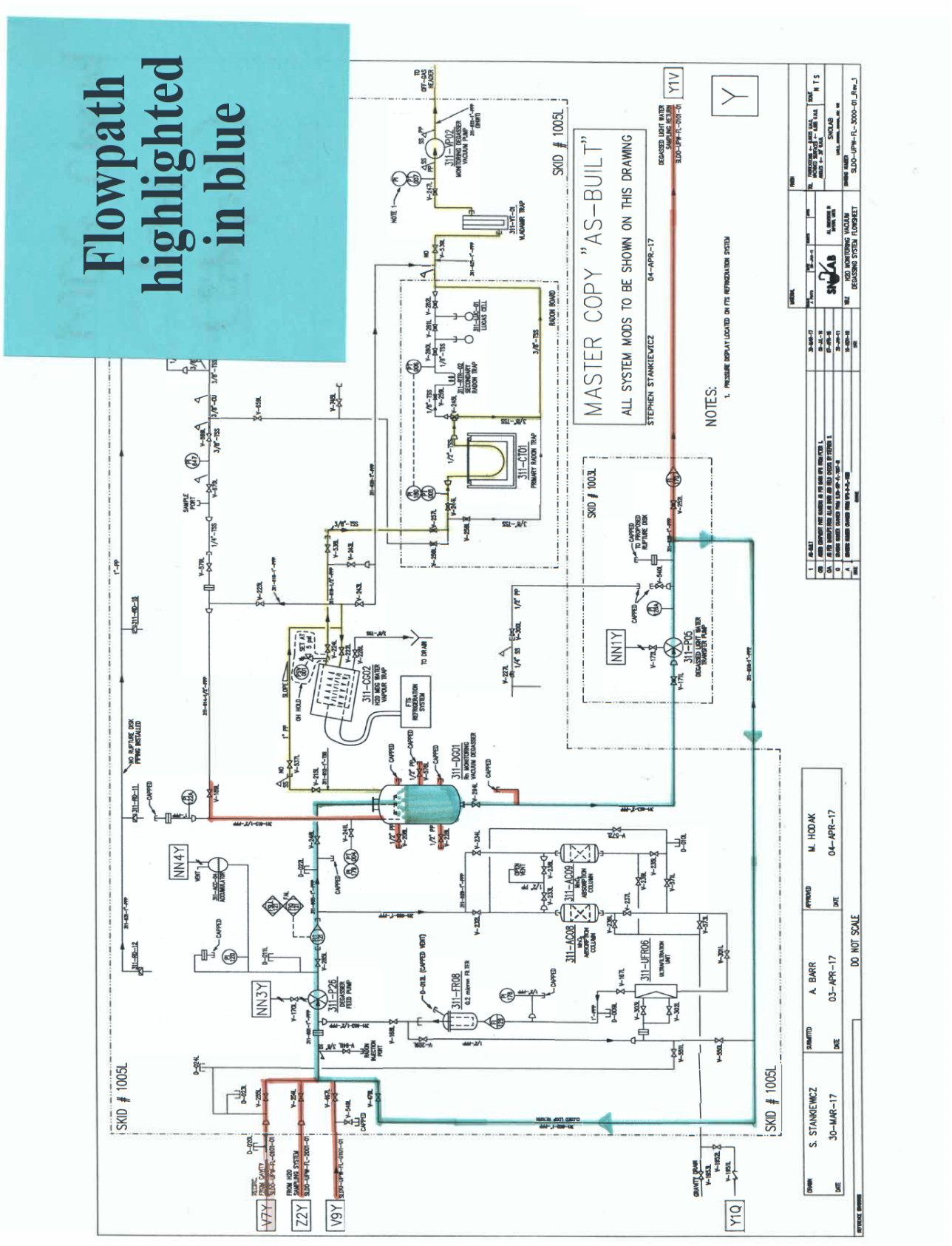

Figure 4.6: Closed-loop configuration for MDG background. Shaded blue line shows the flow-path of water with two diaphragm pumps. The brown lines show complete isolation from the UPW plant.

atoms entered into the assay system per hour. The end of the SNO experiment left the assay system in a decommissioned phase. During the commissioning phase of SNO+ assay system was revived and a closed loop assay was performed which measured 446 radon atoms/day which were in agreement with the SNO measurement. However, In 2018 the assay system developed a lot of leaks which is the reason behind the 31623 Rn/day measurement in 4.2.

Helium leak checking campaign was conducted throughout 2018 and parts of 2019 which were done to identify leaks and fix them and eventually reduce the background to an operational level. The operational level refers to the sensitivity of the assay system which ensures low enough background in order to accurately see the radon contribution coming from the cavity.

Leaks were identified and a leak rate of minimum 10^{-8} mbar l/s was ensured throughout all components of the assay system. This extensive effort led to a background reduction by a factor of ten. Table 4.3 shows the reduction of background level to approximately on average of 3700 atoms per day from 2018. The current background level shows a sensitivity of the board to 10^{-14} gU^{238}/gH_2O or higher. The background level even though higher than the SNO time is acceptable to measure the levels on the orders 10^{-13} g/g magnitude for SNO+. Closed loop assays are performed before a cavity assay to ensure that nothing has changed within the assay system.

All 2019 assays uses a blank background measurement which is an underestimation of the overall background of the system. Prior to Nov 2020, one of the diaphragm pumps were removed and the lines were exposed to mine air. Therefore, doing a closed loop assay (see Appendix A) was necessary and since then it has become a norm before a cavity assay. Once the loop was established, vacuum pump was pulling a significant amount of vacuum which indicates an absence of a leak and ensure secured connections. Interpretations of these results requires that the actual background of the assay system should be higher than what is measured because it excludes the piping that goes to the cavity of the detector. There is no definite way of including those piping into this assay to get an actual measurement of the background.

The Nov 2020 results indicated that about 2800 atoms per day were injected into the radon system which meant only 90 atoms entering the system within 45 minutes. Due to COVID and

	Blank	**Closed-Loop**			
Date	July 15$^{\text{th}}$ 2019	Nov 18$^{\text{th}}$ 2020	April 20$^{\text{th}}$ 2021	July 5$^{\text{th}}$ 2021	July 26$^{\text{th}}$ 2021
LC ID	LC 8	LC 16	LC 17	LC 18	LC 18
$\mathbf{B}_{\text{LC}}$ (cpd)	15	7	5.4	6	6
$\mathbf{t}_{\text{assay}}$(minutes)	60	45	60	45	30
Alphas	90	101	160	20	78
$\mathbf{t}_{\text{delay}}$(hours)	1	2	3	3	2
$\mathbf{t}_{\text{count}}$(days)	1.873	6.958	7.335	0.953	6.125
$\mathbf{R}_{\text{bcg}}$ (Rn/samp)	78.6 ± 20.4	90 ± 23.4	195 ± 51	111 ± 29	76 ± 20
$\mathbf{R}_{\text{bcg}}$ (Rn/day)	1894 ± 492	2884 ± 750	4716 ± 1226	3586 ± 932	3644 ± 947

Table 4.3: Measured levels of the background of the MDG since commissioning of SNO+ since November 2020. April results showed higher concentration than the rest of the measurements.

other scheduling reasons, assays remained on hiatus until April of 2021. In April 2021 assay, 195 radon atoms entered the system within an hour which corresponds to 4716 atoms/day, this number is considerably high and it could be be due to the out-gassing of radon from the system components. The two assays were performed in July 2021, and their results were 111 atoms in 45 minutes (74 atoms in 30 minutes) and 76 atoms in 30 minutes, respectively. The two results were consistent but the first assay of July had very small counting time due to some issue in the data acquisition system that aborted the counting.

4.2.6 Water Assay results

SNO+ shielding is crucial in minimizing non signal events that can leak into the region of interest for $0\nu\beta\beta$ signal. As mentioned in section 4.2.4, radon measurement allows to accurately determine the Uranium-238 concentration within the cavity assuming secular equilibrium. Water purification system include piping that extend into the cavity which are used to sample water for cavity assays. The four sample points that allow access to cavity are listed below and a pictorial representation is shown in Figure 4.7:

- V-202: Bottom of the cavity
- V-203: PSUP Equator
- V-204: Bottom of the PSUP
- V-206: Between PSUP and AV bottom

Water assays are performed in conjunction with the UPW operator present underground. One of the key things that need to be established prior to establishing flow from the cavity is that the Auto fill (cavity re-circulation) needs to be turned offline, in order to ensure that purified water from the plant does not gets mixed up with the incoming cavity water. Procedures written for the assays are thoroughly checked by plant operators to ensure that flow path is correctly established and doesn't pose any threats to the plant.

Location	**V-202**	**V-203**	**V-206**	**V-204**	**V-203**
Date	9^{th} May 2019	5^{th} June 2019	20^{th} June 2019	4^{th} July 2019	23^{rd} July 2019
LC ID	N8	N8	N8	N8	N8
$\mathbf{B}_{\text{LC}}$ (cpd)	15	15	15	15	15
$\mathbf{t}_{\text{assay}}$(minutes)	40	60	60	60	30
Alphas	517	375	481	513	71
$\mathbf{t}_{\text{delay}}$(hours)	1	1	1	2	2
$\mathbf{t}_{\text{count}}$(days)	3.61	5	3.860	4.744	0.875
$\mathbf{F}_{\text{(L/m)}}$	16	14(unstable)	18	18	18
$\mathbf{R}_{\text{bcg}}$ (Rn/sample)	52.7 ± 13.7	78.6 ± 20.4	78.6 ± 20.4	78.6 ± 20.4	39.3 ± 10.2
$\mathbf{R}_{\text{bcg}}$ (Rn/day)	1894 ± 492	1894 ± 492	1894 ± 492	1894 ± 492	1894 ± 492
$\mathbf{R}_{\text{water}}$ (Rn/sample)	1124 ± 292	537 ± 139	922 ± 240	893 ± 232	447 ± 116
$\mathbf{R}_{\text{water}}$ (Rn/day)	40563 ± 10546	12932 ± 3362	22220 ± 5777	21523 ± 5596	21484 ± 5585
C[g U^{238}/g H_2O]	2.97×10^{-13} g/g	1.03×10^{-13}g/g	1.44×10^{-13} g/g	1.40×10^{-13} g/g	1.40×10^{-13}g/g

Table 4.4: Cavity water assay results from 2019 with a constant board background. 5^{th} June assay results had an unstable water flow so the total flow rate is averaged out. Bottom of the cavity is reporting a higher concentration than the rest of the locations.

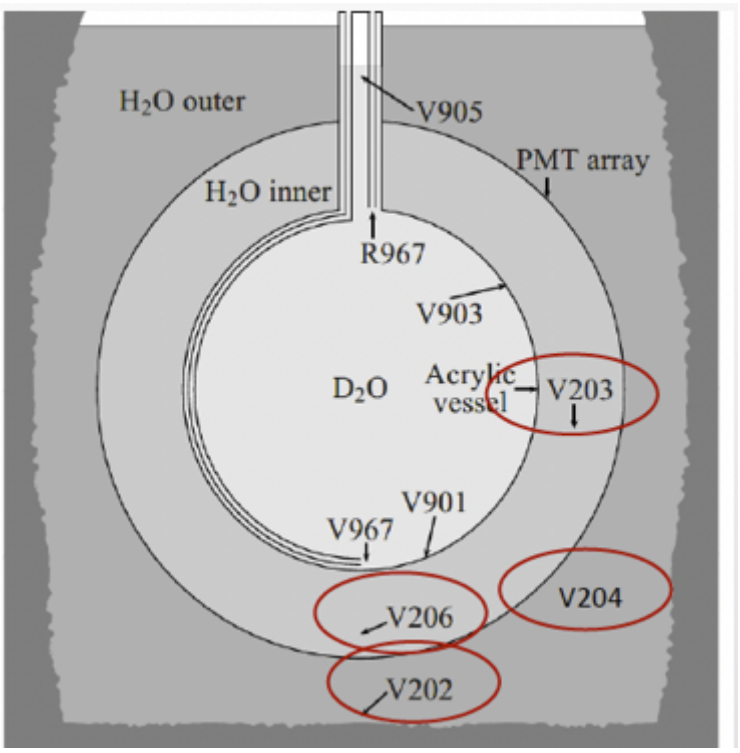

Figure 4.7: Old schematic of SNO detector with highlighted sample points. Sample points remained the same from transitioning of SNO to SNO+ except for the addition of V-204 sample point [25].

After long and extensive efforts, board backgrounds were reduced in early 2019. SNO+ started performing radon assays in order to determine the shielding effect of the cavity. The assay results are summarised in Table 5.6. The first assay performed was in May 2019 from the bottom of the cavity (V-202). The bottom of the cavity reported 2.97×10^{-13} g/g concentration, which is a little more than the set target of 2.1×10^{-13} g/g. Bottom of the cavity was expected to have a higher concentration because of being closer to the mine walls. The next assay performed was of the PSUP equator(V-203) in July 2019. The results showed a concentration of 1.03×10^{-13}g/g which is a factor of three lower than the bottom of the cavity, moreover, this measurement was also repeated in July 2019 and reported a concentration of 1.40×10^{-13}g/g. These two V-203 assays showed consistency between the two measurements and suggested stable background levels in the cavity.

The volume between AV and PSUP bottom (V-206) was also assayed in June 2019. The concentration measured was 1.44×10^{-13} g/g which is not only below the target but also indicates

Location	**V-203**	**V-203**	**V-204**
Date	19^{th} Nov 2020	23^{rd} April 2021	27^{th} July 2021
LC ID	LC 18	LC 18	LC 17
$\mathbf{B}_{\text{LC}}$ (cpd)	5.21	6	5.4
$\mathbf{t}_{\text{assay}}$(minutes)	30	45	45
Alphas	267	663	775
$\mathbf{t}_{\text{delay}}$(hours)	18	3	1
$\mathbf{t}_{\text{count}}$(days)	7.125	2.239	7.499
$\mathbf{R}_{\text{bcg}}$(Rn/day)	2884 ± 750	4716 ± 1226	3644 ± 947
$\mathbf{R}_{\text{water}}$ (Rn/sample)	441 ± 115	2270 ± 590	1208 ± 314
$\mathbf{R}_{\text{water}}$(Rn/day)	18310 ± 4761	68152 ± 17720	35134 ± 9134
$\mathbf{F}_{\text{(L/m)}}$	20	18	18
C[g U^{238}/g H_2O]	1.07×10^{-13}g/g	4.44×10^{-13} g/g	2.26×10^{-13} g/g

Table 4.5: Cavity water assays results over the years 2020 and 2021 with variable assay system backgrounds. 2021 measurements showed higher results due to a change in the mode of cavity re-circulation.

uniform background levels in the entire inner cavity volume. The bottom of the PSUP (V-204) was also assayed and a concentration 1.40×10^{-13} g/g was measured. All four locations showed promising results and showed equilibrium within the internal cavity concentrations. Moreover, the results also indicate that the PSUP structure provides extra shielding to the internal cavity water.

After July 2019, SNO+ shifted its focus to getting the AV filled with the scintillator, and with pandemic hitting early 2020, the water assays were put on pause. Access to SNOLAB was restored towards the end of 2020 and a cavity assay was scheduled. Prior to cavity assay, one of the diaphragm pump used on the assay skid to fill the MDG with water was replaced during early 2020. The replacement caused some of the lines to be exposed to mine air, therefore, closed-loop assay was performed to determine the background of the assay system each time before a cavity assays (see Appendix A). The MDG background results are all summarised in Table 4.3. The first sample point assayed was V-203 which showed a concentration of 1.07×10^{-13} g/g which is very consistent to the measurements taken in 2019. However, in December 2020 SNO+ changed the mode of cavity re-circulation, where water was taken from the bottom and fresh water was injected towards the top of the cavity. The change in circulation was done to cool down the cavity throughout rather than having the cavity being hottest at the top (18 degrees) and with being coolest at the bottom(12 degrees). Disruption of cavity temperature profile was expected to produce a higher concentration in the PSUP assay results. The temperature profiling in the figure 4.8 shows that changing the cavity recirculation cooled the cavity uniformly rather than being hottest at the top and coldest at the bottom.

In April of 2021, approximately 4 months after the change in cavity re-circulation, V-203 assay was performed. The assay showed a considerably high concentration of 4.44×10^{-13} g/g which is a factor of four higher from the last measurement. V-204 was also assayed, which showed a concentration of 2.26×10^{-13} g/g. This measurement was also a factor of two higher than the measurement from 2019. The change in recirculation had a huge impact on the cavity concentrations as it induced convection currents within the cavity which allowed radon to mix within the Cavity.

4.3 Conclusion

SNO+ periodically takes measurements from different locations of the cavity and determine radon levels in the cavity. Moreover, the assay background is also checked for consistency.

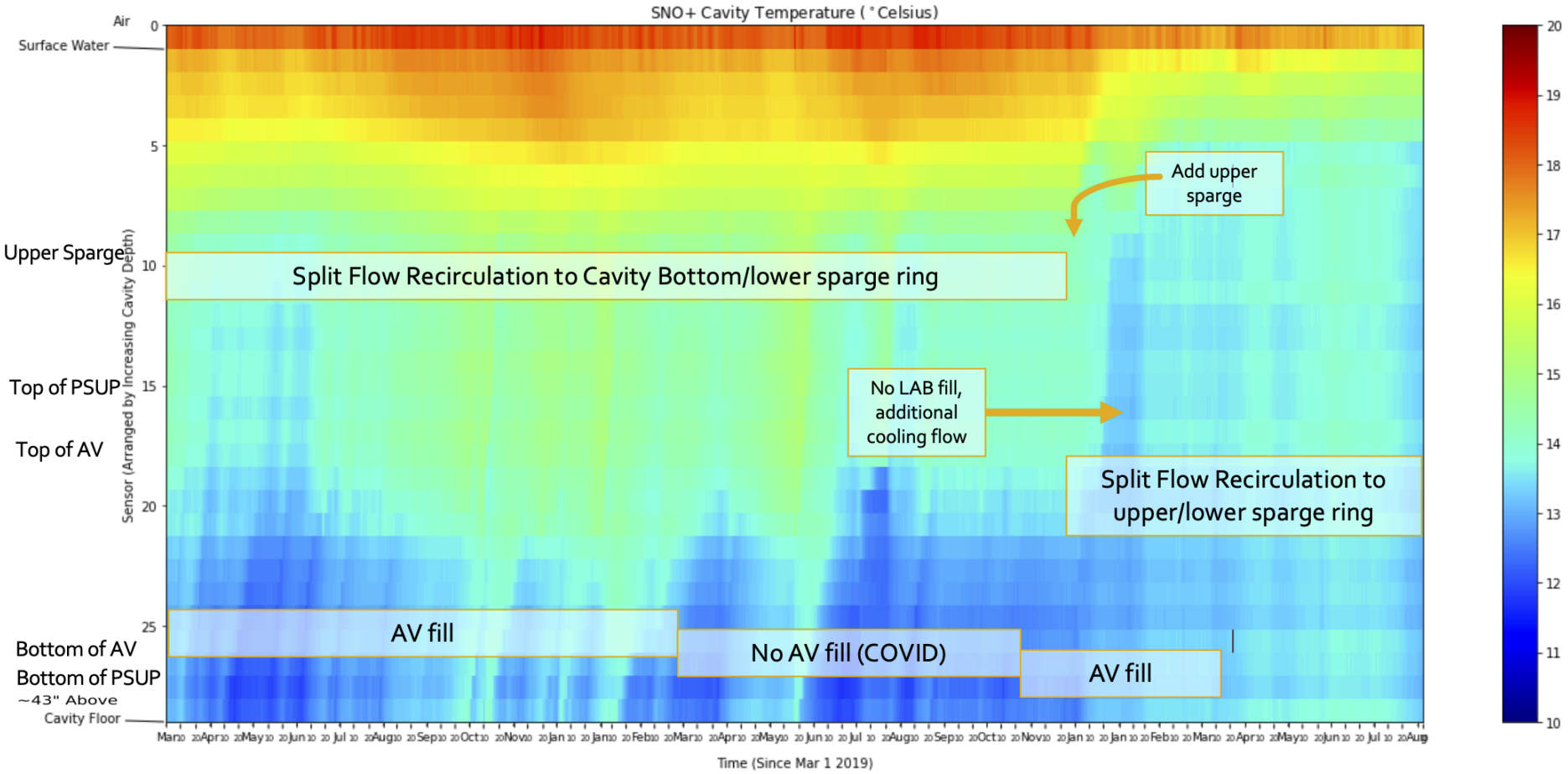

Figure 4.8: Cavity temperature profile from March 2019 to August 2021. In December 2021, cavity recirculation mode was changed that allowed an overall cooling effect in the cavity [54].

The assays results conclusively show that SNO+ is maintaining g/g concentrations within the background budget. Moreover, it can also be seen that the inner cavity volume has reduced background levels than the external cavity, which suggests that PSUP is also providing an additional shielding to the inner water. The temperature profile is very important in controlling the background and prevents radon from mixing in the detector due to convection currents.

The consistency of the results and the increased concentration measurements due to change in cavity recirculation provides evidence about the reliability of our assay systems and serves as a quality check for the ultra-pure water purification plant.

Chapter 5

Gas Radon Assays

5.1 Introduction

The low background budget for SNO+ requires radon exclusion from the detector. As mentioned in Section 2.1, SNO+ detector has a cover-gas over the neck of the AV and over the top of the cavity to mitigate the effect of radon ingress from the mine air. Moreover, purification plants such as the scintillator and tellurium plants have a cover-gas system in design to prevent radon ingress. The extensive cover-gas capabilities of SNO+ requires it to have an assay system which can measure the radon content within the nitrogen cover-gas and determine the reduction factor from the mine air. Performing radon assays on the cover-gas allow a direct measurement for the radon content and determine the effectiveness of cover-gas against the mine air.

5.2 Mobile Gas Radon board

Board History

Mobile radon board was constructed for SNO experiment and was primarily used for emanation measurements. Emanation measurements are crucial in determining the materials to be used within the detector. Ultrasonically cleaned materials are placed within the vacuum sealed chamber; the chamber is then pumped and purged and left to emanate for more than two half

lives of radon. Emanated radon is then assayed using the mobile radon board and emanation rate of the sample is determined. Prior to 2019 this board was tagged out for use due to big leaks in the system.

SNO+ decided to run a leak checking campaign on the board to make the board functional again. Leak checking was done by running vacuum on the lines using a leak checker and spraying helium gas on the lines, a subsequent increase in pressure on the leak checker would indicate a leak. The baseline leak rate was set at 10^{-8} mbar l/s; any leak higher than this would require a replacement of the part. Moreover, SNO+ was not only interested in emanation measurements but wanted to measure the radon levels within the covergas systems of the detector and its components which was different from the previous operational specifications of the board. All emanation measurements were performed under vacuum but in order to measure the radon content within the covergas, nitrogen gas needs to be flown at atmospheric pressure, which requires remeasuring of the gas board efficiencies.

Board Specifications

The gas radon board is built on a movable cart to allow easy access to the covergas source points. The board it self is made of 3/8" inches of stainless steel tube with swagelock connections and gate valves. The fundamental functioning of the gas board is very similar to the water assay board, where radon is cryogenically trapped in a primary trap. Figure 5.1shows the schematic of the updated radon board. The V-source is connected to either the UI, International Dewar, V-01 head tank, or any other possible source point in the future.

Nitrogen gas is flown at 1 L/m from the V-source and into the primary trap. The primary trap is cryogenically cooled down with liquid nitrogen. The V-10, which is a three way valve, is opened to vacuum in order to ensure uninterrupted flow of gases like Ar, N_2 and O_2 into the vacuum pump. Once the Radon extraction is completed, primary trap is isolated from the rest of the board and secondary is cooled down with liquid nitrogen. Extracted radon is then transferred into secondary and then volume shared into the Lucas cell. During the transfer, both traps are heated using a heat gun to ensure maximum transfer efficiency. Unlike the

water assay, this board does not have a back flow trap for preventing mine air ingress from the vacuum pump, or an FTS that prevents vapor from entering the traps.

A normal gas assay requires preliminary setup, which includes a thorough cleaning of the board. The board is pumped and purged for a few hours before the assay is started. Furthermore, all traps on the boards are baked in order to ensure any residual radon from a past assay or emanation gets flushed out. Further upgrades from late 2020 resulted in the addition of a pre-Trap and a 1/4 inch stainless steel line connection to the nitrogen bottle. Anything after the V-source was not included in the original SNO-era design of the board.

The addition of pre-trap enabled the purging of the board prior to each assay. Purging requires the flow of ultra pure nitrogen gas through the cryogenically cooled pre-trap through the entire board.

Radon Calculations

The radon content follows the same setup as shown in Section 4.2.4. Unlike the water board gas board only has one global efficiency. Therefore, the corrected Radon calculations are as follows:

$$\mathrm{R(atoms/sample)} = \frac{\mathrm{N} - \mathrm{B_{lc}} t_{\mathrm{count}}}{\varepsilon(\mathrm{e}^{-\lambda t_{\mathrm{delay}}})(1 - \mathrm{e}^{-\lambda t_{\mathrm{count}}})} - \mathrm{R_{bg}} \tag{5.1}$$

Where $\varepsilon = \varepsilon_{\mathrm{global}}$. Subsequently, the Radon(atoms/day) equation becomes:

$$\mathrm{R(atoms/day)} = \frac{(\mathrm{N} - \mathrm{B_{LC}} t_{\mathrm{count}})\lambda}{\varepsilon(1 - \mathrm{e}^{-\lambda t_{\mathrm{count}}})(1 - \mathrm{e}^{-\lambda t_{\mathrm{assay}}})(\mathrm{e}^{-\lambda t_{\mathrm{delay}}})} - \mathrm{R_{bg}} \tag{5.2}$$

Concentrations of gas assay results are not expressed as g/g, therefore, calculating concentration is much simpler. The concentration is expressed as relative to mine air; where the results of radon/litre is divided by the radon/litre of mine air. The Equation 5.1 then becomes:

$$\mathrm{R(atoms/l)} = \frac{1}{\mathrm{F}}\left[\frac{\mathrm{A} - \mathrm{B_{lc}} t_{\mathrm{count}}}{\varepsilon(\mathrm{e}^{-\lambda t_{\mathrm{delay}}})(1 - \mathrm{e}^{-\lambda t_{\mathrm{count}}})} - \mathrm{R_{bg}}\right] \tag{5.3}$$

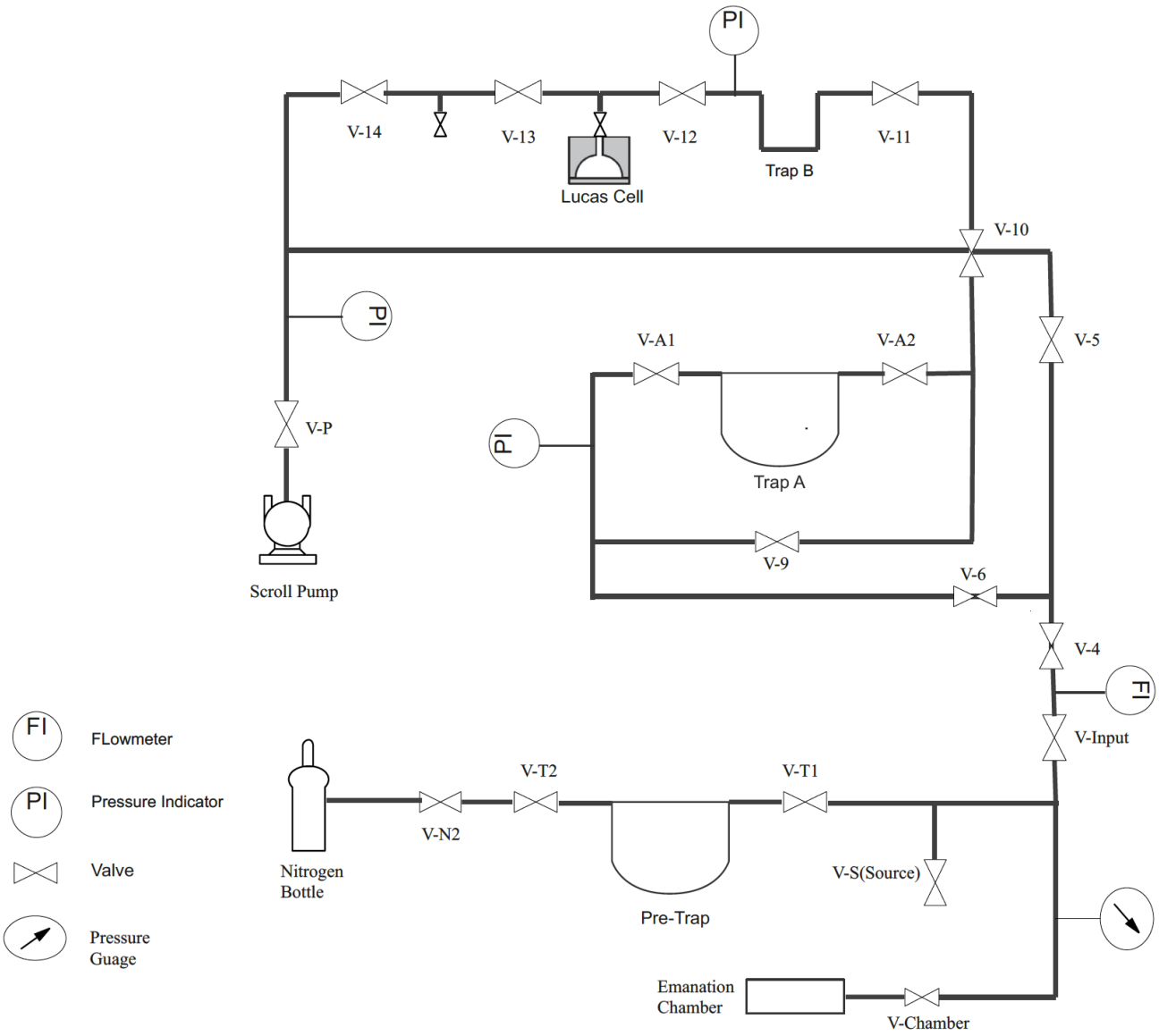

Figure 5.1: Radon Board schematic after 2020 modifications. Trap A and Trap B are the primary and secondary traps of the system. The pre-trap and the nitrogen line is newly added to the system.

Where F is the total flow of the sample gas used and is expressed in litres. In order to correctly measure the concentration, the result from Equation 5.3 is divided by the mine air concentration of 6.4×10^3 atoms/l. The concentration then can be expressed as:

$$\text{Concentration} = \frac{\text{R(atoms/l)}}{(6.4 \times 10^3)\text{atoms/l}} \tag{5.4}$$

5.2.1 Efficiency measurement

Prior to 2019, mobile radon board was used only for emanation measurements. The operational specification included using the board under vacuum, which is similar to the water board, therefore, water board efficiencies were assumed (see Table 4.1). However, that is not true anymore, not only the board is being used under atmospheric pressure but also extensive leak fixing and upgrades have been performed. The efficiency of this assay board needed to be measured and characterized.

The efficiency measurement is performed by flowing a gas of known amount of radon content through the radon board and then comparing it with the measured values. The known source is mine air in this case and the measured value is 1 litre of mine air contains 64000 rn atoms. The primary trap of the board is sensitive to the water vapour i.e it over-pressurizes the trap which greatly affects the transfer and counting efficiencies. Passing mine air also meant high moisture and CO_2 buildup in the lucas cell due to high concentrations in the lab environment. Therefore, drierite and NaOH columns were introduced to absorb the moisture and CO_2 respectively. Furthermore, upon testing it was found that drierite was not enough in trapping all the moisture so an an ice bath which was maintained at less $<$ -10 degrees was introduced and was found effective at preventing moisture from entering the board.

$$\text{Efficiency}(\varepsilon) = e^{(-4.58\times10^{-2})(x_{\text{minutes}})+5.04} \tag{5.5}$$

The efficiency measurements were fitted to an exponential curve with the equation 5.5, where x is assay time in minutes. The efficiency of the board is the global efficiency which includes

Date	Assay Time(min)	Efficiency
20/04/2021	1.5	153 %
16/04/2021	5.5	119 %
07/10/2019	10	92.0%
07/07/2021	30	36.3%
26/07/2021	30	34.5%
06/08/2021	30	44.8%
Averaged	30	38.5 %
07/07/2021	45	23.85%
26/07/2021	60	9.23%

Table 5.1: Efficiency of the board by assaying mine air through the Radon board at 1LPM. The 2019 board efficiency of 92 % is also included in the table.

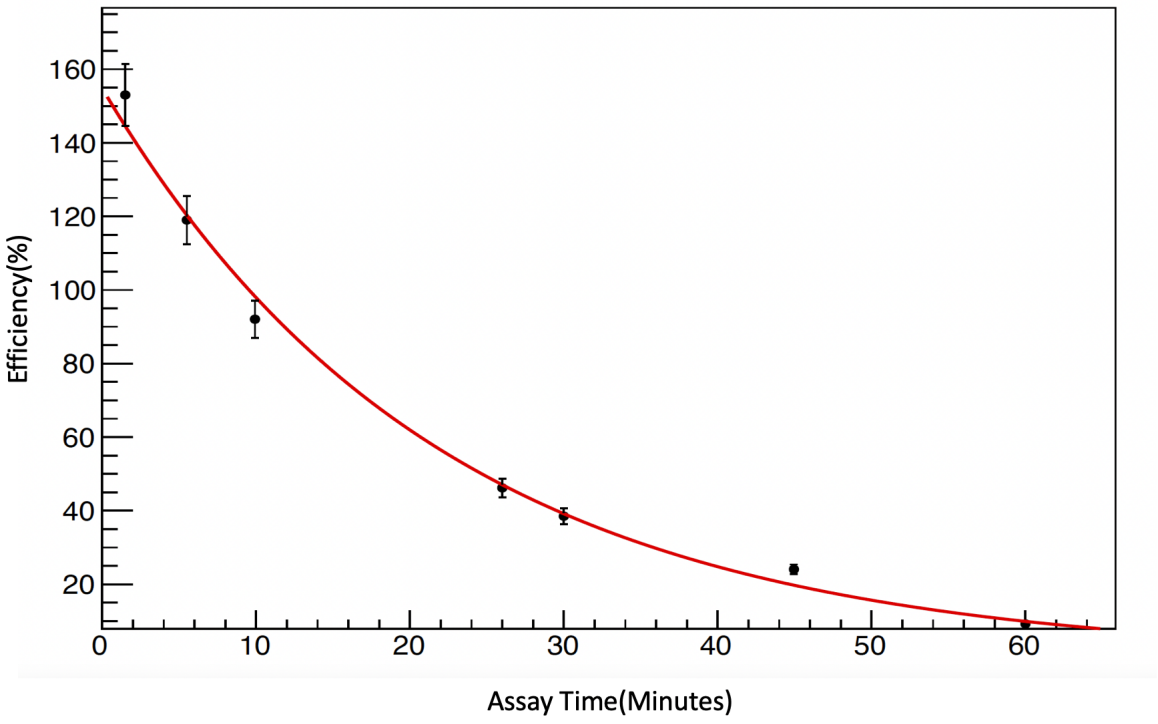

Figure 5.2: Efficiency versus Assay Time at 1 LPM. The global efficiency greatly decreases with time indicating a non constant efficiency of the board.

the three alphas from radon decay, therefore, the efficiency for some of the assay times is more than a 100 %. The equation 5.5 will be used to extrapolate the unknown efficiencies. Efficiency measurements provides evidence of warming up of the primary trap which affects the trapping efficiency and the overall efficiency of the board. Longer assay though an asset for increased statics, have a profound affect on the measurements. The efficiency measurements were also used to determine the uncertainty within the measurement. The 30 minute assay measurements were repeated and the variance between the three measurement was used to find the uncertainty. The uncertainty was calculated from $\sqrt{\text{var}}$ and it was found to be 5.5 %, and this uncertainty will be used throughout this chapter.

5.2.2 Board Background

The board background is measured by pulling a vacuum throughout the board and performing the assay under vacuum conditions. Background measurements are crucial in determining the sensitivity of the radon board. The modifications of the radon board performed in 2020 introduced a pre-trap which allowed any residual radon within the nitrogen gas to be cryogenically trapped for background measurement, however the evidence of trap warming up from efficiency measurements in section 5.2.1 raised concerns on the functionality of the pre-trap as well. If the pre-trap warms up in a similar fashion as the primary trap then it defeats the purpose of the pre-trap. Therefore, the measurements done with using the nitrogen gas was removed and vacuum measurements were used to determine the board background. The efficiency measurement was done at 1 LPM of mine air at atmospheric pressure, therefore, the determined model can not be used to determine the efficiency of the board at vacuum due to which water board efficiency was assumed for this measurement.

5.2.3 Universal Interface Assay

Radon Assay of the Universal interface (UI) is performed to determine the radon concentration within the cover-gas of the detector. Nitrogen gas is extracted from the universal interface at 1 litre/minute using the vacuum pump on the mobile radon gas board. UI consists of the volume

Date	17^{th} Nov 2020
LC ID	LC18
$\mathbf{B}_{\text{LC}}$ (cpd)	7
$\mathbf{t}_{\text{assay}}$(minutes)	60
$\varepsilon_{\text{global}}$	1.42
Alphas	77
$\mathbf{t}_{\text{delay}}$(hours)	2.91
$\mathbf{t}_{\text{count}}$(days)	6.95
$\mathbf{R}_{\text{bcg}}$ (Rn/sample)	47 ± 2.5
$\mathbf{R}_{\text{bcg}}$ (Rn/day)	1135 ± 62.42

Table 5.2: Board background of the board using water board efficiencies from 4.1.

above the liquid scintillator within the neck of the AV. Moreover, this cover gas system consists of three bags which compensate the pressure difference that occur during normal operations of the mine. The Figure 5.3 depicts the SNO+ AV cover gas system.

UI assays were performed both before and after the modification of the radon board in 2020. The sensitivity of the radon board to vapor have resulted in failed attempts to assay the covergas from the UI. To mitigate this effect, an ice bath is prepared with a temperature of $< -10^{\circ}$C. The nitrogen gas passes through the ice bath before it enters the radon board for trapping and counting. The Table 5.6 summarizes all the UI assay results performed from 2019 till 2021.

The allowed background budget for the UI is 650 decays/day. Therefore results presented in Table 5.6 needs to be interpreted in decays/day. The activity is calculated by using the following relations:

$$\text{Activity} = \lambda N \tag{5.6}$$

Where N is the total number of radon atoms present in the UI and λ represents the decay constant of radon. Assay results needs to be normalized for the entire UI volume in order to accurately calculate the total number of atoms present in the UI . The UI consists of about 1950 litres of ultra pure nitrogen gas. Table 5.4 summarizes the UI results in form of total activity within the entire UI.

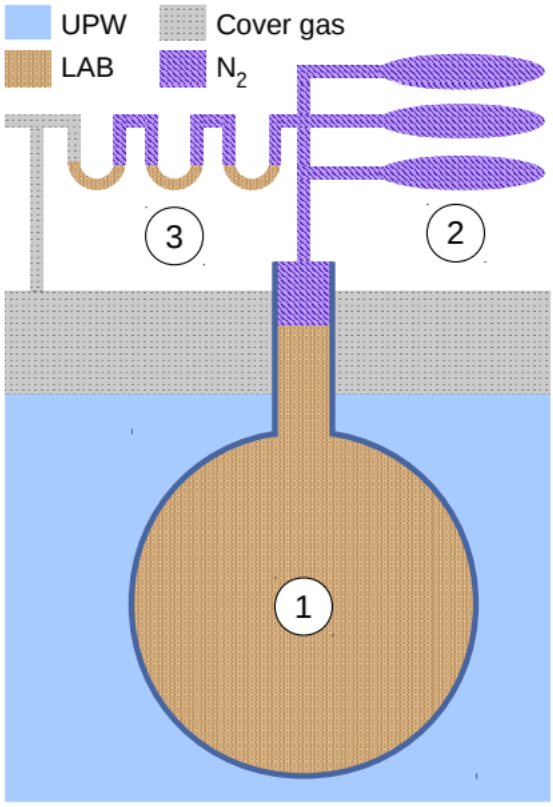

Figure 5.3: Cover-gas systems of SNO+ Detector. (1) shows the scintillator filled AV volume. (2) represent the AV cover-gas system filled with N2, and (3) represent the U-trap which contain both LAB and nitrogen gas. Grey area above the cavity represents the nitrogen cover-gas of the cavity[11]

	Top of UI				Rn Monitor	
Date	18^{th} Dec 2019	15^{th} Jan 2020	30^{th} March 2021	30^{th} March 2021	31^{st} March 2021	31^{st} March 2021
LC ID	LC14	LC14	LC18	LC16	LC21	LC20
$\mathbf{B}_{\mathrm{LC}}$ (cpd)	14	14	7	6	3	3
$\mathbf{t}_{\mathrm{assay}}$(minutes)	15	39	30	30	45	40
Volume(L)	15	39	30	30	45	40
$\varepsilon_{\mathrm{global}}$	0.77	0.258	0.385	0.385	0.238	0.247
Alphas	639	341	75	82	37	77
$\mathbf{t}_{\mathrm{delay}}$(hours)	44	3	3	1.5	18	15
$\mathbf{t}_{\mathrm{count}}$(days)	20.72	6.86	8.47	8.46	7.73	8.72
$\mathbf{R}_{\mathrm{bcg}}$ (Rn/sample)	11.7 ± 0.64	30.6 ± 1.68	23.55 ± 1.29	23.55 ± 1.29	35.3 ± 1.94	31.4 ± 1.72
$\mathbf{R}_{\mathrm{UI}}$ (Rn/sample)	634 ± 34.9	1328 ± 73	29.5 ± 1.62	81 ± 4.5	52.6 ± 2.9	258 ± 14
C[rel. to mine Air]	6.61×10^{-04}	5.32×10^{-04}	1.53×10^{-05}	4.22×10^{-05}	3.05×10^{-05}	1.13×10^{-04}

Table 5.3: UI assay results from over the course of two years. 2019 and 2020 results report higher radon concentration due to exposure of UI to mine air.

Assay Date	Rn Atoms/litre	Total Atoms(N)	A(decays/day)
18^{th} Dec 2019	42	83182	15056
15^{th} Jan 2020	34	66946	12117
30^{th} Mar 2021	0.98	1932	350
30^{th} Mar 2021	2.7	5305	960
31^{st} Mar 2021	1.15	2271	410
31^{st} Mar 2021	6.45	12674	2294

Table 5.4: UI Activity determined from normalized UI assay results. March 2021 results shows that UI activity is mostly lower than the 650 decays/day target.

On 11^{th} December 2019, PFA tubing was deployed in the AV due to which UI was opened for about three hours. PFA tube was deployed through the center of the detector to extract the water from the bottom of the AV in order to facilitate the volume displacement filling of the LAB. Two assays were performed to determine the state of the the UI, one on 18th December 2019 and the second on 15^{th} January 2020. The first assay showed 15056 decays/day and after 28 days the second assay showed a drop in activity down to 12117 decays/day. The first assay is an evidence of an exposure of UI to mine air but the second assay hinted towards a possible leak in the UI because after almost 7 half lives of radon, second assay result was expected to be much lower which was not the case.

A leak checking campaign was conducted early 2021 to fix the leaks on the UI which had an impact on the state of the UI. Four assays were performed from two different locations: Top of UI and Radon monitor. The two subsequent assays from top of UI were performed on the 30^{th} March 2021 and showed 350 decays/day and 960 decays/day. The second set of assays was performed on 31^{st} March 2021. The results were 410 decays/day and 2294 decays/day. The two sets of assay performed in March 2021 showed a higher radon content for the second subsequent assay. The increase seen could be due to radon build up within the connecting line of the UI and radon board or due to the residual radon from the previous assay. All the assays performed in 2021, except one shows a 10^5 reduction factor which indicates proper functioning of the covergas system of SNO+ experiment.

Date	07^{th} Oct 2019	09^{th} Oct 2019	4^{th}Feb 2021
LC ID	LC14	LC14	LC18
$\mathbf{B}_{\mathrm{LC}}$(cpd)	12	12	7
$\mathbf{t}_{\mathrm{assay}}$(minutes)	45	30	50
Volume(L)	45	30	50
$\boldsymbol{\varepsilon}_{\mathrm{global}}$	0.2385	0.385	0.156
Alphas	78	12	77
$\mathbf{t}_{\mathrm{delay}}$(hours)	1	2	2
$\mathbf{t}_{\mathrm{count}}$(days)	1.490	0.489	5.91
$\mathbf{R}_{\mathrm{bcg}}$(Rn/sample)	35.3 ± 2	23.5 ± 1.29	39.25 ± 2.15
R (Rn/sample)	1037 ± 57	292 ± 17	312 ± 17
C[rel. to mine Air]	3.60×10^{-04}	1.52×10^{-04}	9.74×10^{-05}

Table 5.5: International assays results from over the course of two years. The last measurement showed a very low concentration due to poor efficiency at longer assays.

5.2.4 International Dewar Assay

International Dewar is located at SNOLAB that is independent of SNO+, but plays an important role for the experiment. International Dewar is filled with nitrogen and ensure stable flow to the cover gas systems. It provides cover-gas to SNO+ cavity, scintillator purification plant, and tellurium plant.

The radon board is connected to the international dewar by a small polypropylene line by a 1/4' VCR connection. International assays are different than UI assays as there is no presence of water vapour, therefore, establishment of an ice bath is not necessary.

The first International assay was performed on 7^{th} October 2019 which showed a concentration of 3.60×10^{-4} relative to the mine air. The second assay was performed on 9^{th} October 2019 which showed a concentration of 1.52×10^{-4} relative to the mine air. These two measurements showed 10^{-4} reduction factor from the mine air. After the board modification, International assay was repeated in February 2021 which used 50 litres of gas and showed a concentration of 6.82×10^{-5} relative to the mine air.

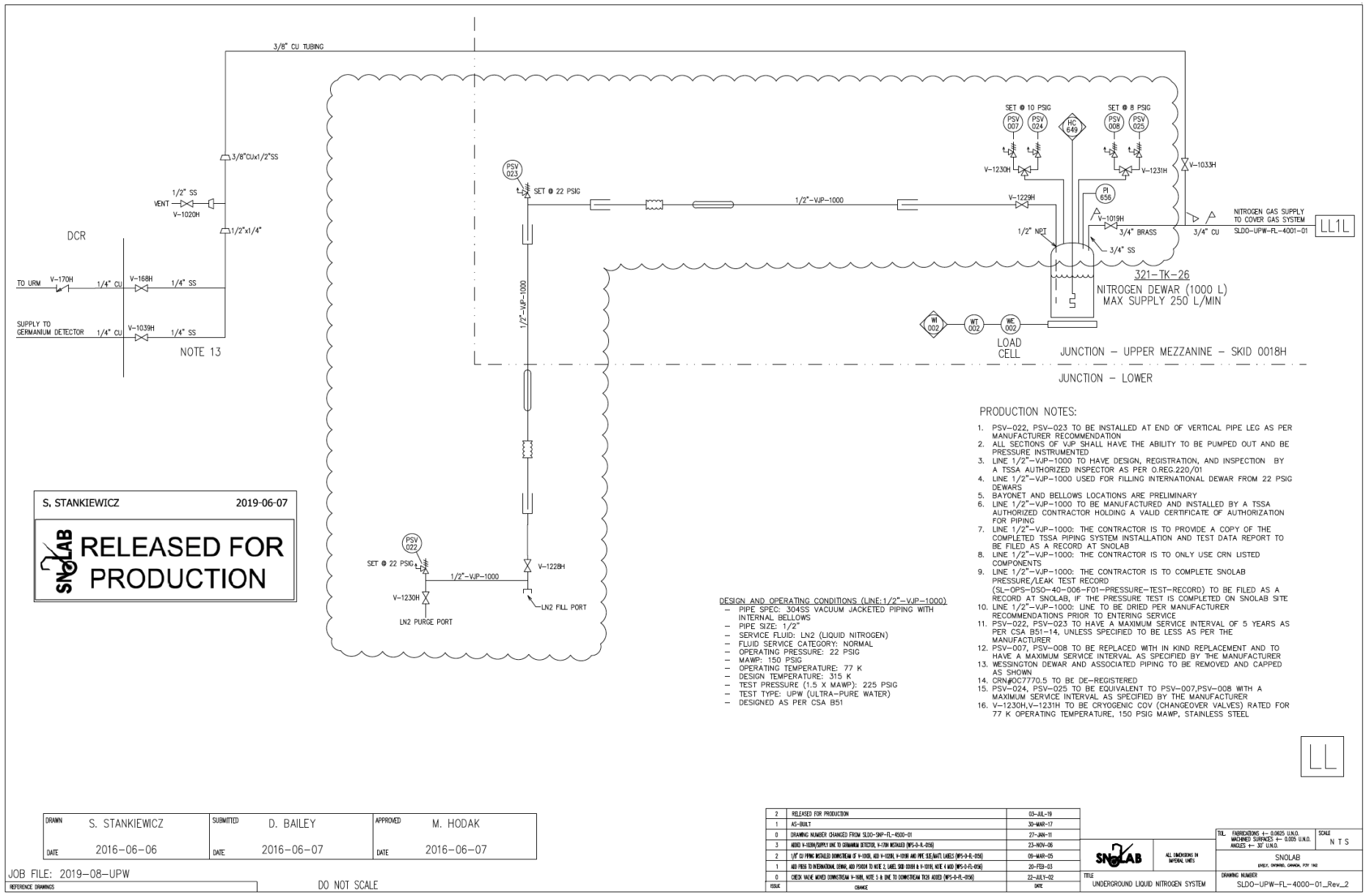

Figure 5.4: International dewar flow sheet. The dewar supplies cover-gas to SNO+ cavity, scintillator purification plant, UPW plant, and Tellurium plant.

5.2.5 VO1 Assay

SNO+ remained in the partial fill phase from 2019 till 2021 where the AV was filled with liquid scintillator. The Scintillator plant is located underground where the LAB is purified before it enters the AV (see Section 3.10 for detail working of the Scintillator plant). VO1 is the final vessel where the LAB is stored before it enters the detector. It has a cover-gas which acts as a barrier from mine air to enter into the vessel. SNO+ experiment has a very low background budget for ^{238}U and ^{232}Th decay chains. Radon assay of the cover gas is necessary to determine the background of the VO1 and to get an insight of the uranium backgrounds of the LAB and the scintillator plant.

Valve D-1225-01 was used to extract cover gas from VO1 at 1 L/m rate. The radon gas board can not handle LAB vapor, therefore, an ice bath was installed right after the outlet of the VO1 and before the inlet to the radon board with a stainless steel line which would freeze the LAB vapor.

The idea was to extract about 30 - 45 litres of gas through the VO1 during active filling. The assays were performed when the AV fill had been online for two to three days so the accurate condition inside the V01 head tank could be assessed. The assay time was increased from 30 minutes depending upon the effectiveness of the ice bath, the stability of the fill, and adjustment of the V01 cover gas. The VO1 configuration during the assay was set at fifty percent LAB volume and fifty percent cover gas.

The first assay extracted 40 litres of gas and reported a concentration of 3.66×10^{-04} lower than the mine air. Following this assay, filling was paused for several months due to the COVID-19 pandemic. The filling resumed towards the end of 2020 and continued filling until March of 2021. The second assay was performed on 25th Feb$^{\text{th}}$ 2021 and assayed 45 litres of nitrogen gas and reported a concentration of 1.01×10^{-04} relative to mine air; which is a factor of three lower concentration than the last measurement. The third and the last assay during the bulk fill was planned on 23$^{\text{rd}}$ March 2021, a week before the fill concluded, and extracted 30 litres of gas and showed a concentration of 5.39×10^{-05} lower than the mine air. The first and the second assay measurements corresponds to the reduction factor of 10^4, which shows consistent

Date	10^{th} Mar 2020	25^{th} Feb 2021	23^{rd} Mar 2021
LC ID	LC16	LC17	LC17
$\mathbf{B}_{\text{LC}}$ (cpd)	4	6	6
$\mathbf{t}_{\text{assay}}$(minutes)	45	45	30
Volume(L)	45	45	30
$\varepsilon_{\text{global}}$	0.2385	0.2385	0.385
Alphas	99	92	85
$\mathbf{t}_{\text{delay}}$(hours)	3	1	1
$\mathbf{t}_{\text{count}}$(days)	2.62	6.46	7.997
$\mathbf{R}_{\text{bcg}}$ (Rn/sample)	35.3 ± 2	35.3 ± 2	23.55 ± 1.29
$\mathbf{R}_{\text{VO1}}$ (Rn/sample)	968 ± 53.2	290 ± 16	103 ± 5.66
C[rel. to mine Air]	3.66×10^{-04}	1.01×10^{-04}	5.36×10^{-05}

Table 5.6: VO1 assay results from over the course of two years during normal LAB filling operations

results from the international tank results mentioned in Table 5.5. These results are a good indication that there is no major leak in the scintillator purification plant and no background is added between the international dewar and VO1. The February 2021 assay does show a higher concentration than the February result of the international dewar which could indicate a leak in VO1 vessel or scintillator plant but was ruled by a lower radon concentration from the March 2021 assay. V01 results can not be used to determine the overall activity in VO1 because of the ever-changing conditions of V01 during filling. The gas and liquid volume is never stable during filling, therefore, an overall activity can not be determined.

5.3 Conclusions

The SNO+ has extensive cover gas systems in place that mitigate the risk of radon ingress into the detector components. The radon board was modified and corrected for any leaks that persisted earlier; resulting in reduced background levels for the board. The board was calibrated using mine air and a time dependency within the efficiency measurement was seen. The board is fully functional and has been successfully taking measurements for different cover-gas locations within SNO+.

Several assays were performed at different locations including the UI, International dewar,

and VO1 head tank. The UI mostly showed some below target levels for uranium backgrounds in 2021. Post modifications, the international and VO1 showed a reduction of 10^{-05} which is an improvement that suggests that board modifications have a profound effect in improving the sensitivity of the board. All covergas systems of SNO+ are working according to the expectation and are very effective in preventing radon ingress into the SNO+ detector.

Chapter 6

External ^{214}Bi Analysis

6.1 Introduction

Chapters 3 and 4 establishes the uranium decay chain as one of the most important background for SNO+ due to it's prevalence within the mine environment and radioactivity that can obscure the physics signals. The Uranium isotope although long lived has a decay chain that can produce daughter nuclei which upon decaying emit radioactive emissions that lie within the region of interest for neutrino-less double beta decay. This chapter goes over the external background that is present within the water volume between the PSUP and the AV, although present externally but can emit high energy gammas that can propagate through the AV wall and into the scintillator volume.

Chapter 4 goes into detail about direct measurements of ^{222}Rn in cavity water through Radon assays (*ex situ*), while this chapter will go over the measurement of beta particles coming from the decay of ^{214}Bi in order to determine the g/g concentration in the cavity water through detector data (*in situ*). The agreement between the *ex situ* and *in situ* measurement would give confirmation about the reliability of the radon assay system and accuracy of the developed algorithms to determine the background concentrations. Moreover, these measurements will also ensure that SNO+ cavity remains under the target background level and will also report any radon ingress into the cavity and provide an early alert for malfunctions in the ultra pure

water purification plant.

6.2 Cherenkov Radiation

Cherenkov radiation is an electromagnetic radiation which is emitted when a charged particle carrying an electric field travels faster than the speed of light in a given medium ($n > \beta$). With n being the refractive index of the given medium and β being defined as v/c, where v is the velocity of the particle and c is the speed of light. The Cherenkov emitted cone has an open angle of:

$$\mathrm{Cos}\vartheta_c = \frac{1}{\beta n}, \tag{6.1}$$

The cherenkov cone with angle ϑ_c is seen in Figure 6.1. Equation 6.1 shows that there is a threshold condition of ($n\beta > 1$) below which no cherenkov radiation will be emitted and also confirms the angular dependence upon the relativistic speed of the particle [28]. Moreover, the radiation emitted will also be in the direction of ϑ_c and interference of waves will prevent the radiation to go in any other direction which allows to determine the position, direction, and energy of a cherenkov event [42]. The rate of the energy radiated by the particle emitting a cherenkov radiation over a length l is given by [42]:

$$W = \frac{e^2 l}{c^2} \int_{n\beta>1} \Big[1 - \frac{1}{n^2\beta^2}\Big] \omega \, d\omega \tag{6.2}$$

Where e is the electron charge, l is the distance travelled along the path of propagation, and ω is the photon frequency. The integral over ω is such that the cherenkov condition of $n\beta > 1$ is met which means that below this threshold no photons will be emitted. One of the most ideal candidate for a cherenkov detector is water with n being 1.33, most famous cherenkov experiments were, SNO [27] and Superkamiokande [43].

During the water phase of the experiment, SNO+ AV was filled with ultrapure water which was known as the water phase of the experiment(explained in detail in section 2.2.1). The cavity

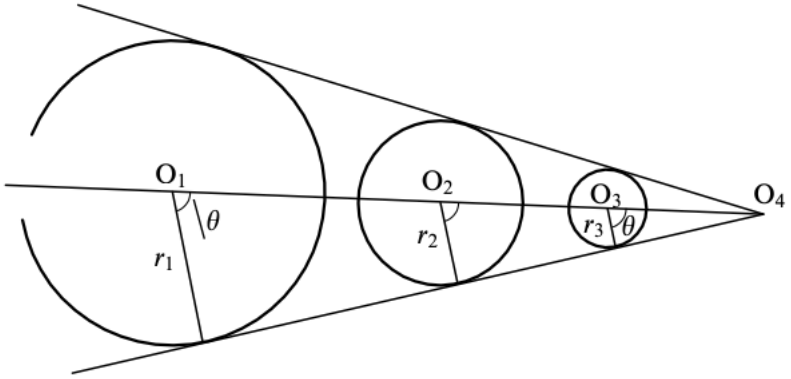

Figure 6.1: Cherenkov radiation cone for a particle travelling from position O_1 to O_4. Spherical waves appear at points where the particle passed [28].

of SNO+ will be kept filled with ultra pure water through all the phases of the experiment. All physics analysis during the water phase and all background measurements in the inner cavity used cherenkov radiation as the main detection technique. This chapter looks at the cherenkov photons being emitted by beta particles coming from ^{214}Bi decay.

6.3 Event Classifiers

6.3.1 Nhits

In determining the events taking place within the SNO+ detector, photomultiplier tube hits is the primary mode of detection and the most basic measure of energy. N_{hits} is defined as the total number of photomultiplier hits in an event within a timing window of 100 ns. In the PSUP water and during the water phase this number depends upon the generation of cherenkov photons from a particle travelling with relativistic speed within the water. While in scintillator phase, PMTs are hit with photons originating from scintillation light. The light yield during the water phase and for the PSUP is 6 N_{hits}/MeV while for Te-loaded phase is 480 N_{hits}/MeV. The significant increase in N_{hits} during Te-loaded phase is due to the high light yield of the scintillator.

6.3.2 Isotropy (β_{14})

The isotropy of the event can be used to distinguish a cherenkov event from a scintillator like event. A Cherenkov event is a very sharp signal and its isotropy can be defined by the angles between the PMTs hits and the fitted event vertex [37]. The angle ϑ_{i} is the angle between the the hit PMT and the reconstructed event vertex while ϑ_{ij} is the angle between the PMTs i and j to the fitted event vertex. The angles subtended by the cherenkov ring can be seen in figure 6.2. The angle ϑ_{ij} is expressed as the the legendre polynomials and the separation variables are defined as [37]:

$$\beta_l = \frac{2}{\mathrm{N(N-1)}}\left[\sum_{\mathrm{i=1}}^{\mathrm{N}}\sum_{\mathrm{j=i+1}}^{\mathrm{N-1}} P_l(\cos\vartheta_{\mathrm{ij}})\right] \tag{6.3}$$

β_l is the beta parameter which gives information about the spatial hit pattern of the event and P_l is the legendre polynomial. This parameter was first defined by SNO experiment to provide a clear separation of electron and neutron events coming from CC or NC interactions (see section 1.3.1). It was found that $\beta_1 + 4\beta_4 = \beta_{14}$ provided the best separation and this classifier has been implemented in SNO+ RAT software for analyzing cherenkov events and reject light that is highly isotropic [37].

6.3.3 ITR Cut

The In Time Ratio(ITR) classifier was also first developed by SNO experiment which makes use of the time residual distribution of the cherenkov events and distinguish them from scintillator events and instrumental backgrounds. The instrumental backgrounds are non radioactive backgrounds mainly dominated by photons emitted from the PMTs during normal operations and are termed as "flashers". The concept behind the ITR cut is based on the sharpness of the cherenkov signal and aims to remove events that have a broader time distribution than that of a cherenkov signal. The ITR cut is constructed by finding the ratio of prompt events in the time residual window of [-2.5 ns, 5.0 ns] to the total number of calibrated hits [57]. The figure 6.3 shows the distribution of backgrounds and neutrino data measured by SNO experiment.

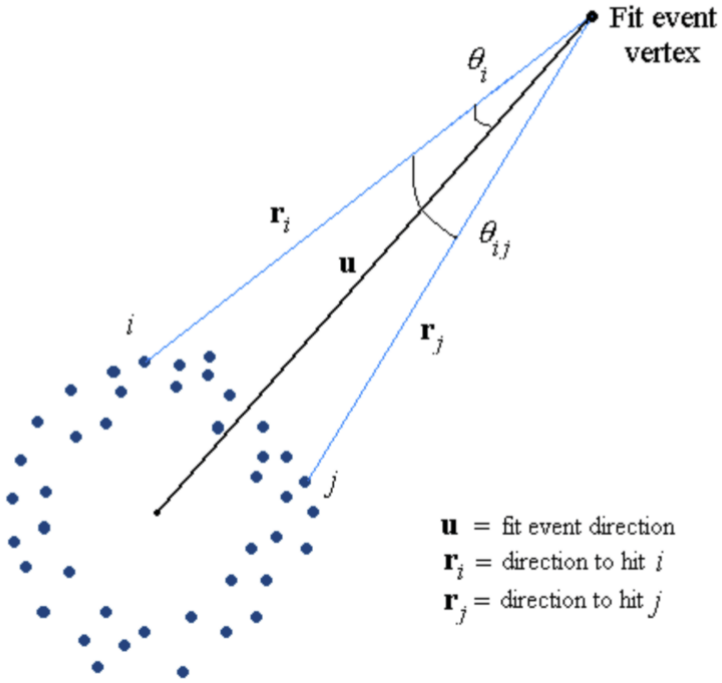

Figure 6.2: A Cherenkov ring with angles respective of fit event vertex. These angles are use to determine the β_{14} Isotropy parameter [37].

The ITR cut of 0.55 is most effective in getting rid of any backgrounds coming from the flashers or neck events while retaining most of the physics signal [57].

6.3.4 Nhitscleaned

An additional cut of nhitscleaned is used which is a another way of removing events coming from the PMT noise. This cut removes all events that have a $N_{hits} < 15$ which is dominated by instrumental backgrounds. Moreover, during data processing SNO+ only reconstructs 10 % of the events below 10 N_{hits}, therefore, this cut only acts as a cleaning cut rather than an event classifier.

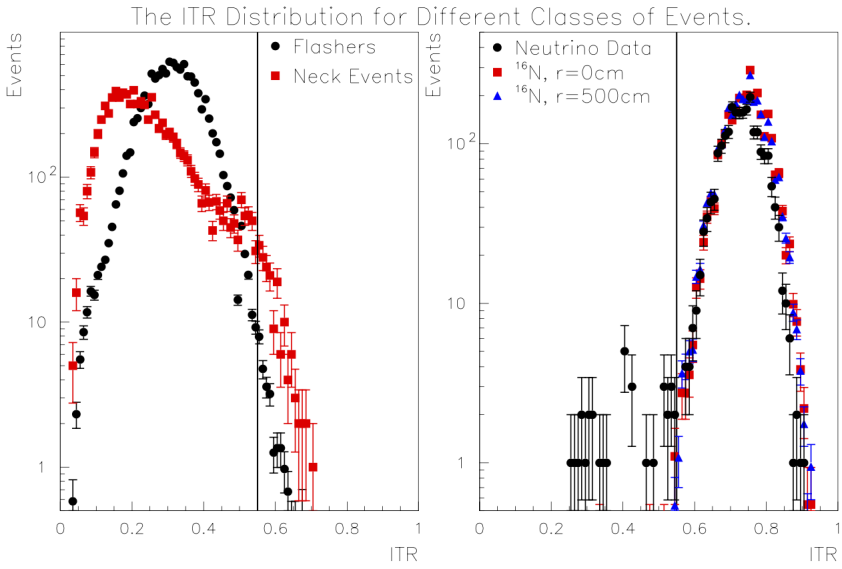

Figure 6.3: The ITR distributions measured by SNO for instrumental backgrounds (left), and calibration data and Neutrino data post instrumental cuts(right) [57].

6.4 Method of Analysis

In July 2019, the addition of PPO and scintillator officially ended the water phase of the experiment and started the partial fill phase. The classifiers like β_{14} and ITR will be used in order to distinguish the cherenkov events from scintillator events and isolate all the cavity events from internal events. Using SNO+ RAT software, beta decays from ^{214}Bi were simulated in the PSUP for the stable regions of filling (i.e where there is no ongoing LAB fill). Monte Carlo (MC) simulations were generated and compared to the detector data with the assumption that all detected events are caused by the ^{214}Bi from the Uranium decay chain.

The analysis is then applied to the reconstructed cherenkov events in stages, the main steps are outlined below:

- Detector data is downloaded from the SNO+ grid. Only those runs are selected that are classified as physics runs and pass the run selection criteria. Analysis is run on a day to day basis which consists of all the physics runs in a day.

- In time ratio(ITR) cut is implemented which looks at the events within a prompt timing window.(See section 6.3.3). This cut is highly efficient in removing all instrumental

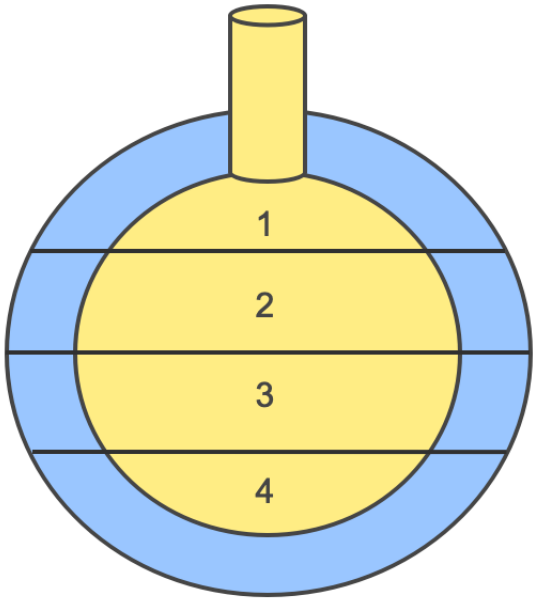

Figure 6.4: Schematic of the detector with four different volume regions for both internal and external volume regions. Radial slices range from -8000 to +8000mm with 0 being the center of the AV.

backgrounds from the data. ITR > 0.55 is used.

- β_{14} classifier is used to reject the emitted light that is highly isotropic (See section 6.3.2). The $\beta_{14} > 0.4$ is used.

- N_{hits} is the energy proxy for SNO+. $N_{hits} < 40$ is used.

- Nhitscleaned < 15 is used to remove all of the PMT noise and low energy events.

- The detector region is divided into four regions of both separate internal AV volume and external PSUP volume, as can be seen in Figure 6.4. Region 1 is from 4000mm $<$ z $<$ 8000mm, Region 2 is from 4000mm $<$ z $<$ 0, Region 3 is 0 $<$ z $<$ -4000mm, and Region 4 is -4000mm $<$ z $<$ -8000mm; with zero being the center of the AV. This chapter only looks at the external regions.

- The Fuducial Volume (FV) cut uses an inner radial cut 6500 $<$ r $<$ 7500 to exclude events that occur within the AV and also events that are very close to the PMTs, this

inevitably reduces the FV cut's efficiency. However, this is a necessary sacrifice to avoid contamination from various sources into this study.

- The total number of surviving Monte Carlo events are then divided by the total number of simulated events which gives the efficiency of the model.
- Expected values of ^{214}Bi events/second are divided by the detector regional volumes and then multiplied by the MC efficiencies to yield true event density of each region. The expected events are taken from Table 3.3.
- The density of each region is then compared with the densities yielding from detector data and their ratio provides a scaling factor.
- The scaling factor is then multiplied by the target value of the 2.1 $\times 10^{-13}$gU^{238}/gH_2O which gives the true purity levels of each region of the detector.
- The event densities and the g U^{238}/gH_2O concentrations are plotted with time. Detector shift reports are checked for any unusual activity for each day and marked on the plots.

6.5 Background levels from August 2019 - October 2019

During the August 2019 to October 2019 time period, filling was briefly paused due to some issues within the scintillator purification plant. MCs were generated to determine the efficiency of the model in order to estimate the purity levels within the PSUP volume. The MC selection criteria is as follows:

- Beta particles of 3.27 MeV from Bi^{214} decays were simulated externally in the UPW with possible mis-reconstruction within the AV.
- Events were simulated in the partially filled scintillator-UPW configuration.
- A total of 5.85×10^7 events were simulated in the detector's external shielding water, equivalent to 0.4 years of expected events.

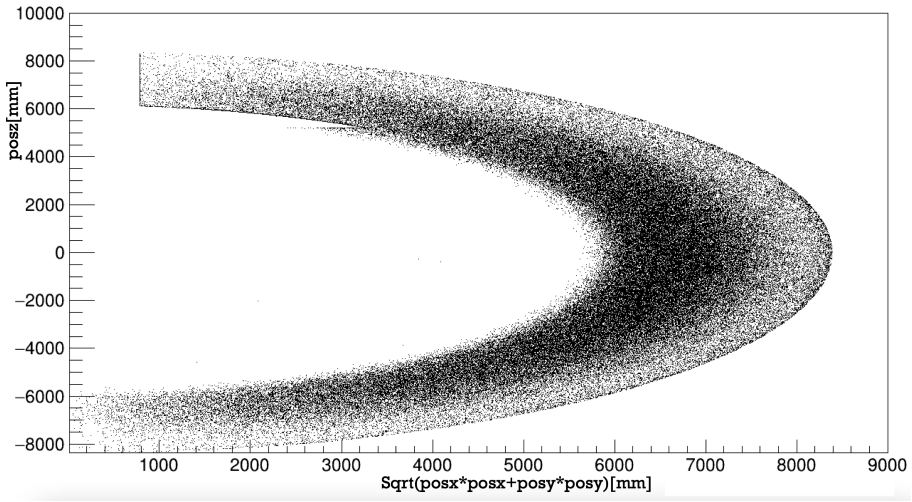

Figure 6.5: Distribution of events after ITR, β_{14}, N_{hits}, and Nhitscleaned cuts are applied. All events are restricted within the cavity and all internal events or misconstructed events were removed.

- The Scintillator interface was set at 5370 mm from the equator of the detector.
- 0.53 gPPO/Litre of LAB.

Surviving MC events with the cuts were used to determine the total efficiency of the model. The same model was applied to a set of MC generated for external ^{208}Th events, in order to determine the degree of contamination within the ^{214}Bi signal coming from ^{208}Th events. The following Tables 6.1 and 6.2 shows the total number of surviving events and their respective efficiencies. ^{208}Th showed very few surviving events and provided evidence of minimal contamination into the distribution of the ^{214}Bi events and was considered safe to be ignored.

Total Simulated	5.85×10^7 events			
Bi-214 External	MC Events	Efficiency	Events/yr	Events/day
$4000 < z < 8000$, external	145938	0.249%	3.28×10^5	900
$0 < z < 4000$ external	91263	0.156%	2.05×10^5	564
$-4000 < z < 0$ external	103348	0.177%	2.33×10^5	640
$-8000 < z < -4000$ external	83889	0.143%	1.88×10^5	517

Table 6.1: Surviving ^{214}Bi events after applying ITR, β_{14}, N_{hits}, and Nhitscleaned cuts and their respective efficiencies.

Total Simulated	3.0×10^7 events			
Th-208 External	MC Events	Efficiency	Events/yr	Events/day
$4000 < z < 8000$, external	3557	0.012%	464	1.27
$0 < z < 4000$ external	7059	0.024%	923	2.53
$-4000 < z < 0$ external	7215	0.024%	943	2.59
$-8000 < z < -4000$ external	5188	0.017%	679	1.86

Table 6.2: Surviving ^{208}Th events that provides contamination to the bismuth-214 events spectrum. The number of events produced in each volume is very low.

The analysis was then carried using the steps mentioned in Section 6.4. The g^{238}U/gH_2O concentration and event density of bismuth events were plotted against time. The shift reports that are generated during normal operations of data taking is thoroughly scanned to look for any unusual activity happening underground. The unusual activity is then labelled on the graphs and any sudden spike in the concentration is conveyed to the collaboration for prompt action.

6.5.1 Results

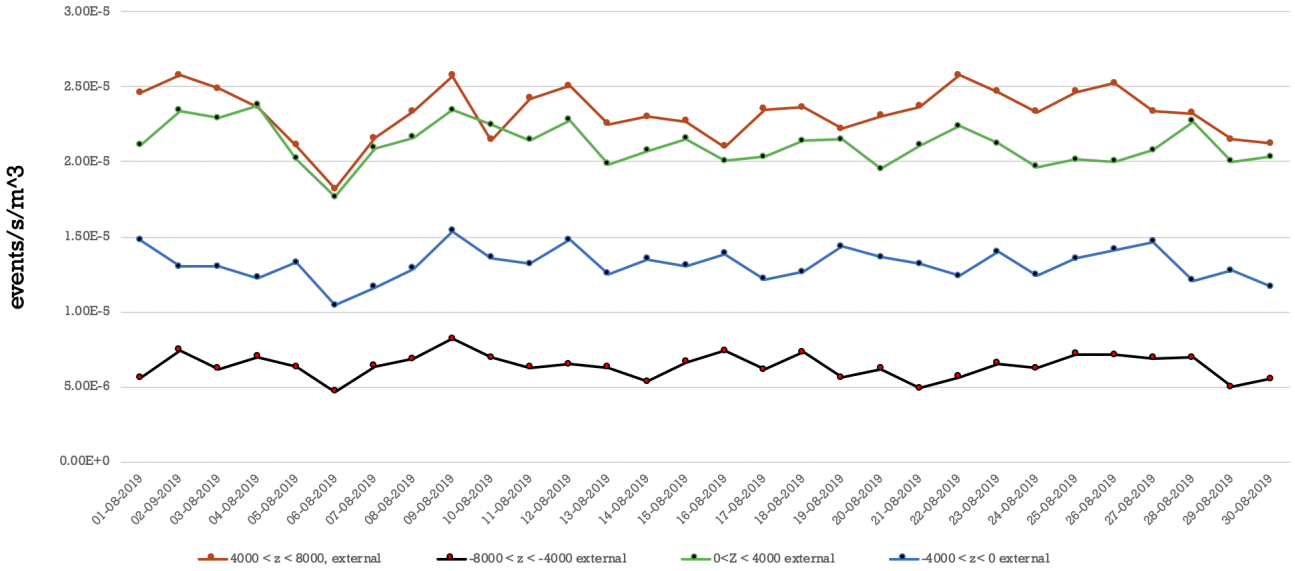

Figure 6.6: Event Density within each section of the PSUP for the month of August 2019

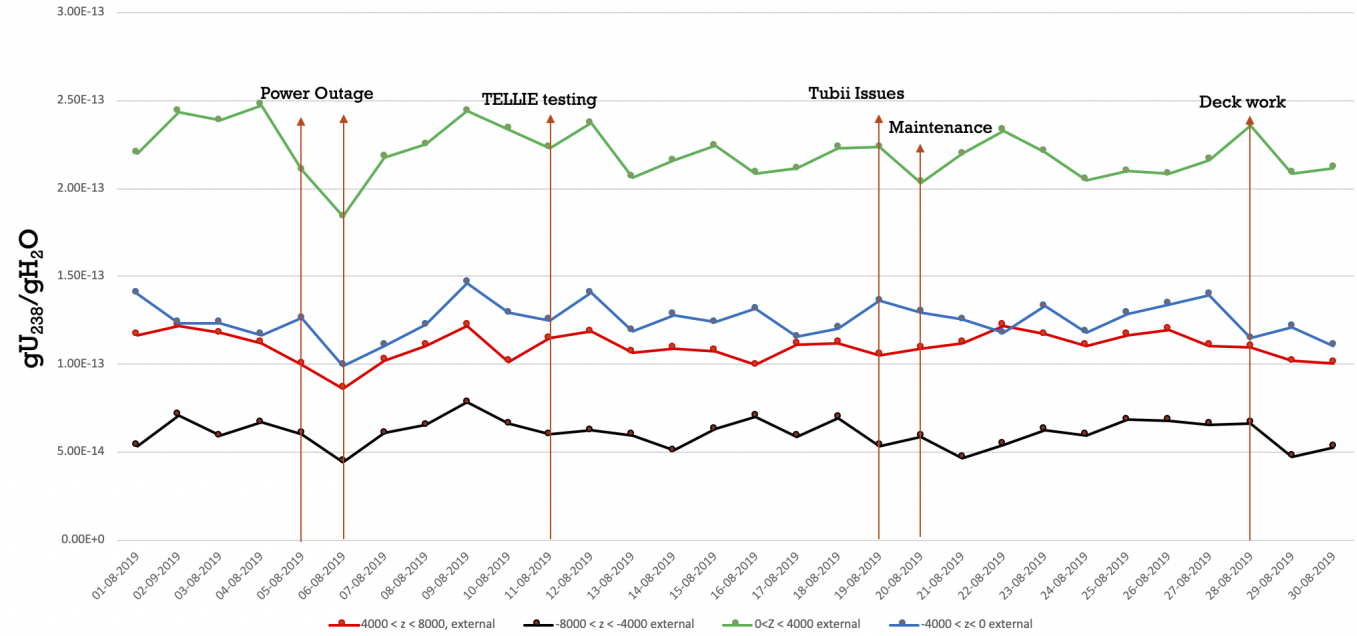

Figure 6.7: $g^{238}U/gH_2O$ concentrations for the month of August 2019. Power outage showed a decrease in concentration due to lost data while deck work showed elevated concentration levels. Other activity includes TELLIE testing and regular maintenance.

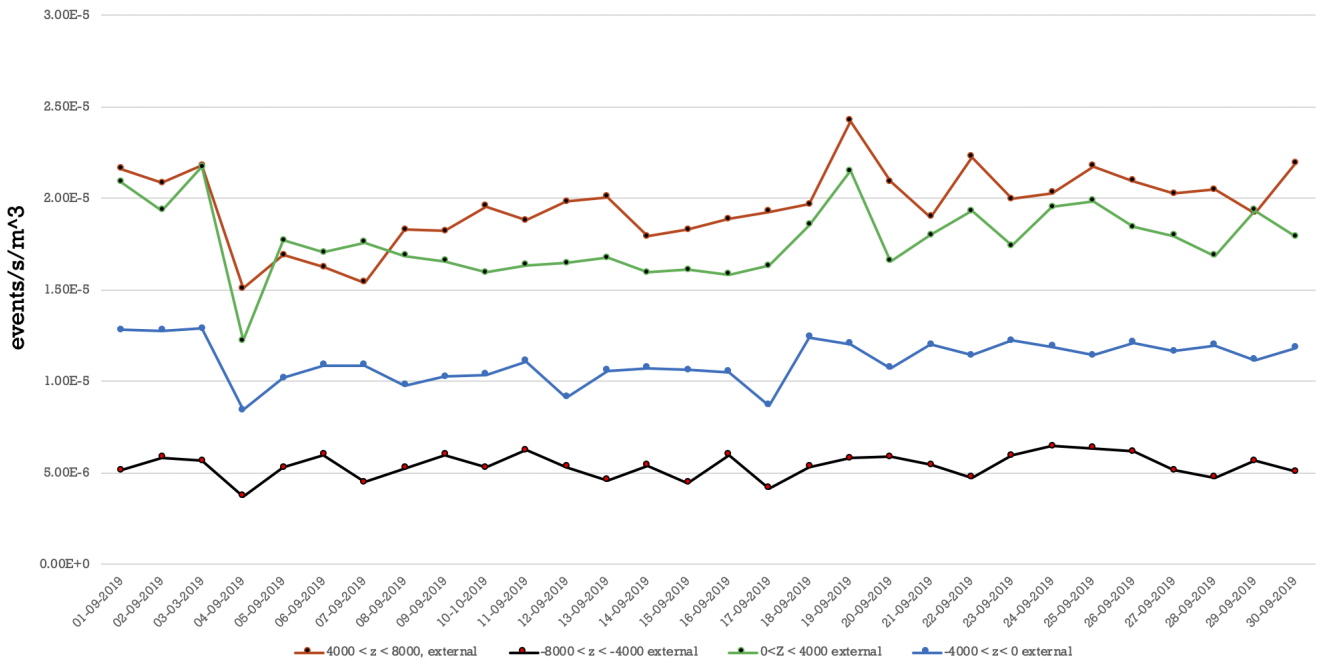

Figure 6.8: Event Density within each section of the PSUP for the month of September 2019

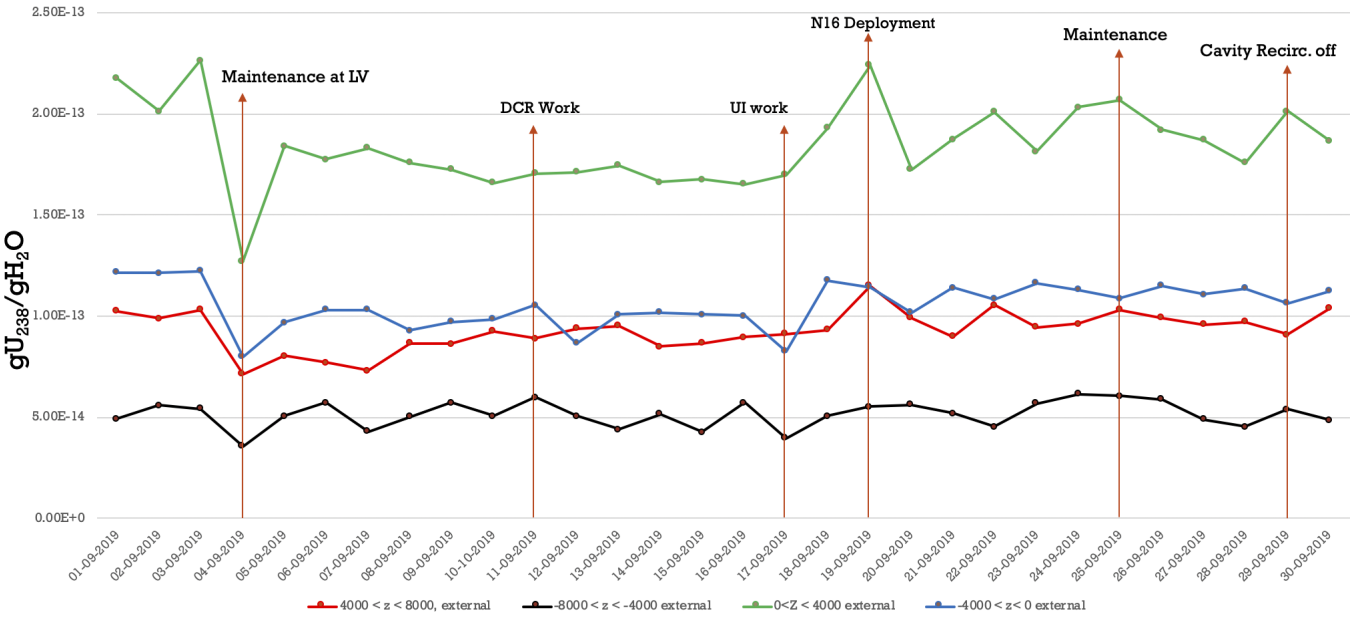

Figure 6.9: $g^{238}U/gH_2O$ concentrations for the month of September 2019. Maintenance at low voltage shows a sharp decrease due to loss of data while external N16 deployment shows increased activity as expected. Lots of on deck and DCR activity shown as well.

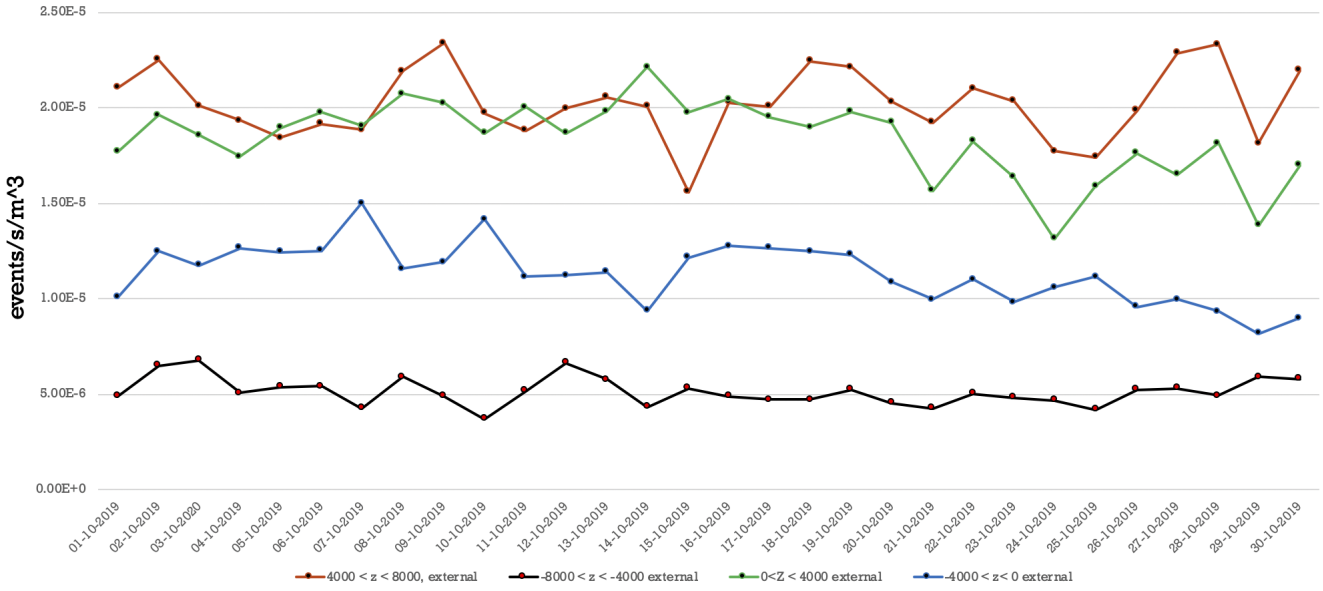

Figure 6.10: Event Density within each section of the PSUP for the month of October 2019

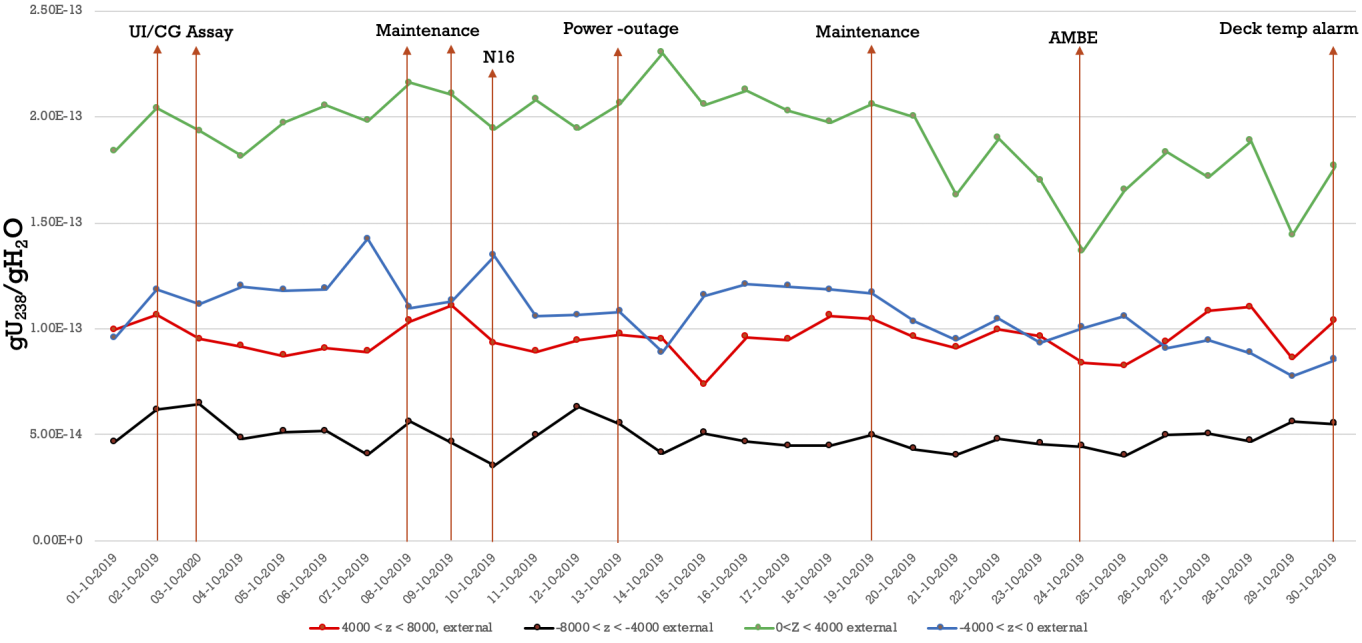

Figure 6.11: $g^{238}U/gH_2O$ concentrations for the month of October 2019. UI assays caused increased activity. Activity also includes calibration work like N16 and AMBE external deployments, and some maintenance work.

The analysis showed that $0 < z < 4000$ had the highest concentration of gU^{238}/gH_2O but is still below the target level of 2.1×10^{-13} g/g which is very promising for SNO+ in maintaining external radioactivity within the background budget. Moreover $-8000 < z < -4000$ showed the least amount of activity as suggested by the MC data while the top z slice of $8000 < z < 4000$ showed lower radioactivity which is contrary to the MC suggestion. The analysis results when compared to the assay results in Tables 5.6 and 4.5 showed an agreement which confirms that our developed algorithms for analyzing ^{214}Bi events and assay systems are working and producing reliable results. The scintillator purification plant resumed normal fill operations after October 2019 and bismuth analysis was concluded for this stable region.

6.6 Background levels from April 2020 - August 2020

SNO+ carried out normal filling operations until COVID-19 pandemic hit and SNOLAB access was restricted which halted the filling operations. From April 2020 until August 2020 there was no filling, which was used as an opportunity to resume external bismuth analysis. The only constraint for this analysis was that external ^{214}Bi analysis is carried out for $N_{hits} < 40$ and due to storage problems processing group was only reconstructing 1 % of events in this region. Very low statistic was expected, therefore, Z slices were changed and only two volume regions were considered: $0 < z < 8000$mm and -8000mm $< z < 0$(See figure 6.12). All the other methodology of the analysis remained the same as mentioned in Section 6.4. MC was generated for this period with the following criteria:

- Beta particles of 3.27 MeV from Bi^{214} decays were simulated externally in the UPW with possible mis-reconstruction within the AV.
- Events were simulated in the partially filled scintillator-UPW configuration.
- A total of 3.0×10^6 events were simulated in the detector's external shielding water.
- The Scintillator interface was set at 750 mm from the equator of the detector.
- 0.53 gPPO/Litre of LAB.

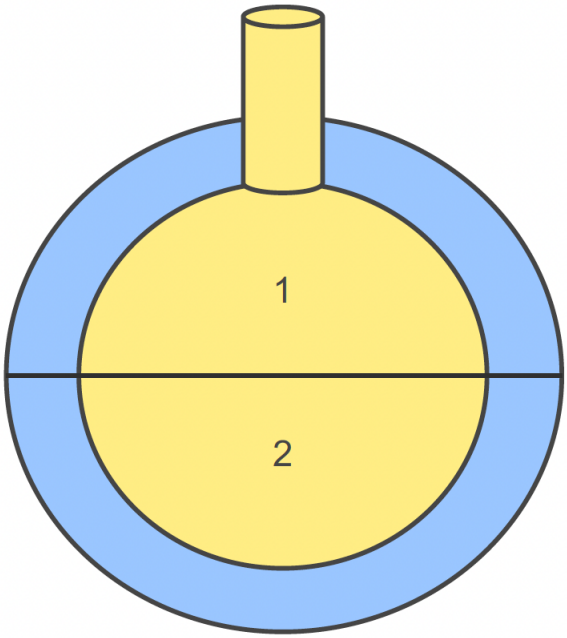

Figure 6.12: Schematic of the detector with two different volume regions for both internal and external volume regions. Radial slices range from -8000 to +8000mm with 0 being the center of the AV.

Surviving MC events with the cuts were used to determine the total efficiency of the model. The Table 6.3 shows the total number of surviving events and respective efficiencies for each detector region.

Bi-214 External	MC Events	1 % Correction	Efficiency	Events/yr	Events/day
Total Cuts	26310	263.1	8.77×10^{-5}	1.15×10^{4}	31.7
$0 < z < 8000$ external	10608	106.08	3.54×10^{-5}	4.62×10^{3}	12.80
$-8000 < z < 0$ external	15702	157.02	5.23×10^{-5}	6.90×10^{3}	18.9

Table 6.3: Surviving MC events after applying ITR, β_{14}, N_{hits}, and Nhitscleaned cuts and their respective efficiencies. 1 % correction is also included to precisely match the detector conditions.

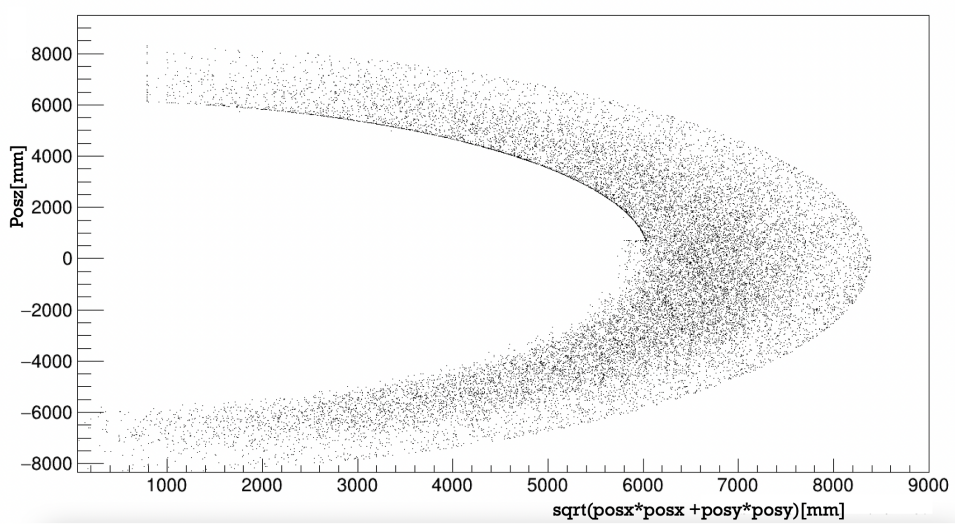

Figure 6.13: Distribution of ^{214}Bi events after applying ITR, β_{14}, N_{hits}, and Nhitscleaned cuts and their respective efficiencies cuts are applied. All events are restricted within the cavity and all internal events or mis-constructed events were removed.

6.6.1 Results

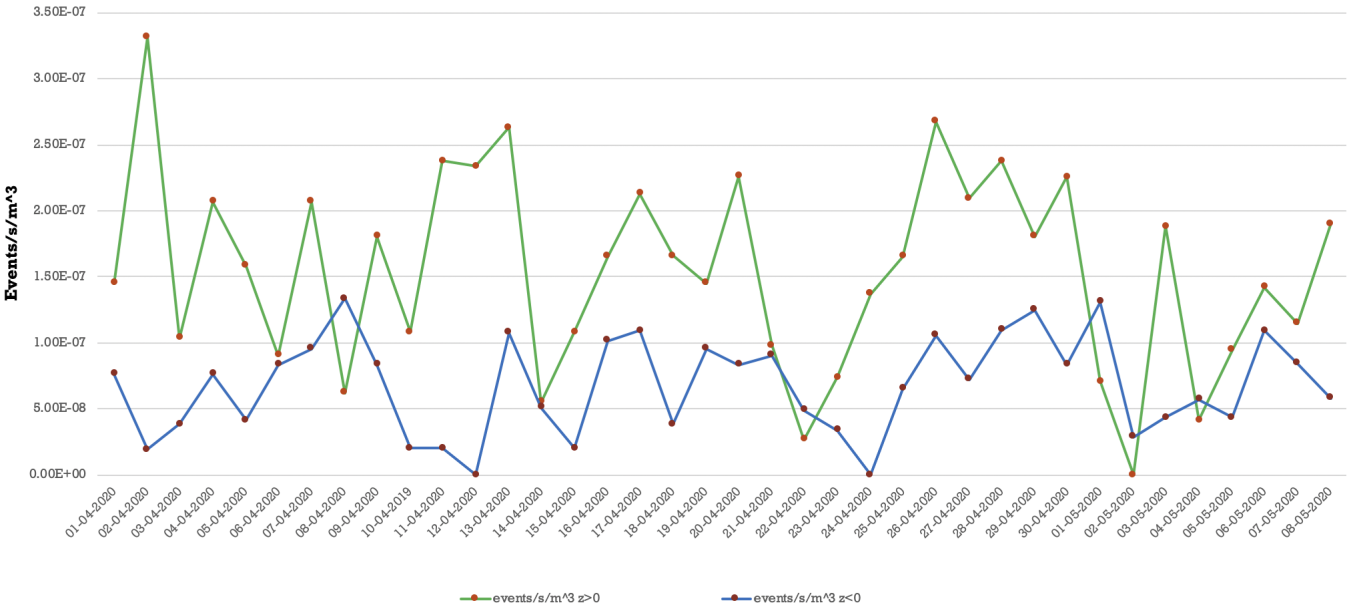

Figure 6.14: Event density within each section of the PSUP for the month of April 2020 and first week of May.

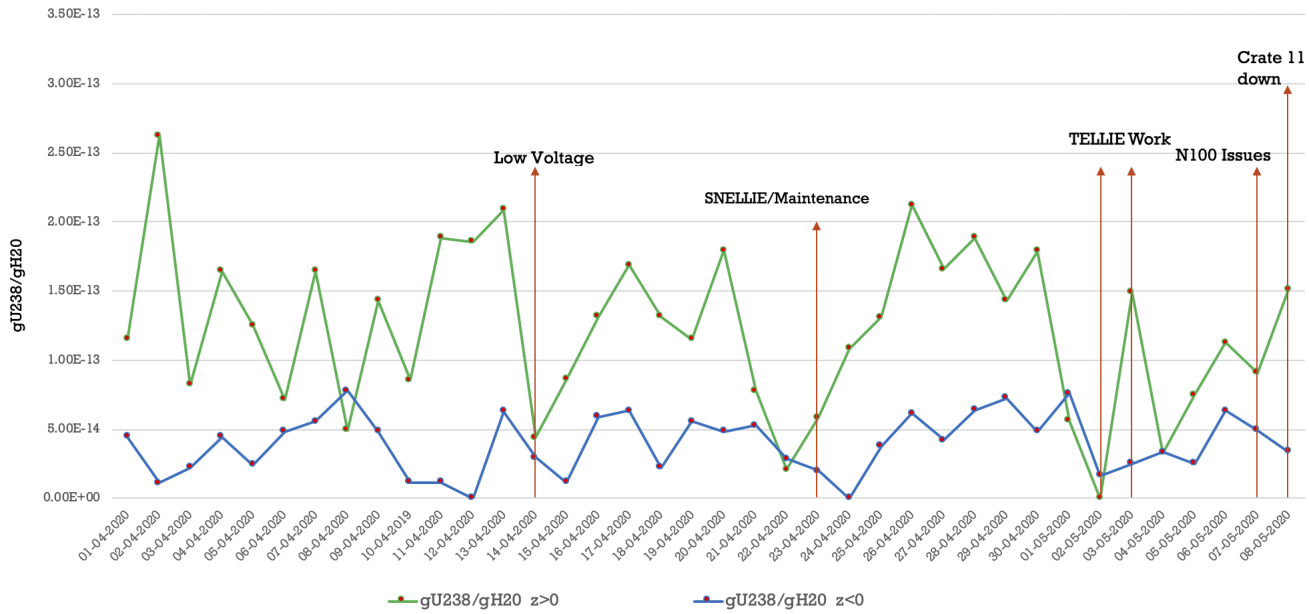

Figure 6.15: gU^{238}/gH_2O concentrations for the month of April and first week of May 2020. Some low voltage and maintenance time with Tellie work and some trigger and crate issues in the end.

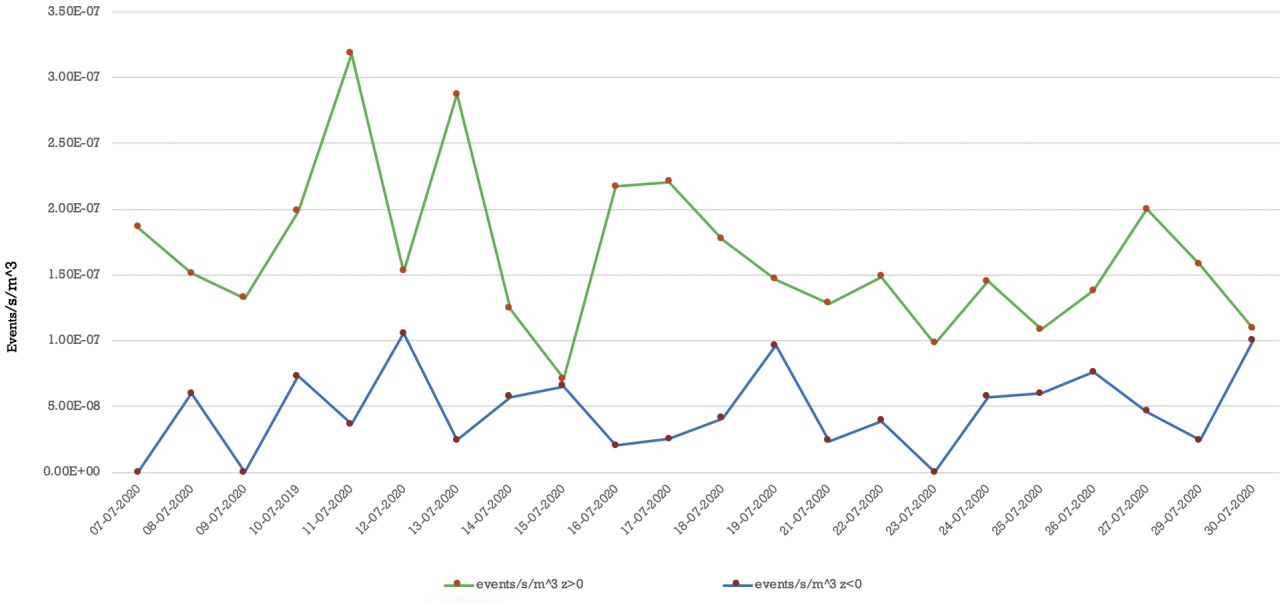

Figure 6.16: Event Density within each section of the PSUP for the month of July 2020. 20thth July data point missing because of no events being reconstructed.

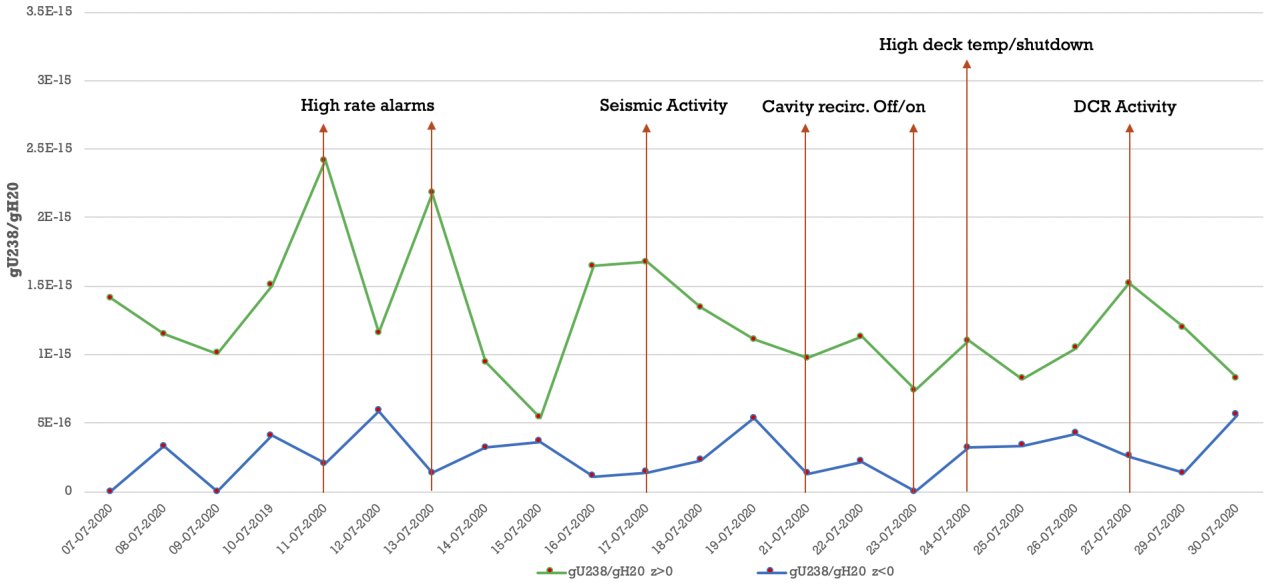

Figure 6.17: g^{238}U/gH_2O concentrations for the month of July 2020. High rate alarms shows some elevated levels with some DCR activity and high deck temperature alarms.

The results from this stable region even though has low statistics showed promising results and does not show any radon ingress in the PSUP volume. During this stable region, the month of June and first week of July data was not included because detector was having a lot of problems like lost crates and trigger issues, therefore, it was decided to omit that data

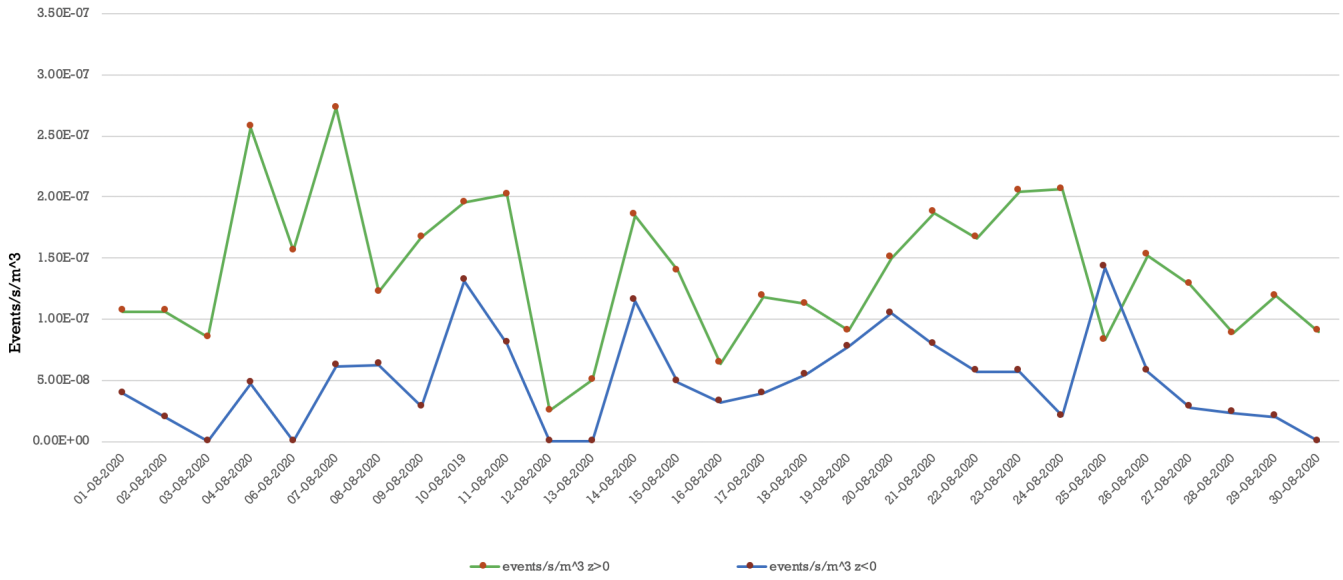

Figure 6.18: Event Density within each section of the PSUP for the month of August 2020

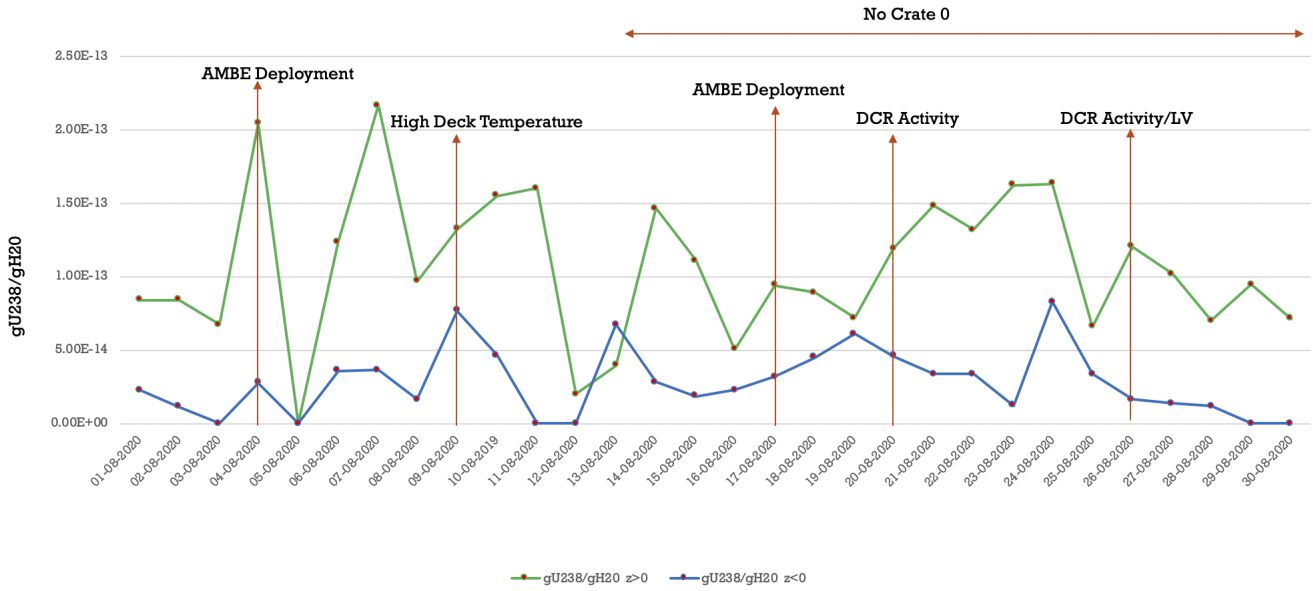

Figure 6.19: $g^{238}U/gH_2O$ concentrations for the month of August 2020. Few external calibration deployments (AMBE) and DCR activities. Crate 0 was removed due to some electronics issue.

from this study. The top half of the detector showed more activity than the bottom half of the cavity which is contrary to the MC suggestion but consistent with the behavior seen from 2019 analysis. Due to lack of statistics a lot of variations were seen and there were some days where

almost no events were seen especially for the z < 0 region. The g/g concentration within the detector volume stayed around or below the target level of 2.1×10^{-13} g/g which suggested a consistent concentration within the PSUP water. Moreover, the background levels shows some fluctuation in the concentration depending upon underground activity such as the DCR work, high deck temperature, calibration source deployments, or the state of the detector.

6.7 Conclusion

The $g^{238}U/gH_2O$ concentration from these two time periods of July-October 2019 and April-August 2020 shows that SNO+ have been successful in maintaining consistent backgrounds levels in the cavity and no radon ingress into the cavity volume was seen. Moreover, this analysis serves as a performance check for the Ultra purification plant (mentioned in 3.9) and confirms its reliability in purifying contaminants from the cavity water. The concentration determined through analysis is consistent from the assay results mention in Chapter 4 which suggests that SNO+ has successfully shown an agreement between the *in-situ* and *ex-situ* measurements. The agreement also serves as a confirmation of proper working of the water radon assay systems and the developed algorithms for analysis. Below target background levels in cavity will also ensure a reduction in the expected gammas originating from uranium decay chain that will propagate into the AV volume and into the ROI for $0\nu\beta\beta$ decay.

Chapter 7

Conclusion

Radon is one of the most problematic isotopes for any underground experiment due to its wide prevalence within the mine environment. SNO+ has a stringent background budget because of the rarity of the exotic physics goals including neutrinoless double beta decay. SNO+ makes use of three purification plants: UPW plant, Scintillator plant, and tellurium plant, in order to ensure any medium added to the detector is pure and meets the standard for low radioactive contamination. Moreover, all purification plants have a moderate nitrogen cover-gas blanket. In addition, the acrylic vessel has a sophisticated covergas system that restrict the radon ingress from mine air into the detector volume.

Due to low background budget, it is crucial to measure and monitor the radon levels within the SNO+ cavity. The water radon assay system allows for a direct measurement of radon levels in the cavity at various locations. During the time of this thesis, the water assay system was fixed and leak checked and new system backgrounds were determined. The water assay results mentioned in Chapter 4 show that under normal conditions, SNO+ has been very successful in maintaining a below target level concentration within the cavity where the target level is $2.1 \times 10^{-13} \mathrm{gU}_{238}/\mathrm{gH}_2\mathrm{O}$. Therefore, the *ex situ* results from the assays concludes that UPW plant and the assay systems have optimum functionality, and assay system has been producing consistent results.

In Chapter 6 Bismuth analysis explains a way of monitoring cavity concentration through

the detector data, also known as *in situ* analysis. In addition, the *in situ* analysis allows to monitor the background levels throughout the PSUP volume while the *ex situ* measurements are only limited to four locations. The background rate through the analysis was also below the target of 2.1×10^{-13} gU^{238}/gH_2O and showed consistent backgrounds in all regions of the inner cavity volume. An agreement between the *ex situ* and *in situ* measurements have been established within this thesis.

During the fill operations of SNO+, higher than expected radon ingress was observed. Therefore, a thorough investigation on the effectiveness of the covergas system became necessary. The SNO era developed an emanation board that was modified and made suitable to perform radon assay on the nitrogen covergas systems of SNO+. The background of the gas board was determined and the overall efficiency of the system was carefully evaluated. This thesis highlights the extensive efficiency measurement campaign that was performed in order to understand the accurate functionality of the board under atmospheric pressure. Moreover, the time dependence upon efficiency was determined and a model was developed through which efficiency on separate assay times can be determined from extrapolation. The vapour sensitivity of the board made it difficult to perform gas assays, therefore the Ice bath was introduced within the assay procedure to successfully perform assay measurements. Most of the locations of the SNO+ experiments had some form of water such as the LAB vapor within the UI and in the scintillator plant, therefore, the use of Ice bath proved very crucial. The UI covergas, VO1(scintillator plant), and International dewar(N_2) were all found to be under the operational budget and showed a reduction level on the order of 10^5. The gas assay measurements performed as part of this thesis work, enabled SNO+ to successfully perform these measurements, as prior to this no such measurements were performed. The use of the functional and calibrated gas assay system will allow SNO+ to monitor the effectiveness of the cover-gas systems and in future will also allow to determine the cover-gas viability in the tellurium plant as SNO+ enters tellurium loading phase.

SNO+ needs to continue using these background mitigation methods and ensure that all shielding contributors such as the cavity and covergas systems are working well. Constant

monitoring of *ex situ* and *in situ* measurements should be continued in all the other phases of the experiment. The gas assay system should built another primary trap with efficiency that does not have assay time dependency. Lastly, the scintillator radon assay board should be constructed so that *ex situ* measurements can be taken from the LAB within the AV volume and *in situ* measurements such as those from Bi-Po coincidences can be verified and checked for consistency.

Bibliography

[1] https://www.snolab.ca/. Accessed: 2021-11-25.

[2] A scintillator purification plant and fluid handling system for sno+. 2015.

[3] MG Aartsen, M Ackermann, J Adams, JA Aguilar, M Ahlers, M Ahrens, D Altmann, T Anderson, C Arguelles, TC Arlen, et al. Searches for extended and point-like neutrino sources with four years of icecube data. *The Astrophysical Journal*, 796(2):109, 2014.

[4] Kevork N Abazajian. Sterile neutrinos in cosmology. *Physics Reports*, 711:1–28, 2017.

[5] JN Abdurashitov, EL Faizov, VN Gavrin, AO Gusev, AV Kalikhov, TV Knodel, II Knyshenko, VN Kornoukhov, IN Mirmov, AM Pshukov, et al. Results from sage (the russian-american gallium solar neutrino experiment). *Physics Letters B*, 328(1-2):234–248, 1994.

[6] M Agostini, K Altenmüller, S Appel, V Atroshchenko, Z Bagdasarian, D Basilico, G Bellini, J Benziger, R Biondi, D Bravo, et al. Sensitivity to neutrinos from the solar cno cycle in borexino. *The European Physical Journal C*, 80(11):1–15, 2020.

[7] M Agostini, GR Araujo, AM Bakalyarov, M Balata, I Barabanov, L Baudis, C Bauer, E Bellotti, S Belogurov, A Bettini, et al. Final results of gerda on the search for neutrinoless double-β decay. *Physical Review Letters*, 125(25):252502, 2020.

[8] B Aharmim, SN Ahmed, JF Amsbaugh, AE Anthony, J Banar, N Barros, EW Beier, Alain Bellerive, B Beltran, M Bergevin, et al. Independent measurement of the total active b 8

solar neutrino flux using an array of he 3 proportional counters at the sudbury neutrino observatory. *Physical Review Letters*, 101(11):111301, 2008.

[9] Q Retal Ahmad, RC Allen, TC Andersen, JD Anglin, JC Barton, EW Beier, M Bercovitch, J Bigu, SD Biller, RA Black, et al. Direct evidence for neutrino flavor transformation from neutral-current interactions in the sudbury neutrino observatory. *Physical review letters*, 89(1):011301, 2002.

[10] S. N. Ahmed, A. E. Anthony, E. W. Beier, A. Bellerive, S. D. Biller, J. Boger, M. G. Boulay, M. G. Bowler, T. J. Bowles, S. J. Brice, and et al. Constraints on nucleon decay via invisible modes from the sudbury neutrino observatory. *Physical Review Letters*, 92(10), Mar 2004.

[11] V Albanese, R Alves, MR Anderson, S Andringa, L Anselmo, E Arushanova, S Asahi, M Askins, DJ Auty, AR Back, et al. The sno+ experiment. *Journal of Instrumentation*, 16(08):P08059, 2021.

[12] M. Anderson et al. Measurement of the ^{8}B solar neutrino flux in SNO+ with very low backgrounds. *Phys. Rev. D*, 99(1):012012, 2019.

[13] M. et al Anderson. Search for invisible modes of nucleon decay in water with the sno+ detector. *Phys. Rev. D*, 99:032008, Feb 2019.

[14] P Anselmann, R Fockenbrock, W Hampel, G Heusser, J Kiko, T Kirsten, M Laubenstein, E Pernicka, S Pezzoni, U Roenn, et al. First results from the 51cr neutrino source experiment with the gallex detector. *Physics Letters B*, 342(1-4):440–450, 1995.

[15] G Anton, I Badhrees, PS Barbeau, D Beck, V Belov, T Bhatta, M Breidenbach, T Brunner, GF Cao, WR Cen, et al. Search for neutrinoless double-β decay with the complete exo-200 dataset. *Physical review letters*, 123(16):161802, 2019.

[16] T Araki, S Enomoto, K Furuno, Y Gando, K Ichimura, H Ikeda, K Inoue, Y Kishimoto,

M Koga, Y Koseki, et al. Search for the invisible decay of neutrons with kamland. *Physical review letters*, 96(10):101802, 2006.

[17] J. Argyriades, R. Arnold, C. Augier, J. Baker, A. S. Barabash, A. Basharina-Freshville, M. Bongrand, G. Broudin, V. Brudanin, A. J. Caffrey, E. Chauveau, Z. Daraktchieva, D. Durand, V. Egorov, N. Fatemi-Ghomi, R. Flack, Ph. Hubert, J. Jerie, S. Jullian, M. Kauer, S. King, A. Klimenko, O. Kochetov, S. I. Konovalov, V. Kovalenko, D. Lalanne, T. Lamhamdi, K. Lang, Y. Lemière, C. Longuemare, G. Lutter, Ch. Marquet, J. Martin-Albo, F. Mauger, A. Nachab, I. Nasteva, I. Nemchenok, F. Nova, P. Novella, H. Ohsumi, R. B. Pahlka, F. Perrot, F. Piquemal, J. L. Reyss, J. S. Ricol, R. Saakyan, X. Sarazin, L. Simard, F. Šimkovic, Yu. Shitov, A. Smolnikov, S. Snow, S. Söldner-Rembold, I. Štekl, J. Suhonen, C. S. Sutton, G. Szklarz, J. Thomas, V. Timkin, V. Tretyak, V. Umatov, L. Vála, I. Vanyushin, V. Vasiliev, V. Vorobel, and Ts. Vylov. Measurement of the double-β decay half-life of ^{150}Nd and search for neutrinoless decay modes with the nemo-3 detector. *Phys. Rev. C*, 80:032501, Sep 2009.

[18] E Armengaud, C Augier, AS Barabash, F Bellini, G Benato, A Benoît, M Beretta, L Bergé, J Billard, Yu A Borovlev, et al. New limit for neutrinoless double-beta decay of mo 100 from the cupid-mo experiment. *Physical review letters*, 126(18):181802, 2021.

[19] R Arnold, C Augier, JD Baker, AS Barabash, A Basharina-Freshville, S Blondel, S Blot, M Bongrand, D Boursette, V Brudanin, et al. Measurement of the 2 ν β β decay half-life and search for the 0 ν β β decay of cd 116 with the nemo-3 detector. *Physical Review D*, 95(1):012007, 2017.

[20] Robert G Arns. Detecting the neutrino. *Physics in Perspective*, 3(3):314–334, 2001.

[21] E Arushanova, AR Back, SNO+ collaboration, et al. Physics capabilities of the sno+ experiment. 888(1):012245, 2017.

[22] O. Azzolini, M. T. Barrera, J. W. Beeman, F. Bellini, M. Beretta, M. Biassoni, C. Brofferio,

C. Bucci, L. Canonica, S. Capelli, and et al. First result on the neutrinoless double-decay of se82 with cupid-0. *Physical Review Letters*, 120(23), Jun 2018.

[23] H.O. Back, M. Balata, A. de Bari, T. Beau, A. de Bellefon, G. Bellini, J. Benziger, S. Bonetti, C. Buck, B. Caccianiga, and et al. New limits on nucleon decays into invisible channels with the borexino counting test facility. *Physics Letters B*, 563(1-2):23–34, Jun 2003.

[24] Steven Biller and Szymon Manecki and. A new technique to load 130te in liquid scintillator for neutrinoless double beta decay experiments. *Journal of Physics: Conference Series*, 888:012084, sep 2017.

[25] I Blevis, J Boger, E Bonvin, BT Cleveland, X Dai, F Dalnoki-Veress, G Doucas, J Farine, H Fergani, D Grant, et al. Measurement of 222rn dissolved in water at the sudbury neutrino observatory. *Nuclear Instruments and Methods in Physics Research Section A: Accelerators, Spectrometers, Detectors and Associated Equipment*, 517(1-3):139–153, 2004.

[26] J Boger, RL Hahn, JK Rowley, AL Carter, B Hollebone, D Kessler, I Blevis, F Dalnoki-Veress, A DeKok, J Farine, et al. The sudbury neutrino observatory. *Nuclear Instruments and Methods in Physics Research Section A: Accelerators, Spectrometers, Detectors and Associated Equipment*, 449(1-2):172–207, 2000.

[27] J Boger, RL Hahn, JK Rowley, AL Carter, B Hollebone, D Kessler, I Blevis, F Dalnoki-Veress, A DeKok, J Farine, et al. The sudbury neutrino observatory. *Nuclear Instruments and Methods in Physics Research Section A: Accelerators, Spectrometers, Detectors and Associated Equipment*, 449(1-2):172–207, 2000.

[28] Boris M Bolotovskii. Vavilov – cherenkov radiation: its discovery and application. 52(11):1099–1110, nov 2009.

[29] Laurie M Brown. The idea of the neutrino. *Physics Today*, 31(9):23, 1978.

[30] James Chadwick. Possible existence of a neutron. *Nature*, 129(3252):312–312, 1932.

[31] Bruce T Cleveland, Timothy Daily, Raymond Davis Jr, James R Distel, Kenneth Lande, CK Lee, Paul S Wildenhain, and Jack Ullman. Measurement of the solar electron neutrino flux with the homestake chlorine detector. *The Astrophysical Journal*, 496(1):505, 1998.

[32] BT Cleveland, T Daily, R Jr Davis, J Distel, K Lande, CK Lee, P Wildenhain, and J Ullman. Update on the measurement of the solar neutrino flux with the homestake chlorine detector. *Nuclear Physics B Proceedings Supplements*, 38:47, 1995.

[33] W Noel Cottingham and Derek A Greenwood. *An introduction to the standard model of particle physics*. Cambridge university press, 2007.

[34] M Cribier, W Hampel, G Heusser, J Kiko, T Kirsten, M Laubenstein, E Pernicka, W Rau, U Rönn, C Schlosser, et al. Results of the whole gallex experiment. *Nuclear Physics B-Proceedings Supplements*, 70(1-3):284–291, 1999.

[35] Gaillard Danby, Jean Maurice Gaillard, Konstantin Goulianos, Leon M Lederman, Nariman Mistry, Melvin Schwartz, and Jack Steinberger. Observation of high-energy neutrino reactions and the existence of two kinds of neutrinos. *Physical Review Letters*, 9(1):36, 1962.

[36] Raymond Davis. Solar neutrinos. ii. experimental. *Phys. Rev. Lett.*, 12:303–305, Mar 1964.

[37] Jessica A. Dunmore. *The separation of CC and NC events in the Sudbury Neutrino Observatory*. PhD thesis, 2004.

[38] Steven R. Elliott and Petr Vogel. Double beta decay. *Annual Review of Nuclear and Particle Science*, 52(1):115–151, Dec 2002.

[39] Andringa et al. Current status and future prospects of the sno+ experiment. *Advances in high energy physics.*, 2016.

[40] Guido Fantini. Search for double beta decay of 130te to the 0+ states of 130xe with the cuore experiment. 2020.

[41] The LEP Working Group for Higgs, ALEPH Collaboration, DELPHI Collaboration, L3 Collaboration, OPAL Collaboration, et al. Search for the standard model higgs boson at lep. *Physics Letters B*, 565:61–75, 2003.

[42] IETIM Frank and Ig Tamm. Coherent visible radiation of fast electrons passing through matter. In *Selected Papers*, pages 109–114. Springer, 1991.

[43] S Fukuda, Y Fukuda, T Hayakawa, E Ichihara, M Ishitsuka, Y Itow, T Kajita, J Kameda, K Kaneyuki, S Kasuga, et al. The super-kamiokande detector. *Nuclear Instruments and Methods in Physics Research Section A: Accelerators, Spectrometers, Detectors and Associated Equipment*, 501(2-3):418–462, 2003.

[44] W. H. Furry. On transition probabilities in double beta-disintegration. *Phys. Rev.*, 56:1184–1193, Dec 1939.

[45] Pauline Gagnon. The standard model: a beautiful but flawed theory. *Quantum Diaries [cited 20171211] Available from: https://www. quantumdiaries. org/2014/03/14/the-standard-model-a-beautiful-but-flawed-theory*, 2014.

[46] Carlo Giunti and Chung W Kim. *Fundamentals of neutrino physics and astrophysics*. Oxford university press, 2007.

[47] M. Goeppert-Mayer. Double beta-disintegration. *Phys. Rev.*, 48:512–516, Sep 1935.

[48] Reyco Henning. Reviews in physics. pages 29–35, 2016.

[49] K. S. Hirata, T. Kajita, T. Kifune, K. Kihara, M. Nakahata, K. Nakamura, S. Ohara, Y. Oyama, N. Sato, M. Takita, Y. Totsuka, Y. Yaginuma, M. Mori, A. Suzuki, K. Takahashi, T. Tanimori, M. Yamada, M. Koshiba, T. Suda, K. Miyano, H. Miyata, H. Takei, K. Kaneyuki, H. Nagashima, Y. Suzuki, E. W. Beier, L. R. Feldscher, E. D. Frank, W. Frati, S. B. Kim, A. K. Mann, F. M. Newcomer, R. Van Berg, and W. Zhang. Observation of ^{8}B solar neutrinos in the kamiokande-ii detector. *Phys. Rev. Lett.*, 63:16–19, Jul 1989.

[50] Lillian Hoddeson, Laurie M Brown, Laurie Brown, Michael Riordan, and Max Dresden. *The rise of the standard model: A history of particle physics from 1964 to 1979*. Cambridge University Press, 1997.

[51] J.Rumleskie. Evaluating sno+ backgrounds through ^{222}rn assays and the simulation of 13c$(\alpha, \mathrm{n})^{16}$c reactions during water phase". *Masters thesis*, 2015.

[52] K Kodama, N Ushida, C Andreopoulos, N Saoulidou, G Tzanakos, P Yager, B Baller, D Boehnlein, Walter Freeman, B Lundberg, et al. Observation of tau neutrino interactions. *Physics Letters B*, 504(3):218–224, 2001.

[53] Michiji Konuma, Masako Bando, Haruyoshi Gotoh, Hisao Hayakawa, Kohji Hirata, Kazuyuki Ito, Kenji Ito, Kazuyuki Kanaya, Daisuke Konagaya, Taichiro Kugo, et al. The legacy of hideki yukawa, sin-itiro tomonaga, and shoichi sakata: Some aspects from their archives. In *Proceedings of the 12th Asia Pacific Physics Conference (APPC12)*, page 013009, 2014.

[54] Brian Krar and Alex Wright. Water system update. *SNO+ Internal Document SNO+-doc-7091-v1.*, 2021.

[55] David Lindley. Landmarks—discovery of a 2nd kind of neutrino. *Physics*, 8:75, 2015.

[56] Manqing Liu, HW Lee, and AB McDonald. 222rn emanation into vacuum. *Nuclear Instruments and Methods in Physics Research Section A: Accelerators, Spectrometers, Detectors and Associated Equipment*, 329(1-2):291–298, 1993.

[57] Neil K McCauley. *Producing a Background Free Data Set for Measurement of the Charge Current Flux and DayNight Asymmetry at the Sudbury Neutrino Observatory*. PhD thesis, 2001.

[58] Gordon A McGregor. First results from the sudbury neutrino observatory. *arXiv preprint nucl-ex/0205006*, 2002.

[59] D.-M. Mei and A. Hime. Muon-induced background study for underground laboratories. *Phys. Rev. D*, 73:053004, Mar 2006.

[60] WB Oatway, KA Jones, S Holmes, JR Simmonds, G Etherington, J Marsh, RGE Haylock, and CR Muirhead. Background material on nature of radioactive contamination at the university of manchester and possible health risks: Task 1 report.

[61] M. L. Perl, G. S. Abrams, A. M. Boyarski, M. Breidenbach, D. D. Briggs, F. Bulos, W. Chinowsky, J. T. Dakin, G. J. Feldman, C. E. Friedberg, D. Fryberger, G. Goldhaber, G. Hanson, F. B. Heile, B. Jean-Marie, J. A. Kadyk, R. R. Larsen, A. M. Litke, D. Lüke, B. A. Lulu, V. Lüth, D. Lyon, C. C. Morehouse, J. M. Paterson, F. M. Pierre, T. P. Pun, P. A. Rapidis, B. Richter, B. Sadoulet, R. F. Schwitters, W. Tanenbaum, G. H. Trilling, F. Vannucci, J. S. Whitaker, F. C. Winkelmann, and J. E. Wiss. Evidence for anomalous lepton production in $e^+ - e^-$ annihilation. *Phys. Rev. Lett.*, 35:1489–1492, Dec 1975.

[62] G. Prior. The sno+ experiment physics goals and background mitigation, 2017.

[63] Frederick Reines. Giant liquid scintillation detectors and their applications. *Liquid scintillation counting*, pages 246–57, 1958.

[64] M. Schwartz. Feasibility of using high-energy neutrinos to study the weak interactions. *Phys. Rev. Lett.*, 4:306–307, Mar 1960.

[65] Michael Spira, Abdelhak Djouadi, D Graudenz, and RM Zerwas. Higgs boson production at the lhc. *Nuclear Physics B*, 453(1-2):17–82, 1995.

[66] T Tanimori. Recent results on solar neutrinos from kamiokande-11.

[67] V. I. Tretyak, V. Yu. Denisov, and Yu. G. Zdesenko. New limits on dinucleon decay into invisible channels. *Journal of Experimental and Theoretical Physics Letters*, 79(3):106–108, Feb 2004.

[68] S. Umehara, T. Kishimoto, I. Ogawa, R. Hazama, H. Miyawaki, S. Yoshida, K. Matsuoka, K. Kishimoto, A. Katsuki, H. Sakai, D. Yokoyama, K. Mukaida, S. Tomii, Y. Tatewaki,

T. Kobayashi, and A. Yanagisawa. Neutrino-less double-β decay of ^{48}Ca studied by caf$_2$(eu) scintillators. *Phys. Rev. C*, 78:058501, Nov 2008.

[69] JD Vergados, H Ejiri, and F Šimkovic. Theory of neutrinoless double-beta decay. *Reports on Progress in Physics*, 75(10):106301, 2012.

[70] Victor T Voronchev, Yasuyuki Nakao, and Yukinobu Watanabe. Comparative roles of p p chain reactions as a trigger for suprathermal processes in the solar core. *Physical Review C*, 96(5):055803, 2017.

[71] Pooja Woosaree. 222rn measurements within the water phase of the sno+ experiment, msc thesis, 2018.

Appendix A

MDG Background Procedure

SNOLAB	**Closed Loop: MDG Background with Water**

Document Number: SL-OPS-PCS-30-351-P		**Revision Number: 0**
Document Owner: Syed Adil Hussain		
Reviewer: Sanford Clark		
Name:	**Signature:**	**Date: <YYYY-MM-DD>**
Approval Authority: Operations Manager		
Name:	**Signature:**	**Date: <YYYY-MM-DD>**

1. Scope

This procedure provides steps to perform a Radon (Rn) assay to determine the MDG background with water. The Radon board traps radon from the monitor degasser into Lucas cells to be taken to the surface lab for counting. Before assaying, the FTS water trap is emptied of any residual H_2O, which is collected and the volume recorded. To supply pressure to clear the water trap, a flow of "clean" nitrogen from a gas cylinder is used to fill the trap. A checklist must be filled in when running the procedure.

2. Procedure

2.1 Authorization to Implement

One of the key changes to this procedure has been to add several places where UPWSS authorization is required. The first UPW authorization is for the tasks of draining the FTS trap and Vlad trap. This is specifically authorized even though it is a fairly benign task because it is frequently done a day or two before the actual assay, and is the only action completed that day. The second UPW authorization is for baking and pumping on the Radon board. Normally this is also an activity that does not affect the water systems, but it is normally done first thing the morning of a H_2O Rn assay, and the UPW needs to be aware of the activity taking place. The UPW may also choose to authorize both of these first two places at the beginning of the day of the assay, to allow the Assay Operator to get all of their preparations done without further interaction with the UPW required. The third UPW authorization is required before the assay proper is allowed to begin. This is the most important authorization, because water system valves are to be opened, pumps started, etc.

2.2 Draining the Traps

2.2.1 UPW Authorization

See above explanation. This is more of a UPW notification than authorization.

2.2.2 Defrosting the FTS (if required)

♦ If required, the FTS can be defrosted by using the defrost function. Normally this is not required.

2.2.3 Preliminary Confirmed Closed List

♦ Follow and fill in section 2.2.3 of the checklist to confirm closed valves to prepare to drain the trap.

2.2.4 Preliminary Confirmed Open List

♦ Follow and fill in section 2.2.4 of the checklist to confirm valves that are normally left open.

2.2.4 Preliminary Setup

♦ Follow and fill in section 2.2.4 to ensure the N2 gas bottle supply is connected, and the regulator and needle valve are set properly.

2.2.5 Flushing the Lines

♦ Follow and fill in section 2.2.5 to flush air out of the N2 lines

2.2.6 Valve Open List

♦ Follow and fill in section 2.2.6 to open a path from the trap to the pressure gauge.

2.2.7 Pressurizing and Draining the Trap

♦ Follow and fill in section 2.2.7 to pressurize and drain the trap

♦ Note that attention must be paid to only pressurize the trap with a slight positive pressure. There is no safety relief valve on the trap, so if it is over pressurized it would break, perhaps explosively.

2.2.8 Return System to Normal Configuration

♦ Follow and fill in section 2.2.8 to return the valves to a normal configuration. Often draining the trap is done the day before the day of the assay, but assays can be cancelled or deferred, so it is important to leave the system in a normal or standard configuration.

2.2.9 Draining the "Vlad" Trap

♦ Follow and fill in section 2.2.9 if the Vlad trap needs to be drained. This is not done as frequently as draining the Titan Trap, so is considered an optional section. If there are two people working on the Rn assay, it can also be done simultaneously with draining the Titan Trap to save time.

2.3 Pumping the Trap, Flushing Lucas Cells, and Baking the Board

2.3.1 UPW Authorization

See explanation in section 2.1. This is also more of a UPW notification than authorization, because it doesn't affect the rest of the water systems.

2.3.2 Initial Set-up

♦ Follow and fill in section 2.3.2 of the checklist to turn on the FTS system and the vacuum pump.

2.3.3 Cool 'Vlad' Trap

♦ Follow and fill in section 2.3.3 of the checklist to fill the Vlad trap with LN2. Note that the Assay Operator must also be authorized on the LN2 handling procedure, SL-OPS-PCS-10-010.

2.3.4 Pumping the Trap

♦ Follow and fill in section 2.3.4 of the checklist to confirm closed valves on the Radon board and open a path from the vacuum pump to the vapour trap.

2.3.5 Evacuating Lucas Cells

♦ Follow and fill in section 2.3.5 to flush and evacuate Lucas cells.

2.3.6 Baking the Radon Board

♦ Follow and fill in section 2.3.5 to bake the Radon board lines with a heat gun to drive off any moisture in the lines.

2.4 Main Assay

2.4.1 UPW Authorization

See explanation in section 2.1. This is the most critical UPW authorization, because actions taken after this affect the water systems and the water in the cavity.

2.4.2 Initial Considerations

♦ Follow and fill in section 2.4.2 to make notes on the assay run plan for the day. Notes taken here will help later interpretation of the assay results, and also help the Assay Operator and UPW consider all the potential implications of the assay on the water systems.

2.4.3 Confirm Closed Valves

♦ Follow and fill in section 2.4.3

2.4.4 Confirm Open Valve

♦ Follow and fill in section 2.4.4 to confirm the valve that is normally left open.

2.4.5 Confirm/Establish Initial Set-up

♦ Follow and fill in section 2.4.5 to set up the two diaphragm pumps in preparation for the assay flow path to be established.

2.5 OPTION #1 Loop Sample Assay (Optional if MDG contains water)

2.5.1 Confirm Closed or Close Key Valves

♦ Follow and fill in section 2.6.1 to confirm that key valves are closed. These are valves that may have been opened if OPTION #1 has been completed first. If the valves need to be closed, which would be the normal situation, enter a check mark on each line. If the valves are already closed, it probably means that you did not complete a sample line assay first, and you should enter 'CC' on each line for Confirm Closed.

2.5.2 Loop Adjustments

♦ Ask the UPW to follow and fill in section 2.6.2 to adjust the H_2O purification loop. This is required because for a loop sample assay, the assay flow is returned to the loop between the P15 throttle valve V-536L, and the inlet of the PDG. The UPW can add throttle to V-536L, which will reduce the pressure after V-536L, and allow P05 to stroke when it is turned on. The UPW may also want or need to adjust the throttle on V-165L at the inlet to the PDG, to bring the pressure at the inlet to the PDG down, although they will need to make sure they don't lower it too far (no lower than 15 psi), or the PDG will trip offline on low inlet pressure

2.5.3 Valve Open List

♦ Follow and fill in section 2.6.3 to open the loop sample flow path valves.

2.5.4 Establishing Flow for Loop Sample

♦ Follow and fill in section 2.6.4. This part of the procedure requires coordination between the UPW and the Assay Operator.

2.6 MDG Flow Establishment

♦ Follow and fill in sections 2.6.1 – 2.6.4 to complete the MDG fill, and run the MDG in a closed loop.

2.9– 2.13 Radon Assay Sheets

♦ Note that Sections 2.9 to 2.13 have been set up to run a number of Radon assays, following identical steps so that there are no differences in procedure between assays.

2.8 Assay Details

2.8.1 Subsequent Assay Preparations

♦ Follow and fill in section 2.9.1 of the checklist for subsequent assays only (i.e. not required for the first sample line assay nor for the first loop sample assay). Note that the main purpose of this section is to make a note of the sample valve selected, and then open it.

2.8.2 Recommence Flow Through the MDG

♦ Follow and fill in section 2.9.2 to restart the two diaphragm pumps and to open the inlet and outlet valve to the MDG.

2.8.3 Running the Vacuum Degasser

♦ Follow and fill section 2.9.3 of the checklist to bleed P-26 and make final preparations before starting the extraction

2.9 Extraction from the water

♦ Follow and fill out section 2.10.1-2.10.4 to extract the radon from the gas coming out the vacuum degasser. Periodic checks of pressures, every 15 minutes, are to be recorded as indicated on the MDG extraction sheet and the liquid Nitrogen filled every 30-40 minutes in the "Vlad" trap (311-VT-01). Follow and fill in section 2.10.3 of the checklist during the extraction time. At the end of the assay follow and fill in section 2.10.5 to shut off the water flow and prepare for the transfer of radon.

2.10 Transfer of Radon

♦ Follow 2.11.1-2.11.5 to transfer the radon to the Lucas cell. Note that the transfer time from trap A to trap B is 15 minutes, and the transfer time from Trap B to the Lucas cell is 10 minutes. During the warming of trap B, the pressure in B may rise off scale (>700 on gauge B). If so, open to the cell immediately and record the time. Should the pressure still continue to rise too quickly, open the valve either to the next cell in line or to the small closed section of piping between where the cells should be. There is some margin of error, but at a pressure greater than 1500 or so (well off scale) the meter will be damaged.

2.11 Bake Board again

♦ To prepare for the next assay follow section 2.12 to evacuate the traps.

2.12 Assay Shutdown and Preparation for Next Assay

♦ Follow and fill in section 2.13 to record the current sample valve and close it. Note that instructions are given here to go back to the beginning of Section 2.9 for the next sample point or to move on to OPTION #2 or tocontinue on to a full shutdown of the procedure

2.13 System Shutdown at the End of All Assays

♦ Follow and fill in section 2.14.1 – 2.14.4 to proceed with a full shutdown of the procedure. Note that thereare some valves that will already be closed. If valves are already closed, enter CC for confirm closed. If the valves require closing, enter a check mark.

2.14 Checklist Completion and Filing

♦ Follow and fill in section 2.15.1– 2.15.2 to prepare and file the checklist and complete the assay.

3. Potential Hazards and Risks

The following are considered to be hazards to be aware of in the implementation of this procedure:

- Opening wrong valves can disrupt the closed loop configuration and will not give accurate background of the MDG.
- Opening wrong valves can interfere with the UPW plant operations.
- The sample line part of this procedure draws H_2O directly from the cavity. Although previous experience has shown it does not to generate a large amount of light, the detector operator must be notified and care exercised when opening the sample line valves.
- Potential for H_2O loss which would upset the levels in the detector.
- Proper equipment must be used when working with and pouring liquid nitrogen. Gloves for pouring, and a protective face shield. Note also that any LN2 spills may drip through the mezzanine floor onto people below, so the utmost care must be used when pouring LN2 and if needed, the people working below should bewarned and asked to move away from the area.
- Too much air entering P15 through V-544L will trip the whole H_2O recirculation system.
- When draining the FTS, do not over pressurize with nitrogen gas, exercise caution while workingwith compressed nitrogen bottle
- When warming the radon trap, watch the pressure rise. If it gets too high, then open the appropriate valves to relieve the pressure.

Note

Note:

4. Revision History

ORIGINATING DATE: 2020-01-30			
REV NO.	**EFFECTIVE DATE (YYYY-MM-DD)**	**AUTHOR**	**SUMMARY OF CHANGE**
0	2020-01-30	S.Hussain	Initial procedure development based on based on SL-OPS- PCS-30-350-P- rev7

SL-OPS-PCS-30-351-P Rev 00
Closed loop: MDG background with water

Personnel: _____

_____

Day/Date: _____

Time: _____

2.1 Authorization to Implement (Explanation)

Note: UPWSS authorization is required in **3 places** for this procedure (2.2 - Draining the Trap, 2.3 - Pumping the Trap, Flushing Lucas Cells, and Baking the Board, 2.4 - Main Assay Procedure).

Sometimes the UPWSS will be asked by the assay operator for authorization for 2.2 (Draining the Traps) onthe day prior to the assay. This might be all that is done on a given day.

The day of the assay, the UPWSS may be asked for authorization for 2.2 and 2.3 together or 2.3 byitself, and then will normally wait until these sections are complete before asking for authorization to complete from 2.4 on (Main Assay Procedure).

2.2 Draining the Traps

2.2.1 Authorization to implement

UPWSS initials to implement Section 2.2 Draining the Trap	

2.2.2 Defrosting the FTS (if required)
***** OPTIONAL SECTION *****

One may melt the ice on the coils of the FTS simply by leaving it over night with the power off **OR**	
Press and hold the defrost button and wait for a click. (if not done, enter NR)	
Monitor trap when defrosting. Turn off defrost before the temp. exceeds 40 °C. (if not done, enter NR)	

2.2.3 Preliminary Confirmed Closed List

Valve on top of degasser	[Y]	V-215L	Confirm Closed	
Behind control panel	[Y]	V-189L	Confirm Closed	
Beside FTS	[Y]	V-243L	Confirm Closed	
Beside FTS	[Y]	V-224L	Confirm Closed	
Beside FTS	[Y]	V-222L	Confirm Closed	
Beside FTS – green	[Y]	V-226L	Confirm Closed	
N2 supply to vapour trap	[Y]	V-669L	Confirm Closed	
N2 flush line (behind MDG skid)	[Y]	V-659L	Confirm Closed	

2.2.3 Preliminary Confirmed Open List

Formerly actuated valve (normally left open)	[Y]	V-537L	Confirm Open	

2.2.4 Preliminary Setup

Ensure regulator is connected to the N2 cylinder, located on the first floor directly beneath the Rn skid				
Main N2 bottle supply valve		[Y]	Lift Red Switch	
Regulator diaphragm valve (N2 cylinder - first floor)		[Y]	OPEN P ~ 5 psi	
Black valve	[Y]	V-660L	OPEN 1 Turn	

2.2.5 Flushing the Lines

Back of MDG Skid, N2 Flush valve	[Y]	V-659L	OPEN	
Open V-745L	[Y]	V-745L	OPEN	
Flush the line for 20 seconds.				
Close V-745L	[Y]	V-745L	CLOSE	
Back of MDG Skid	[Y]	V-659L	CLOSE	

2.2.6 Valve Open List NOTE: Be sure to open the valves slowly

N2 PP Isolation valve (upstairs, backside of skid)	[Y]	V-225L	OPEN slowly	
MDG Vapour Trap N2 inlet (backside of skid)	[Y]	V-222L	OPEN slowly	
N2 SS supply line (backside of skid)	[Y]	V-579L	OPEN slowly	
Note: Pressure gauge along the line should drop to –30 inches of Hg (red scale) if FTS is under vacuum.				

2.2.7 Pressurizing and Draining the Trap

Important Note: The Vapour Trap must not be over-pressurized (>2 psi) or it will break.					
Watch PI 647 during the next two steps to pressurize the trap to 0.5 psi					
N2 supply valve (backside of skid)	[Y]	V-669L	OPEN Slowly		
N2 supply valve (backside of skid)	[Y]	V-669L	CLOSE P ~ 0.5		
Place a bucket below the outlet drain pipe			Bucket Placed		
FTS Drain	[Y]	V-226L	OPEN		
Drain water only to a level just above the outlet tube					
Drain of FTS	[Y]	V-226L	CLOSE		
NOTE: If the gauge indicates that the pressure has fallen below atmosphere, repeat the above steps					

2.2.8 Return System to Normal Configuration

N2 PP Isolation valve (upstairs, backside of skid)	[Y]	V-225L	CLOSE	
MDG Vapour Trap N2 inlet (backside of skid)	[Y]	V-222L	CLOSE	
N2 SS supply line (backside of skid)	[Y]	V-579L	CLOSE	
Drain of FTS	[Y]	V-226L	Confirm Closed	
N2 Supply Valve (behind MDG)	[Y]	V-669L	Confirm Closed	
Measure the amount of water taken from the FTS, Record this number in the MDG log book				
NOTE: Mark the following 3 steps as "NR" if flushing Lucas Cells today:				
Main N2 bottle supply valve [Red Switch]		[Y]	CLOSE	
Regulator diaphragm valve		[Y]	BACK OFF	
Black valve	[Y]	V-660L	CLOSE	

2.2.9 Draining "Vlad" Trap (321-VT-01)
***** OPTIONAL SECTION, May be Done in Parallel With Draining the FTS Trap*****

Inlet to Vlad Trap (near VP02, Alcatel pump)	[Y]	V-539L	Confirm Closed	
Outlet of Vlad Trap (near VP02, Alcatel pump)	[Y]	V-247L	Confirm Closed	
Loosen one clamp (NW vacuum fitting style) and vent the vacuum				
Reconnect / tighten clamp once vented				
Remove top section of Vlad trap				
Use syringe to draw water out of Vlad trap				
Measure the amount of water in Vlad trap and record amount in MDG log book				

Notes:

2.3 Pumping the Trap, Flushing Lucas Cells, and Baking the Radon Board

2.3.1 Authorization to implement

UPWSS initials to implement Section 2.3 Pumping the Trap, Flushing Lucas Cells, and Baking the Radon Board	

2.3.2 Initial Setup

Turn on Control Panel power				
Turn on FTS main power and activate the cooling cycle by depressing the Start/Stop button. The button may have to be pressed twice. Ensure the green light comes on.				
Record Time:			hh:mm	
Inlet to Vlad Trap (near VP02, Alcatel pump)	[Y]	V-539L	Confirm Closed	
Outlet of Vlad Trap (near VP02, Alcatel pump)	[Y]	V-247L	Confirm Closed	
Make sure V_exhaust is open and confirm oil in the exhaust line of the vacuum pump	[Y]	V_Exhaust	OPEN	
Start the Alcatel vacuum pump. The switch is on the control panel.				

2.3.3 Cool "Vlad" Trap (321-VT-01)

Confirm Vlad trap is connected	
Obtain Liquid N_2 according to SL-OPS-PCS-10-010 (LN2 handling procedure)	
Place caution tape on main floor below Rn skid in case LN2 drips below	
Cool "Vlad" trap by filling with liquid N_2. Fill to black line on the blue zip tie next to the Vlad trap	
NOTE: do not overfill as O-ring will freeze and trap will begin leaking	

2.3.4 Pumping Trap

Drain of FTS	[Y]	V-226L	Confirm Closed	
Rn Board (Radon Trap bypass)	[Y]	V-258L	Confirm Closed	
Rn Board (3-way valve after Radon Trap)	[Y]	V-245L	Confirm Closed	
Rn Board (outlet of last Lucas Cell)	[Y]	V-262L	Confirm Closed	
Rn Board (capped)	[Y]	V-256L	Confirm Closed	
Rn Board (inlet to Radon trap)	[Y]	V-244L	Confirm Closed	
Rn Board (secondary isolation from FTS)	[Y]	V-243L	Confirm Closed	
Radon Board bypass to Vlad Trap and vacuum pump	[Y]	V-242L	Confirm Closed	
Valve on top of degasser	[Y]	V-215L	Confirm Closed	
N2 PP Isolation valve (backside of skid)	[Y]	V-225L	Confirm Closed	
Rn Board, valve **normally left open**	[Y]	V-257L	Confirm Open	
Rn Board, valve **normally left open**	[Y]	V-538L	Confirm Open	
Formerly actuated valve (**normally left open**)	[Y]	V-537L	Confirm Open	
* Outlet of Vlad Trap. Open in small increments	[Y]	V-247L	OPEN Slowly	
* Inlet to Vlad Trap (near VP02, Alcatel pump)	[Y]	V-539L	OPEN Slowly	
* Watch pressure on FTS panel, make sure it is going down or else check for leaks before continuing.				
Confirm pressure is below 20 mTorr before proceeding.				
Record pressure reading (PT 007, display on FTS panel)			mTorr	
Confirm FTS has cooled for 10 minutes before pumping on it				
Record Time:			hh:mm	
Vapour Trap inlet, beside FTS	[Y]	V-222L	OPEN	
Vapour Trap outlet, beside FTS	[Y]	V-224L	OPEN	
* Radon Board bypass to Vlad trap and vacuum pump	[Y]	V-242L	OPEN Slowly	
Note: Open V-242L in small stages, not letting the Alcatel pump to strain too much from the gas load.				
Check and Fill "Vlad" trap when needed (~ every 30-40 min)				
Confirm pressure is below 50 mTorr before proceeding.				
Record pressure reading (PT 007, display on FTS panel)			mTorr	
Radon Board bypass to Vlad Trap and vacuum pump	[Y]	V-242L	CLOSE	
Plug in trap/MDG pressure gauges (2 plugs) and heat gun (120 VAC)				

2.3.5 Flushing the Lucas Cells

Two Lucas Cells may be flushed at the same time, even if only one is being used for the actual assay.				
Rn Board (Radon Trap bypass)	[Y]	V-258L	Confirm Closed	
Rn Board (3-way valve after Radon Trap)	[Y]	V-245L	Confirm Closed	
Rn Board (between Lucas Cell ports)	[Y]	V-261L	Confirm Closed	
Rn Board (outlet from last Lucas Cell)	[Y]	V-262L	Confirm Closed	
Rn Board bypass to Vlad trap and vacuum pump	[Y]	V-242L	Confirm Closed	
Rn Board (secondary isolation from FTS)	[Y]	V-243L	Confirm Closed	
Rn Board (Radon trap inlet)	[Y]	V-244L	Confirm Closed	
N2 Supply valve (backside of skid)	[Y]	V-669L	Confirm Closed	
N2 Supply (side of skid)	[Y]	V-668L	Confirm Closed	
Near Vlad Trap	[Y]	V-539L	Confirm Open	
Outlet of Vlad Trap (near VP02, Alcatel pump)	[Y]	V-247L	Confirm Open	
Rn Board, valve **normally left open**	[Y]	V-257L	CLOSE	
Remove the blue plastic protective cap from the Lucas cell and nozzle. Attach the Lucas Cell to quick connect port 2 for a single Lucas Cell, or ports 1 and 2 for two Lucas Cells	[Y]	311-LUC-01	Attach Lucas Cells	
Open Rn Board (outlet from last Lucas Cell) for LC evacuation until pressure is stable (P < 10mTorr)	[Y]	V-262L	OPEN	
If using Port 1	[Y]	V-261L	OPEN	
Rn Board (outlet from last Lucas cell)	[Y]	V-262L	CLOSE	
Near Vlad trap	[Y]	V-539L	CLOSE	
Rn Board	[Y]	V-256L	OPEN	
Open black circular valve on regulator of N2 cylinder. Establish pressure of 6psi.	[Y]	V-660L	OPEN	
Back of MDG Skid	[Y]	V-659L	OPEN	
Open Rn Board (outlet from last Lucas Cell)	[Y]	V-262L	OPEN	
LC N2 Flush #1: Fill LC with N2 (should be fast, <10 s)				
RnBoard (Radon trap bypass)	[Y]	V-258L	OPEN	
Close Rn Board (radon trap bypass)	[Y]	V-258L	CLOSE	
Let LC flush for 30 sec				
Open near Vlad trap valve for evacuation. Wait for stable pressure (P < 10mTorr)	[Y]	V-539L	OPEN	
Near Vlad trap	[Y]	V-539L	CLOSE	
LC N2 Flush #2: Fill LC with N2	[Y]			
RnBoard (Radon trap bypass)	[Y]	V-258L	OPEN	
Close Rn Board (radon trap bypass)	[Y]	V-258L	CLOSE	
Let LC flush for 30 sec				
Open near Vlad trap valve for evacuation. Wait for stable pressure (P < 10mTorr)	[Y]	V-539L	OPEN	
Near Vlad trap	[Y]	V-539L	CLOSE	
LC N2 Flush #3: Fill LC with N2	[Y]			
RnBoard (Radon trap bypass)	[Y]	V-258L	OPEN	
Close Rn Board (radon trap bypass)	[Y]	V-258L	CLOSE	
Let LC flush for 30 sec				
Open near Vlad trap valve for evacuation. Wait for stable pressure (P < 10mTorr)	[Y]	V-539L	OPEN	
Record pressure reading (PT 007, display on FTS panel)			mTorr	
Rn Board (outlet from last Lucas Cell)	[Y]	V-262L	CLOSE	
If using 2 Lucas Cells, Rn Board (between Lucas Cells)	[Y]	V-261L	CLOSE	
Remove Lucas Cells and reattach blue caps				
Rn Board (Radon trap bypass)	[Y]	V-258L	Confirm Closed	
Rn Board (outlet from last Lucas Cell)	[Y]	V-262L	Confirm Closed	

Rn Board (between Lucas Cells)	[Y]	V-261L	Confirm Closed	
Back of MDG Skid	[Y]	V-659L	CLOSE	
Rn Board	[Y]	V-256L	CLOSE	
Rn Board, valve	[Y]	V-257L	OPEN	
Near Vlad trap	[Y]	V-539L	Confirm Open	
Regulator valve		[Y]	BACK OFF	
Needle valve on regulator	[Y]	V-660L	CLOSE	
Red Clip down				

2.3.6 Baking the Radon Board

Use heat gun to bake the two radon traps (311-CT01, 311-RTR02). Take care not to point heat gun at FTS chamber or wiring for pressure gauges A and B. Traps should be heated until they are hot to touch (approx. 40°C)				
Radon Board bypass to Vlad Trap and vacuum pump	[Y]	V-242L	Confirm Closed	
Radon Board (isolation from N2 supply)	[Y]	V-243L	Confirm Closed	
Radon Board (Radon Trap inlet)	[Y]	V-244L	Confirm Closed	
Radon Board (outlet from last Lucas Cell)	[Y]	V-262L	OPEN	
Radon Board (between Lucas Cells)	[Y]	V-261L	OPEN	
Radon Board (inlet to first Lucas Cell)	[Y]	V-260L	OPEN	
Radon Board (inlet to Secondary Radon Trap)	[Y]	V-259L	OPEN	
Heat Trap B (311-RTR-02)				
Close when P < 15 mTorr	[Y]	V-259L	CLOSE	
Record pressure reading (PT 007, display on FTS panel)			mTorr	
Radon Board (inlet to first Lucas Cell)	[Y]	V-260L	CLOSE	
Radon Board (between Lucas Cells)	[Y]	V-261L	CLOSE	
Radon Board (outlet from last Lucas Cell)	[Y]	V-262L	CLOSE	
Radon Board (3-way valve after Radon Trap)	[Y]	V-245L	OPEN Down	
Heat Trap A (311-CT01)				
Close when P < 15 mTorr	[Y]	V-245L	CLOSE	
Record pressure reading (PT 007, display on FTS panel)			mTorr	
Note the baseline pressures on the "MDG extraction/ experiment record sheet."				

************Emergency Shut Down Procedure for Sections 2.1 - 2.3************

IF YOU ARE RETURNING:				
Leave everything as is. If you can, ensure there is enough LN2 in the Vlad trap. The system is stable at this point.				
IF YOU ARE NOT RETURNING (or unsure of your return):				
Radon Board (outlet from last Lucas Cell)		[Y]	V-262L	CLOSE
Rn Board (Radon trap bypass)		[Y]	V-258L	CLOSE
FTS inlet valve		[Y]	V-222L	CLOSE
FTS outlet valve		[Y]	V-224L	CLOSE
Shut off Cooling Switch on FTS	[Y]	FTS Panel, (**on/off**)		OFF
Turn off FTS	[Y]	FTS Panel, (**1/0**)		0
Near Vlad trap		[Y]	V-539L	CLOSE
Shut off vacuum pump	[Y]	Control Panel		OFF
Vent vacuum pump			[Y]	VENT
Near Vlad trap		[Y]	V-247L	CLOSE
Bring Lucas Cell(s) with you				

Notes:

2.4 Main Assay

2.4.1 Authorization to Implement

UPWSS initials to implement Section 2.4 – Main Assay	

2.4.2 Initial Considerations (to be completed with help from the UPWSS)

Run SL-OPS-PCS-30-403 to purge sample line if assay is following H_2O MnOx or HTiO assay	
Confirm that SL-OPS-PCS-30-200-P is running	
Record cavity level (LT-103)	
Make notes describing the current circulation & run plan, i.e.: - Is cavity automake-up active (checked in DeltaV)? Is this what we want? - Is this a closed loop assay for some reason? - Is the (new) polishing RO on-line or off-line? - Is parallel flow (the cavity cooling flow path through the UFR bank) on-line or off-line? - Have there been any SDS trips in the last 24 hours? - Any other unusual circumstances?	

2.4.3 Confirm Closed Valves

Above FTS, back	[Y]	V-550L	Confirm Closed	
On side of degasser	[Y]	V-208L	Confirm Closed	
MDG Skid, back near P26	[Y]	V-168L	Confirm Closed	
MDG Skid, by P26 (P26 outlet valve)	[Y]	V-285L	Confirm Closed	
Near Dummy Column	[Y]	V-232L	Confirm Closed	
Near Dummy Column	[Y]	V-234L	Confirm Closed	
MDG Skid, above P26	[Y]	V-255L	Confirm Closed	
MDG Skid, above P26	[Y]	V-254L	Confirm Closed	
MDG Skid, above P26	[Y]	V-467L	Confirm Closed	
MDG Skid, above P26	[Y]	V-479L	Confirm Closed	
MDG Skid, by UF (Injection Port)	[Y]	V-641L	Confirm Closed	
On side of Degasser	[Y]	V-228L	Confirm Closed	
Top of Degasser	[Y]	V-189L	Confirm Closed	
Top of Degasser	[Y]	V-215L	Confirm Closed	
Inlet to Degasser	[Y]	V-248L	Confirm Closed	
Beside Degasser (Capped)	[Y]	V-576L	Confirm Closed	
Bottom of Degasser	[Y]	V-294L	Confirm Closed	
UFR06 permeate	[Y]	V-302L	Confirm Closed	
UFR06 permeate	[Y]	V-303L	Confirm Closed	
MDG skid (beside FTS)	[Y]	V-209L	Confirm Closed	
Above FTS	[Y]	V-551L	Confirm Closed	
Loop sample valve after PDG (by UV skid)	[V]	V-535L	Confirm Closed	
P15 inlet loop sample and return line (downstairs)	[V]	V-544L	Confirm Closed	
To Forced Drain (downstairs)	[V]	V-558L	Confirm Closed	
Loop sample valve after HX01 and new RO (downstairs)	[V]	V-229L	Confirm Closed	
P15 outlet return line (downstairs, PDG pit)	[V]	V-470L	Confirm Closed	
To drain (downstairs, PDG pit)	[V]	V-471L	Confirm Closed	
PDG pit	[Y]	V-171L	Confirm Closed	
PDG pit	[Y]	V-252L	Confirm Closed	
PDG pit	[Y]	V-540L	Confirm Closed	

2.4.4 Confirm Open Valve

Above Degasser, by PT-004 (normally left open)	[Y]	V-241L	Confirm Open	

2.4.5 Confirm/Establish Initial Set-Up

Compressed air valve for P05 (PDG Pit)	[NN]	V-577L	Confirm Open	
Set P_{air} to bottoms pump P05 (PDG Pit)	[NN]	PCV-135	Set to 40 psi	
P05 inlet (PDG Pit)	[Y]	V-171L	OPEN	
Compressed air valve for P05 (PDG Pit)	[Y]	V-172L	OPEN	
P26 outlet valve (upstairs)	[Y]	V-285L	OPEN	
Set P_{air} to degasser feed pump P26	[NN]	PCV-132	Set to 60 psi	
Compressed air valve for P26	[Y]	V-170L	OPEN	

Notes:

Note:
This procedure has been re-designed so that at this point, the Assay Operator can initiate a sample line assay (OPTION #1, V-201 to 206), or a loop sample assay (OPTION #2, V-535, 544, or 229).

Closed Loop or Loop Troubleshooting Assay Suite
For troubleshooting Radon ingress into the purification loop, sometimes a series of loop sample point assays are required. OPTION #1 Section 2.5 is selected for the first loop sample point, and subsequent loop sample points are covered in Sections 2.7 to 2.12. This option is required only if the MDG is empty and doesn't required to be filled with water.

Other permutations and combinations are possible, but should be planned in advance with Richard Ford.

***OPTION 1 –LOOP SAMPLE: FILLING THE MDG WITH UPW LOOP (Optional, if the MDG already contains water)**

***Proceed only if the MDG is empty, otherwise skip to section 2.7**

2.5 Flowpath Preparation

2.5.1 Confirm Close or Close Key Valves

Confirm closed OR close possible return path valve	[Y]	V-550L	Confirm Closed (CC) or CLOSE (checkmark)	
Confirm closed OR close possible return path valve	[Y]	V-551L	Confirm Closed (CC) or CLOSE (checkmark)	
Confirm closed OR close possible skid inlet	[Y]	V-254L	Confirm Closed (CC) or CLOSE (checkmark)	
Confirm closed OR close possible return to loop valve	[V]	V-544L	Confirm Closed (CC) or CLOSE (checkmark)	

2.5.1 Loop Adjustments

Ask the UPW to reduce the outlet pressure between V-536L and the PDG inlet by adding more throttle to V-536L and or taking throttle off the PDG inlet valve – UPW to target ~12 psi at the PDG inlet	
Loop adjustment(s) complete UPW's checkmark required here→	

2.5.2 Valve Open List

Open P05 outlet valve (PDG pit)	[Y]	V-252L	OPEN	
Open return path to loop	[V]	V-470L	Slowly OPEN	
Open inlet valve to skid	[Y]	V-255L	Slowly OPEN	

2.5.3 Establishing Flow for Loop Sample

Note: The Assay Operator needs to work with the UPW for this section. The UPW will slowly open the loop sample valve – we are sampling from the loop here, not returning to the loop as we do for a sample line assay. The Assay Operator will simultaneously open the flow path in and out of the MDG, with an eye on the MDG level.				
UPW and Assay Operator activities discussed, and both people in position				
Turn on solenoid valve power for P26 (feed pump)		Control Panel	TOGGLE ON	
Increase P_{air} to bottoms pump P05 (PDG Pit)	[NN]	PCV-135	Set to 70 psi	
List the loop sample valve (V-229L, V-535L or V-544L)				
Do the next four steps in quick succession (Assay Operator can call down to the UPW to proceed):				
Slowly open H_2O sample valve	[V]	V-535L	Slowly OPEN	
Inlet to MDG (Assay Operator)	[Y]	V-248L	OPEN	
P05 power (bottoms pump) (Assay Operator)		Control Panel	ON	
Outlet of MDG (Assay Operator)	[Y]	V-294L	OPEN	
(MDG Vacuum Valve) Top of MDG	[Y]	V-215L	OPEN	
Open Slowly until Pressure reads 3HHH (off scale, MDG Skid)	[Y]	V-242L	OPEN Slow	
Ensure P05 is pumping				
If P05 will not stroke, then follow the next 5 steps, otherwise mark them as NR (not required)				
Assay Operator to close inlet to MDG	[Y]	V-248L	CLOSE	
UPW to adjust P05 air pressure	[Y]	PCV-135	Adjust	
and/or UPW to adjust V-536L throttle	[V]	V-536L	Adjust	
and/or UPW to adjust V-165L throttle	[X]	V-165L	Adjust	
When P05 starts stroking then Assay Operator to open V-248L	[Y]	V-248L	OPEN	

Notes:

2.6 Flow Adjustments

2.6.3 Adjusting Flow

Adjust P26/P05 air pressures to about 73 psi to get a steady flow of 20 – 24 lpm				
Note flow after adjustments are made		FIT121		lpm

2.6.4 Accumulator (ACC04) Setup and Flow Dampening (if required)

Record P26 outlet pressure	[Y]	PI 120		psi
Air supply isolation valve (above sink in chem. area)	[Y]	V-578A	Confirm OPEN	
Set accumulator regulator to ~50 psi on associated gauge	[Y]	PCV-137	Set to 50 psi	
Monitor the flow; should read about 24 lpm when stable	[Y]	FIT-121		lpm
Skip ahead to 2.8 Assay Details				

2.6.5 Note Diaphragm Pump Air Supply Pressures

Record P26 air supply pressure	[Y]	PCV-132	psi
Record P05 air supply pressure	[Y]	PCV-135	psi

2.6.6 Start time of steady flow

Start time of steady flow	

2.7 MDG Flow Establishment

2.6.7 MDG Fill Completion [PROCEED QUICKLY]

After **30 min** of steady flow:				
P05 Power (bottoms pump)		Control	Off Quickly	
P26 Power (feed pump)		Control	Off Quickly	
MDG inlet	[Y]	V-248L	CLOSE	
MDG outlet	[Y]	V-294L	CLOSE	
Loop sample valve after PDG (by UV skid)	[V]	V-535L	CLOSE	
MDG Skid, above P26	[Y]	V-255L	CLOSE	
PDG Pit	[Y]	V-252L	CLOSE	
P15 outlet return line (downstairs, PDG pit)	[V]	V-470L	CLOSE	

2.6.8 Return H2O System to Standard Configuration

If Option2: Loop Assay was run, then ask the UPW to increase the outlet pressure between V-536L and the PDG inlet by adding less throttle to V-536L and/or adding throttle to the PDG inlet valve	
Loop adjustment(s) complete UPW's checkmark required here→	

2.6.9 Valve Open List

Closed Loop Return	[Y]	V-479L	OPEN	

2.7 Establishing Flow for Loop Sample

Note: The Assay Operator needs to work with the UPW for this section. The UPW will slowly open the loop sample valve – we are sampling from the loop here, not returning to the loop as we do for a sample line assay. The Assay Operator will simultaneously open the flow path in and out of the MDG, with an eye on the MDG level.				
UPW and Assay Operator activities discussed, and both people in position				
Turn on solenoid valve power for P26 (feed pump)		Control Panel	TOGGLE ON	
Increase P_{air} to bottoms pump P05 (PDG Pit)	[NN]	PCV-135	Set to 70 psi	
Do the next four steps in quick succession (Assay Operator can call down to the UPW to proceed):				
Inlet to MDG (Assay Operator)	[Y]	V-248L	OPEN	
P05 power (bottoms pump) (Assay Operator)		Control Panel	ON	
Outlet of MDG (Assay Operator)	[Y]	V-294L	OPEN	
(MDG Vacuum Valve) Top of MDG	[Y]	V-215L	OPEN	

Open Slowly until Pressure reads 3HHH (off scale, MDG Skid)	[Y]	V-242L	OPEN Slow	
Ensure P05 is pumping				
If P05 will not stroke, then follow the next 5 steps, otherwise mark them as NR (not required)				
Assay Operator to close inlet to MDG	[Y]	V-248L	CLOSE	
UPW to adjust P05 air pressure	[Y]	PCV-135	Adjust	
and/or UPW to adjust V-536L throttle	[V]	V-536L	Adjust	
and/or UPW to adjust V-165L throttle	[X]	V-165L	Adjust	
When P05 starts stroking then Assay Operator to open V-248L	[Y]	V-248L	OPEN	

Notes:

************Emergency Shut Down Procedure for Sections 2.4 - 2.8************

IF YOU ARE RETURNING:				
Radon Board	[Y]	V-244L	CLOSE	
P05 Power (bottoms pump)	[Y]	Control	OFF	
P26 Power (feed pump)	[Y]	Control	OFF	
MDG Inlet	[Y]	V-248L	CLOSE	
MDG Outlet	[Y]	V-294L	CLOSE	
Rn Board	[Y]	V-245L	CLOSE	
IF YOU ARE NOT RETURNING (or unsure of your return):				
Radon Board	[Y]	V-244L	CLOSE	
P05 Power (bottoms pump)	[Y]	Control	OFF	
P26 Power (feed pump)	[Y]	Control	OFF	
MDG Inlet	[Y]	V-248L	CLOSE	
MDG Outlet	[Y]	V-294L	CLOSE	
Rn Board	[Y]	V-245L	CLOSE	
Radon Board (outlet from last Lucas Cell)	[Y]	V-262L	CLOSE	
Rn Board (Radon trap bypass)	[Y]	V-258L	CLOSE	
FTS inlet valve	[Y]	V-222L	CLOSE	
FTS outlet valve	[Y]	V-224L	CLOSE	
Shut off Cooling Switch on FTS [Y]	FTS Panel, (**on/off**)		OFF	
Turn off FTS [Y]	FTS Panel, (**1/0**)		0	
Near Vlad trap	[Y]	V-539L	CLOSE	
Shut off vacuum pump [Y]	Control Panel		OFF	
Vent vacuum pump	[Y]		VENT	
Near Vlad trap	[Y]	V-247L	CLOSE	
Bring Lucas Cell(s) with you				

2.8 Assay Details

	Sample Line Assays			Loop Sample Assays		
Assay Valve #						
Lucas Cell Number LC #						
Record baseline pressures on extraction sheet						

2.8.1 Subsequent Assay Preparations (for subsequent assays only)

Record amount of air in the 5 ft pipe section above sample valve	% air							
List new sample line valve or loop sample valve								
Open new sample line valve or loop sample valve								
On your way back to the Utility Room, let the detector operator know you've opened your sample valve and will be starting the sample line flow								

2.8.2 Recommence flow through MDG (for subsequent assays only)

Turn on P26 (local control panel)								
Open MDG inlet	[Y]	V-248L	OPEN					
Turn on P05 (local control panel)								
Open MDG outlet	[Y]	V-294L	OPEN					
Adjust P26 and P05 pressures if needed to maintain MDG level								
Gradually open to pump down MDG	[Y]	V-242L	Slowly OPEN					

2.8.3 Running the Vacuum Degasser (311-DG01)

Start time of water flow						
Watch Alcatel pressure, it should settle to ~2500 mTorr, with V-242 wide open. MDG pressure should settle around ~ –453						
CLOSE V-242L						
OPEN V-258L						
Bleed the air from P26 by opening D-011*						
*Bleed air by holding a jar under the plastic tubing located on the bleed valve D-011 and **slowly open** the valve until no more air is escaping. **Be careful that tube does not pop off due to pressure**.						
Wait at least **25 minutes** with a water flow of 20 lpm						

2.9 Extraction from the Water

2.9.1 Radon Trap Setup

Fill the large Dewar with LN2 and place it around the Trap A (311-CT01). Use the support elevator to lift the Dewar until the top is even with the Swagelok elbow at the top of the trap.					

2.9.2 Trap A Extraction

Turn on pump **stroke counter**					
CLOSE **V-258L**, quickly open **V-244L**, turn **V-245L** downward and start pump **stroke counter**					
Record Start Time: run for **~30 min, or as required** (At this point the gas flow is into the board through V-257L, through the primary trap, and out V-245L)					

2.9.3 Record Data

Flow rate FIT-121	Behind Rn Board (yellow)	lpm					
Feed Pump Pressure	PI-120 (range)	psi					
Feed Pump Air Pressure	PI-171 (maximum)	psi					
Strokes P26	Time per 20 strokes	sec					
Bottoms Pump Pressure PI-126A	Near P05	psi					
Bottoms Pump Air Pressure	PI-172 (maximum)	psi					
Strokes P05	Time per 20 strokes	sec					
Temperature of MDG walls	Thermometer (after 25 mins)	ºC					

Trap A = Primary Radon Trap = 311-CT01 ; Trap B = Secondary Radon Trap = 311-RTR-02

2.9.4 Extraction Monitoring

	Sample Line Assays			Loop Sample Assays		
Check the Vlad trap periodically and fill with LN_2 as required (every 30-40 min)						
Fill out the Rn extraction log sheet every **15 min**						

2.9.5 Water Extraction Completion [PROCEED QUICKLY]

Radon Board	V-244L	CLOSE						
P05 Power (bottoms pump)	Control Panel	Off Quickly						
P26 Power (feed pump)	Control Panel	Off Quickly						
MDG inlet	V-248L	CLOSE						
MDG outlet	V-294L	CLOSE						
Rn Board, close when P<100 mTorr	V-245L	CLOSE						
Record Time **Immediately (time of V-244L closure)**		Time						
Record time and pump stroke counter final number on the Rn extraction log sheet as well								

2.10 Transfer of Radon

2.10.1 Preparing Trap A and Trap B

Remove Dewar from **Trap A**.								
Cool **Trap B** with LN2 using the smaller Dewar. Support it with wooden box and scissors jack								
Heat trap A to approx room temp								
Record pressure of gauge A on the Radon extraction sheet								
NOTE: If pressure on trap A exceeds +200, abort by opening V-245L into the down position								

2.10.2 Transfer from Trap A to Trap B

Radon Board	V-259L	OPEN						
Radon Board (**start of transfer**)	V-245L	OPEN Upwards						
Allow the transfer to continue for **15 minutes** (meanwhile continue with 2.11.3)								

2.10.3 Preparing the Lucas Cell

Remove the blue plastic protective cap from the Lucas cell and nozzle, secure one Lucas cell to the left quick connect port								
Record Lucas Cell #		LC #						
Radon Board	V-261L	OPEN						
Radon Board	V-262L	OPEN						
Cell normally jumps to 20-30 mTorr on FTS and drops to stable pressure <2 mTorr								
Record maximum pressure		Pmax: mTorr						
Record low stable pressure		Pstable: mTorr						
Radon Board	V-261L	CLOSE						
Radon Board	V-262L	CLOSE						

2.10.4 End of Transfer from Trap A to Trap B

V-259L Close at 15 min mark (**end of transfer**)	Radon Board	CLOSE						
Record Pressures **A** and **B** on Rn Extraction Sheet								
V-245L Turn to downward position to pump trap A	Radon Board	OPEN Down						

2.10.5 Transfer from Trap B to the Lucas Cell

			Sample Line Assays			Loop Sample Assays		
Remove the liquid Nitrogen from **Trap B**								
Heat Trap B until it is warm (approx. room temp)								
If pressure on gauge **B** goes above **+600**, open **V-260L** to relieve the pressure and allow the radon to flow into the Lucas cell.								
Record Pressure **B** on Extraction Sheet								
Start Transfer to Lucas Cell	V-260L	OPEN						
Record Pressure **B** immediately after start of transfer on Extraction Sheet								
Note transfer start time (or use stop watch):								
Bake **Trap A** for ~ 5 min (start of bake)	Radon Board	Bake						
Close when P < 15 mTorr (end of bake)	V-245L	CLOSE						
Note time: (having allowed transfer to take place for 10 minutes)								
Before removing Lucas cell, note Pressure	Trap B							
Remove the Lucas cell and re-attach the blue caps								
Note Pressure B again	Trap B							
Close (end of transfer)	V-260L	CLOSE						
Extraction is now complete.								

2.11 Bake Trap B

Use the heat gun to bake Trap B (311-RTR-02). Take care not to point the heat gun at the FTS chamber or the wiring for the pressure gauges A and B. Trap B should be heated until hot to touch (approx. 80°C)								
Radon Board	V-262L	OPEN						
Radon Board	V-261L	OPEN						
Radon Board	V-260L	OPEN						
Radon Board	V-259L	OPEN						
Heat Trap B (~ 3 min)								
Rn Board Close when P <15mTorr	V-259L	CLOSE						
Radon Board	V-260L	CLOSE						
Radon Board	V-261L	CLOSE						
Radon Board	V-262L	CLOSE						

2.12 Assay Shutdown

2.12.1 Sample Line Assay Completion

Record amount of air in 4 foot pipe section **above V-254L**	% air							
Notify Detector Operator of assay shutdown and whether or not you are doing another sample line assay								
Record number of currently open sample valve on deck	Valve #							
Close currently open sample line valve	CLOSE							
If doing another sample line assay, go back to the beginning of Section 2.8, otherwise enter “done”								
If done the sample line assays and moving on to a loop sample assay go to Section 2.4 Option 2, otherwise enter “done” again and go to Section 2.13.								

2.12.2 Loop Sample Assay Completion

Record number of currently open loop sample valve	Valve #		479L		
Close currently open loop sample valve	CLOSE				
If doing another loop sample assay, go back to the beginning of Section 2.8, otherwise enter “done”, and go to Section 2.13.					

2.13 System Shutdown at the End of All Assays

2.13.1 Degasser Shutdown

Valve on top of degasser	[Y]	V-215L	CLOSE	
Record Time	Time			hh:mm

2.13.2 Valve Close List

MDG Skid, P26 outlet	[Y]	V-285L	CLOSE	
Turn down P_{air} to P26 MDG Skid, above control panel	[NN]	PCV-132	BACK OFF	
MDG Skid, by P26, compressed air to P26	[Y]	V-170L	CLOSE	
Confirm close or close skid inlet	[Y]	V-255L	CLOSE	
Confirm close or close skid inlet	[Y]	V-254L	CLOSE	
Downstairs Near P05	[Y]	V-171L	CLOSE	
PDG Pit, by P05, Turn down P_{air} to P05	[NN]	PCV-135	BACK OFF	
PDG Pit, by P05, compressed air to P05	[Y]	V-172L	CLOSE	
Confirm close or close P05 outlet (downstairs)	[Y]	V-252L	CLOSE	
Confirm close or close sample line return to loop (downstairs)	[V]	V-544L	CLOSE (UPW)	
Confirm close or close loop sample return (downstairs)	[V]	V-470L	CLOSE	

2.13.3 FTS and Radon Board

FTS, inlet valve	[Y]	V-222L	CLOSE	
FTS, outlet valve	[Y]	V-224L	CLOSE	
Shut off Cooling Switch on FTS	FTS Panel, **(on/off)**		OFF	
Turn off FTS	FTS Panel, **(0/l)**			
Near Vlad Trap	[Y]	V-539L	CLOSE	
Shut off vacuum pump	Control Panel		OFF	
Vent vacuum pump, at Vlad trap			Vent	
Near Vlad Trap	[Y]	V-247L	CLOSE	
Unplug heat gun, meter for A/B and meter for MDG			Unplug	
Store liquid N2 (fill XRF detector in the junction if needed)			Store	
Remove caution tape			Remove	

2.13.4 Return H2O System to Standard Configuration (Option 2 Only)

If Option2: Loop Assay was run, then ask the UPW to increase the outlet pressure between V-536L and the PDG inlet by adding less throttle to V-536L and/or adding throttle to the PDG inlet valve	NR
Loop adjustment(s) complete UPW's checkmark required here→	NR

2.14 Checklist Completion and Filing

2.14.1 Ultrapure Water Systems Supervisors Review and Sign-off

Signature of the Ultrapure Water System Shift Supervisor

2.14.2 Copy and File Checklist, Report	
* Xerox checklist pages and send the copy to surface with the cell(s) * File Completed checklist in the "Completed Basket" * Fill in the "Shift Report"	

Notes:

2.15 MDG Extraction Experiment Record Sheet

DATE_____/_____/20_____
m d y

Operators:_____

MDG EXTRACTION EXPERIMENT

Rn extraction is made from the monitor degasser. On surface the Lucas cell is put onto the appropriate PMT and counted to determine number of Rn atoms extracted.

DESCRIPTION of the EXPERIMENT:_____
_____
_____
_____
_____

COUNTING of the LUCAS CELL

Lucas cell #_____Segment _____

Start: _____/_____/20_____, _____ HV On ?? (Y/N) _____
m d y time

Stop:_____/_____/20_____, _____ File Name: _____
m d y time

Counts/ Live time:

Bkg:_____Net Counts/day _____

COMMENTS_____
_____
_____
_____
_____
_____
_____

SETTING UP: Baseline pressures A: _____ B: _____ Alcatel: _____ mTorr

EXTRACTION DETAILS

Extraction: Start_____ Stop_____ Elapsed_____

Lucas cell #_____

Outlet Pressure (PI-120, psig): _____ Inlet Pressure (PI-171, psig): _

MDG Temp (°C): _____ Flow Rate (FIT 121, lpm): _

Time	MDG Temp (°C)	Trap A Pressure	Alcatel Pressure (mTorr)	Trap Temp (°C)	Strokes (Sec/20 strokes)	Comments

Total Strokes On Meter: _____

A → B TRANSFER

A reading when warm: _____

Start time of transfer: _____

Stop time of transfer: _____ Transfer duration: _____

A reading at end of transfer: _____

B reading at end of transfer: _____

B → LC TRANSFER

B reading when warm: _____

Start time of transfer: _____

B reading just after start of transfer: _____ Transfer duration: _____

Stop time of transfer: _____

B reading with LC attached: _____

B reading with LC dis-tached: _____

Appendix B

Gas Board Procedures

Background Assay Procedure for Mobile Radon Board

Title:
Date:
Crew:

1.0 Preparation of the board for extraction

1.1 Preliminary Confirmed Closed List

V-P	Confirm Closed	
V-5	Confirm Closed	
V-4	Confirm Closed	
V-input	Confirm Closed	
V-chamber (Green Valve)	Confirm Closed	
V-S(Source)	Confirm Closed	
V-T1	Confirm Closed	
V-T2	Confirm Closed	
V-N2	Confirm Closed	
V-6	Confirm Closed	
V-9	Confirm Closed	
V-A1	Confirm Closed	
V-A2	Confirm Closed	
V-10	Confirm Closed	
V-11	Confirm Closed	
V-12	Confirm Closed	
V-13	Confirm Closed	
V-14	Confirm Closed	

2.0 Preliminary Setup

Plug in board power bar and Pump	
Turn on the Scroll Pump	
Turn on PT Flow	
Turn on PT Pump	
Turn on PT Traps	

Notes:

3.0 Pumping/Baking the Traps

3.1 Baking and pumping the Nitrogen trap:

V-P	Open	
Record Time:	hh:mm	
Ensure Pressure is below 150 mT. (Allow up to 15 minutes)		
Record Pressure on PT pump	mTorr	
Record Final Time	hh:mm	
V-5	Open	
V-4 **normally left Open**	Open	
V-S	**Confirm Closed**	
V-N2	**Confirm Closed**	
V-Input	Open	
V-T1	Open	
V-T2	Open	
Bake Trap N for twenty minutes		
Record Bake start time	hh:mm	
Record Bake end time	hh:mm	
Record Pressure on PT pump	mTorr	
V-T2	Close	
V-T1	Close	
V-Input	Close	
V-5	Close	

3.2 Baking and pumping the Primary trap A:

V-10	Open (Pen Downwards)	
V-9	Open	
V-6	Open	
V-A1	Open	
V-A2	Open	
Bake trap A for 15 minutes		
Record Initial trap A Pressure		
Record Bake start time	hh:mm	
Record Bake end time	hh:mm	
Record Pressure on PT pump	mTorr	
Record Final trap A Pressure		
V-6	Close	
V-9	Close	
V-A1	Close	

V-A2	Close	
V-10	Close	

3.3 Baking and pumping the Primary trap B:

V-14	Open	
V-13	Open	
V-12	Open	
V-11	Open	
Bake Trap B for 10 minutes		
Record Initial trap B Pressure		
Record Bake start time hh:mm		
Record Bake end time hh:mm		
Record Pressure on PT pump mTorr		
Record Final trap B Pressure		
V-11	Close	
V-12	Close	
V-13	Close	
V-14	Close	
Attach Lucas Cell to second port (Leak in First one)		
V-14	Open wait for pressure to go down	
Record Pressure on PT pump: mTorr		
V-14	Close	

4.0 Purging the entire system for two hours.

- **Ensure Board is securely connected to the nitrogen bottle.**
- **Inspect the line before use.**

Cool down Trap N with Liquid nitrogen		
V-Input	Open	
V-5	Open	
V-6	Confirm Closed	
V-A1	Open	
V-A2	Open	
V-10	Confirm Close	
V-11	Open	
V-12	Open	
V-13	Open	
V-14	Confirm Closed	
Turn regulator to < 10 PSI. Caution(Make sure it doesn't go above 10 PSI. Periodically check the pressure on the guage.		
V-N2	Open	
V-T2	Open	

V-T1	Slowly open until 1L/M	
Initial Time: hh:mm		
Let it run for 5 minutes.		
V-6	Open (After 5 minutes)	
V-10	Open (Pen Upwards)	
V-14	Open	
V-5	Close	
After two hours, record time: hh:mm		
V-N2	Close	
Allow 5 minutes before proceeding in order to pull vacuum		
Record pressure on PT pump: mTorr		
V-T2	Close	
V-T1	Close	
V-Input	Close	
V-6	Close	
VA1	Close	
VA2	Close	
V-10	Close	
V-11	Close	
V-12	Close	
V-13	Close	
V-14	Close	

5.0 Preparation for the Assay:

V-P	Confirm Closed	
V-5	Confirm Closed	
V-4	Confirm Closed	
V-input	Confirm Closed	
V-chamber (Green Valve)	Confirm Closed	
V-S(Source)	Confirm Closed	
V-T1	Confirm Closed	
V-T2	Confirm Closed	
V-N2	Confirm Closed	
V-6	Confirm Closed	
V-9	Confirm Closed	
V-A1	Confirm Closed	
V-A2	Confirm Closed	
V-10	Confirm Closed	

V-11	Confirm Closed	
V-12	Confirm Closed	
V-13	Confirm Closed	
V-14	Confirm Closed	

5.1 Main Assay

5.1.1

Cool down Trap A in liquid N2. Follow SNOLAB Liquid N2 procedure: SL-OPS-ANS-10-004-P		
V-S	**Confirm Closed**	
V-Input	Open	
V-4	Confirm Open	
V-6	Close	
V-5	Open	
Establish line between the source and board		
V-S	Open(Allow. 15minutes to run vacuum on the line)	
(Allow 15minutes to run vacuum on the line)		
V-S	**Close**	
Source	Open	
V-S	Open at 1L/M	
V-9	**Confirm Closed**	
V-A1	Open	
V-A2	Open	
V-10	Open (Pen Downwards)	
V-6	Open	
V-5	Close	
Record Assay start time: hh:mm		
Record Trap A Initial Pressure		
Record Assay Finish time: hh:mm		
V-S	Close	
V-6	Close	
VA-1	Close	
V-A2	Close	
V-10	Close	
Source	Close	
Record Final Trap A pressure:		

5.1.2 Transfer from A to B

Remove Dewar from Trap A.	
Cool Trap B with LN2 using the smaller Dewar.	
Heat trap A to approx. room temp	
Record pressure of gauge A:	

V-10	Pen upwards	
V-11	Open	
V-A2	Open	
Record Time(15 Minutes)	hh:mm	
Bake Trap A during Transfer		
V-14(If lucas cell Attached)	Open	
Wait for pressure to go to original value		
V-14	**Close**	
V-A2	Close	
V-11 **End of transfer**	Close	
V-10	Close	
Record Final Time:	hh:mm	
Record PT Trap A pressure:		

5.1.3 Transfer from B to Lucas cell

Remove the liquid Nitrogen from Trap B		
Heat Trap B until it is warm (approx. room temp)		
Record Pressure on B(PT Trap)		
V-14	**Confirm Closed**	
V-12	Open	
V-13	Open	
Record Time (10 minutes):	hh:mm	
Heat Trap B throughout transfer		
V-12	Close	
V-13	Close	
Record final time (End of Transfer)	hh:mm	
Record Pressure on B(PT Trap)		
Detach Lucas Cell.		
Record Final Pressure on B(PT Trap)		

6.0 Shut down Procedure

V-P	Close	
Scroll Pump	Turn Off	
PT pressure	Turn Off	
PT Flow	Turn Off	
PT trap	Turn Off	

Assay Procedure for Emanation

Title:
Date:
Crew:

1.0 Preparation of the board for extraction

1.1 Preliminary Confirmed Closed List

V-P	Confirm Closed	
V-5	Confirm Closed	
V-4	Confirm Closed	
V-input	Confirm Closed	
V-chamber (Green Valve)	Confirm Closed	
V-S(Source)	Confirm Closed	
V-T1	Confirm Closed	
V-T2	Confirm Closed	
V-N2	Confirm Closed	
V-6	Confirm Closed	
V-9	Confirm Closed	
V-A1	Confirm Closed	
V-A2	Confirm Closed	
V-10	Confirm Closed	
V-11	Confirm Closed	
V-12	Confirm Closed	
V-13	Confirm Closed	
V-14	Confirm Closed	

2.0 Preliminary Setup

Plug in board power bar and Pump	
Turn on the Scroll Pump	
Turn on PT Flow	
Turn on PT Pump	
Turn on PT Traps	

Notes:

3.0 Pumping/Baking the Traps

3.1 Baking and pumping the Nitrogen trap:

V-P	Open	
Record Time:	hh:mm	
Ensure Pressure is below 150 mT. (Allow up to 15 minutes)		
Record Pressure on PT pump	mTorr	
Record Final Time	hh:mm	
V-5	Open	
V-4 **normally left Open**	Open	
V-S	**Confirm Closed**	
V-N2	**Confirm Closed**	
V-Input	Open	
V-T1	Open	
V-T2	Open	
Bake Trap N for twenty minutes		
Record Bake start time	hh:mm	
Record Bake end time	hh:mm	
Record Pressure on PT pump	mTorr	
V-T2	Close	
V-T1	Close	
V-Input	Close	
V-5	Close	

3.2 Baking and pumping the Primary trap A:

V-10	Open (Pen Downwards)	
V-9	Open	
V-6	Open	
V-A1	Open	
V-A2	Open	
Bake trap A for 15 minutes		
Record Initial trap A Pressure		
Record Bake start time	hh:mm	
Record Bake end time	hh:mm	
Record Pressure on PT pump	mTorr	
Record Final trap A Pressure		
V-6	Close	
V-9	Close	
V-A1	Close	

V-A2	Close	
V-10	Close	

3.3 Baking and pumping the Primary trap B:

V-14	Open	
V-13	Open	
V-12	Open	
V-11	Open	
Bake Trap B for 10 minutes		
Record Initial trap B Pressure		
Record Bake start time hh:mm		
Record Bake end time hh:mm		
Record Pressure on PT pump mTorr		
Record Final trap B Pressure		
V-11	Close	
V-12	Close	
V-13	Close	
V-14	Close	
Attach Lucas Cell to second port (Leak in First one)		
V-14	Open wait for pressure to go down	
Record Pressure on PT pump: mTorr		
V-14	Close	

4.0 Purging the entire system for two hours.

- **Ensure Board is securely connected to the nitrogen bottle.**
- **Inspect the line before use.**

Cool down Trap N with Liquid nitrogen		
V-Input	Open	
V-5	Open	
V-6	Confirm Closed	
V-A1	Open	
V-A2	Open	
V-10	Confirm Close	
V-11	Open	
V-12	Open	
V-13	Open	
V-14	Confirm Closed	
Turn regulator to < 10 PSI. Caution(Make sure it doesn't go above 10 PSI. Periodically check the pressure on the guage.		
V-N2	Open	
V-T2	Open	

V-T1	Slowly open until 1L/M	
Initial Time: hh:mm		
Let it run for 5 minutes.		
V-6	Open (After 5 minutes)	
V-10	Open (Pen Upwards)	
V-14	Open	
V-5	Close	
After two hours, record time: hh:mm		
V-N2	Close	
Allow 5 minutes before proceeding in order to pull vacuum		
Record pressure on PT pump: mTorr		
V-T2	Close	
V-T1	Close	
V-Input	Close	
V-6	Close	
VA1	Close	
VA2	Close	
V-10	Close	
V-11	Close	
V-12	Close	
V-13	Close	
V-14	Close	

5.0 Preparation for the Assay:

V-P	Confirm Closed	
V-5	Confirm Closed	
V-4	Confirm Closed	
V-input	Confirm Closed	
V-chamber (Green Valve)	Confirm Closed	
V-S(Source)	Confirm Closed	
V-T1	Confirm Closed	
V-T2	Confirm Closed	
V-N2	Confirm Closed	
V-6	Confirm Closed	
V-9	Confirm Closed	
V-A1	Confirm Closed	
V-A2	Confirm Closed	
V-10	Confirm Closed	

V-11	Confirm Closed	
V-12	Confirm Closed	
V-13	Confirm Closed	
V-14	Confirm Closed	

5.1 Main Assay

5.1.1

Cool down Trap A in liquid N2. Follow SNOLAB Liquid N2 procedure: SL-OPS-ANS-10-004-P		
V-S	**Confirm Closed**	
V-5	**Confirm Closed**	
V-Input	Open	
V-4	Confirm Open	
V-9	**Confirm Closed**	
V-A1	Open	
V-A2	Open	
V-10	Open (Pen Downwards)	
V-6	Open	
V-green	**Open**	
Record Assay start time: hh:mm		
Record Trap A Initial Pressure		
Record Assay Finish time: hh:mm		
V-green	Close	
V-Input	Close	
V-6	Close	
VA-1	Close	
V-A2	Close	
V-10	Close	
Record Final Trap A pressure:		

5.1.2 Transfer from A to B

Remove Dewar from Trap A.		
Cool Trap B with LN2 using the smaller Dewar.		
Heat trap A to approx. room temp		
Record pressure of gauge A:		
V-10	Pen upwards	
V-11	Open	
V-A2	Open	
Record Time(15 Minutes) hh:mm		
Bake Trap A during Transfer		
V-14(If lucas cell Attached)	Open	
Wait for pressure to go to original value		

V-14	**Close**	
V-A2	Close	
V-11 **End of transfer**	Close	
V-10	Close	
Record Final Time: hh:mm		
Record PT Trap A pressure:		

5.1.3 Transfer from B to Lucas cell

Remove the liquid Nitrogen from Trap B		
Heat Trap B until it is warm (approx. room temp)		
Record Pressure on B(PT Trap)		
V-14	**Confirm Closed**	
V-13	**Confirm Closed**	
V-12	Open	
Record Time (10 minutes): hh:mm		
Heat Trap B throughout transfer		
V-12	Close	
V-13	Close	
Record final time (End of Transfer) hh:mm		
Record Pressure on B(PT Trap)		
Detach Lucas Cell.		
Record Final Pressure on B(PT Trap)		

6.0 Shut down Procedure

V-P	Close	
Scroll Pump	Turn Off	
PT pressure	Turn Off	
PT Flow	Turn Off	
PT trap	Turn Off	

Appendix C

Scintillator Bio-Flex Hose Assay

Bio-flex hoses

Introduction

Bio-flex[1] hoses are one of the sample lines connected from UI to scintillator fill lines. There are three flux hoses attached to the detector and they are suspected to be one of the candidates for ingress of radon into the detector. One of the sample lines was removed with the goal of investigating the diffusion rate of radon from the mine Air to its inner volume. The hose specifications are as follows:

For all of the following calculations, lab temperature is assumed to be 300 K.

Bio-Flex Hose Assay

The first goal was to clean the hose well enough to remove any LAB or any vapor on the Hose. The Hose was removed and hung vertically in the DCR while flushing nitrogen overnight. The

[1]Bioflex hoses are highly flexible Polytetrafluorethylene lined hose which is used for transfer of processed fluids(Linear Alkylbenzene in our case).

Inner diameter	1.5 inch	0.0381m
Length	80 inch	2.0320m
Surface Area	380 in^2	0.24 m^2

Table C.1: Dimensions of the Bio-Flex hoses

initial setup included that the hose was attached to the nitrogen bottle on one end and to the vacuum pump on the other end with pressure gauge attached. Moreover, valves were attached to facilitate pumping and purging. The hose was pumped and purged several times before the hose was filled with Nitrogen gas.

Nitrogen gas was filled just above the atmospheric pressure of the lab until the pressure reached 1100 Torr (146654 Pascal). The Hose was left to sit for an hour before the extraction; the goal was to check if there is any leak in the pipe. The nitrogen gas added to the Hose was used to perform radon assays to measure the diffusion and emanation of radon from the mine Air into the hose and eventually determine the ingress of radon into LAB during filling.

10^{th} October 2019 Extraction

Once it was ensured that the Hose wasn't leaking, an extraction of the gas was performed. One end of the hose was attached to the the mobile radon board. Gas was extracted at 0.1 litre/minute for 12 minutes until the pressure on the Hose dropped from 1100 Torr (146654 pa) to 575 Torr (76660 pa). Ideal gas law was used to determine the number of moles in order to normalise the gas samples extracted.

$$\mathrm{PV} = \mathrm{nRT}$$

$$\mathrm{n} = \frac{146654 * 2.3131 \times 10^{-3}\mathrm{m}^3}{8.31 * 300\mathrm{K}} \tag{C.1}$$

$$\mathrm{n_i} = 0.1363\,\mathrm{mol} \tag{C.2}$$

$$\mathrm{n_f} = 0.0712\,\mathrm{mol} \tag{C.3}$$

$$\mathrm{d_n} = 0.0650\,\mathrm{mol} \tag{C.4}$$

Using the ideal gas equation at STP, number of moles were use to determine the extracted volume, the first extraction was a total of $1.453 \times 10^{-3}\mathrm{m}^3$ or 1.456 L of gas.

The gas was passed through the radon board where radon was injected into the Lucas cell and taken to surface lab for counting. The number of radon atoms were calculated using the following equation.

$$\text{Radon atoms/sample} = \frac{N_{\text{Alphas}} - B_{\text{LC}} t_{\text{count}}}{\varepsilon_{\text{total}}(\exp^{-\lambda t_{\text{Delay}}})(1 - \exp^{-\lambda t_{\text{Count}}})} \tag{C.5}$$

where N_{Alphas} is the measured alphas in the lucas cell, B_{LC} is the alpha background of the Lucas cell, t_{count} is the total counting period of the assay in days, $\varepsilon_{\text{total}}$ is the total efficiency of the radon board, and t_{delay} is the time from the end of the assay to the start of the counting.

The total efficiency of the board is not known at 0.1 LPM so the efficiencies of the water assay system underground will be assumed. The calculations presented in this report uses the water board efficiencies. The efficiencies are as follows:

Board	$\varepsilon_{\text{counting}}$	$\varepsilon_{\text{trapping}}$	$\varepsilon_{\text{transfer}}$	$\varepsilon_{\text{Total}}$
Water Board	0.74	0.64	1	1.42
Queens Board	0.74	0.8	0.9	1.59

The assay was counted for 3.45 days; 960 alphas were counted. The Lucas cell background was 12 alphas/day which corresponds to 42 alphas/counting period. After subtracting the Lucas cell background 918 alphas were measured with a delay time of two hours. This results in 1411 radon atoms in the gas sample collected.

$$\text{Radon Atoms /sample} = 1411\text{Rn/sample} \tag{C.6}$$

We use the pressure difference to correct the total number radon atoms in the Hose before the Assay.

$$\text{RadonAtoms (Hose)} = 1411\,\text{Rn}(\frac{1100\,\text{Torr}}{1100\,\text{Torr} - 575\,\text{Torr}}) \tag{C.7}$$

If we interpret this count as the rate of radon ingress over the one hour of exposure:

$$\text{Rn Atoms (Hose)/hr} = 2957\,\text{Rn/Hr} \tag{C.8}$$

The remaining radon atoms in the Hose after the extraction is just the difference between equation (8) and (9).

$$\text{Remaining Rn Atoms (Hose)} = 1546/\text{Atoms} \tag{C.9}$$

18^{th} October 2019 Extraction

The Sample was left to emanate for 7.97 days. The starting pressure on October 10th was 575 Torr. Immediately before the extraction the pressure was 593 Torr. The dP 18 torr (24 mbar).

$$\text{Q} = 1.1 \times 10^{-5}\,\text{Torr(l/s)} \tag{C.10}$$

With this leak rate it can be concluded that about 3.4% of the Hose air is mine air which entered into the Hose over the total period of emanation time.

The atoms left in the Hose from the previous extraction needs to be accounted. 1546 atoms remained in the Hose at the end of the first extraction. Emanation time is almost 2 half life of radon according to which only 365 radon atoms should remain on October 18th 2019 at the time of extraction.

The second extraction was 12 minutes long just like the previous one. The pressure in the hose dropped from 593 Torr to 387 Torr. This difference in pressure is 206 torr (27464 pa). The assay was counted for 2.62 days; 207 alphas were counted. The Lucas cell background was 12 alphas/day which corresponds to 31 alphas/counting period. After subtracting the Lucas cell background, 175 alphas were measured with a delay time of two hours. This results in 331.615 radon atoms in the gas sample collected.

$$\text{Radon Atoms/sample} = 331\,\text{Rn}(\frac{593\,\text{Torr}}{593\,\text{Torr} - 387\,\text{Torr}}) \tag{C.11}$$

$$\text{Radon atoms (Hose) A} = 954.5\text{Rn/Hose} \tag{C.12}$$

In order to determine the actual number of Radon atoms that emanated through the wall of the Hose, number of atoms in eq C.12 needs to be corrected for 365 radon atoms that remained

inside the Hose after the October 10th extraction.

$$\text{Radon atoms}_{\text{emn}} = 589\text{Rn atoms} \tag{C.13}$$

As the emanation time was about two half lives of radon this number needs to be corrected in order to account for the radon atoms that entered the Hose and decayed in the Hose. The following equation will be used to do the correction:

$$\text{Radon atoms}_{\text{Total}} = \frac{A\lambda t_{\text{em}}}{(1 - \exp^{-\lambda t_{\text{em}}})} \tag{C.14}$$

Where A is the the total number of Radon atoms in the Hose.

$$\text{Radon atoms}_{\text{emanation}} = 1114.6\,\text{Rn atoms} \tag{C.15}$$

$$\text{Radon atoms/day} = \frac{1114.6\,\text{Rn}}{7.97\,\text{days}} \tag{C.16}$$

$$\text{Radon atoms/day} = 139\text{Rnatoms/day} \tag{C.17}$$

$$\text{Radon atoms/hr} = 5.82\text{Rnatoms/hr} \tag{C.18}$$

$$\text{Radon atoms/hr/in}^2 = 0.0153\text{Rn atoms/hr(in}^2) \tag{C.19}$$

At the end of the extraction the remaining atoms in the Hose that was left to emanate was:

$$\text{Radon atoms(Hose)} = 955\,\text{Rn} - 331.6\text{Rn}$$

$$\text{Radon atoms(Hose)} = 622.98\,\text{Radon atoms} \tag{C.20}$$

28^{th} October 2019 Extraction

The Sample was left to emanate for 9.49 days. The pressure at the end of the extraction was 387 Torr and after 9.49 the pressure on the Hose raised to 440 Torr. The third extraction was also 12 minutes long just like the previous ones.The pressure dropped from 440 Torr to 1 Torr. The goal was to extract all the gas from the hose until it reaches vacuum.

The remaining atoms in Hose in eq C.20 decayed by almost 2.5 half lives of radon. Using the half life equation only 111 atoms should remain in the Hose from the previous extraction. After a counting period of 0.749 days, a total of 145 alphas were counted.The Lucas cell has a background of 12 alphas/day which corresponds to 9 alphas/counting. After subtracting the lucas cell background, 136 alphas were measured. Which results in 765 radon/sample atoms using equation number 3. The radon atoms/sample and radon atoms/Hose is the same. as the entire. volume of gas was extracted:

$$\text{Radon(Hose)} = 765\,\text{RnAtoms} \tag{C.21}$$

In order to determine the actual number of Radon atoms that emanated through the wall of the Hose, number of atoms in eq C.21 needs to be subtracted with 111 radon atoms that remains inside the Hose after the last extraction in order to determine the radon atoms that entered the Hose during the emanation time.

$$\text{Radon atoms}_{\text{emanation}} = 653\text{Rn atoms} \tag{C.22}$$

Using the same steps as the last extraction, using eq C.14 we correct for the total number of atoms that emanated through the walls and decayed before the extraction.

$$\text{Radon atoms/hose(corrected)} = 1370\,\text{Rn atoms} \tag{C.23}$$

The total number of Rn atoms entering the Hose can be determined by dividing with the

emanation time:

$$\text{Radon atoms/day} = \frac{1370\,\text{Rn}}{9.49} \tag{C.24}$$

$$\text{Radon atoms/day} = 144\text{Rn atoms/day} \tag{C.25}$$

$$\text{Radon atoms/hr} = 6.01\,\text{Rnatoms/hr} \tag{C.26}$$

$$\text{Radon atoms/hr/in}^2 = 0.0158\text{Rn atoms/hr(in}^2) \tag{C.27}$$

At the end of this extraction vacuum was pulled on the Hose and was left to pump for quite a bit. We will now consider the fact that after pumping we essentially had zero radon atoms left in the Hose.

7^{th} November 2019 Extraction

The Sample was left to emanate for 8.965 days under vacuum. The pressure at the end of the extraction on October 28th was 1 Torr and after the emanation time it was 90 Torr. This extraction will determine the radon emanating into the Hose. This assay was also for 12 minute just for the sake of keeping the backgrounds of the radon board consistent.

After a counting period of 7.865 days, a total of 694 alphas were counted. The Lucas cell background was 12 alphas/day which results in 94 alphas/counting period.After subtracting the lucas cell background 599 alphas were measured which results to a total number of 665.95 radon atoms using equation number 3. We now calculate the number of radon atoms entering the hose in a day.

The results from this extraction also needs to be corrected for the radon atoms that entered into the Hose and decayed over the period of the emanation time. Equation (13) will be used to determine the total number of radon atoms that entered into the hose.

$$\text{Radonatoms/emanation} = 1348\text{Rn/emanation} \tag{C.28}$$

$$\text{Radonatoms/day} = \frac{1348\text{Rn}}{8.965} \tag{C.29}$$

$$\text{Radonatoms/day} = 150\text{Rnatoms/day} \tag{C.30}$$

$$\text{Radon atoms/hr} = 6.26\,\text{Rnatoms/hr} \tag{C.31}$$

$$\text{Radonatoms/day/in}^2 = 0.0164\text{Rnatoms/hr(in}^2\text{)} \tag{C.32}$$

Efficiency = 1.42	10^{th} Oct 2019	18^{th} Oct 2019	18^{th} Oct 2019	7^{th} Nov 2019
Emanation time(days)	0.0416	7.97	9.49	8.965
Radon/sample	1411	331.61	765.4	665.9
Radon/Hose	2957.8	954.6	765.4	665.9
Remaining Radon(After Extraction)	1546	622.9	0	0
Rn left over from prev measurement	0	365.38	111.8	0
Radon Atoms by emanation	2957.8	589.2	653.6	665.9
Radon Atoms by emanation (Corrected)	2973	1114.6	1370	1348
Radon Atoms/day	70987	139.8	144.3	150.3
Radon Atoms/Hr	2973 ± 891	5.82 ± 1.7	6.01 ± 1.8	6.26 ± 1.87
Radon Atoms/Hr/$inch^2$	7.82	0.01533	0.01583	0.0164

The similar calculations were performed using the Queens board efficiency just to have a relative measurement because the total efficiency of the radon board at which these measurements took place is unknown.

Efficiency = 1.59	10^{th} Oct 2019	18^{th} Oct 2019	18^{th} Oct 2019	7^{th} Nov 2019
Emanation time(days)	0.0416	7.97	9.49	8.965
Radon/sample	1254.8	294.7	680.3	592
Radon/Hose	2629	848.5	680.3	592
Remaining Radon(After Extraction)	1374	553.7	0	0
Rn left over from prev measurement	0	324.8	99.3	0
Radon Atoms by emanation	2629	523.7	580.9	591.9
Radon Atoms by emanation (Corrected)	2642	990.7	1218	1198
Radon Atoms/day	63100	124	128.3	133.6
Radon Atoms/Hr	2642 ± 793	5.17 ± 1.55	5.34 ± 1.60	$5.57 \pm .1.67$
Radon Atoms/Hr/inch^2	6.95	0.0136	0.01407	0.0146

Conclusion

Successful measurements of the bio-flex Hoses were taken and radon emanating through the walls of the hoses were determined. This result will be further used to determine the radon background entering the detector during the filling through these Hoses.